INDUCED PLURIPOTENT STEM CELL-DERIVED MESENCHYMAL PROGENITOR CELLS: PROMOTION OF NEURITOGENESIS AND AXON ELONGATION THROUGH NEUROTROPHIN AND CYTOKINE PRODUCTION

by

Rachel Mai-Lan Brick

B.S. in Biotechnology, Pennsylvania State University, 2011

B.S. in Immunology and Infection Diseases, Pennsylvania State University, 2011

Submitted to the Graduate Faculty of

University of Pittsburgh School of Medicine in partial fulfillment

of the requirements for the degree of

Doctor of Philosophy

University of Pittsburgh

2017

UNIVERSITY OF PITTSBURGH

School of Medicine

This dissertation was presented

by

Rachel M. Brick

It was defended on

June 12, 2017

and approved by

Charleen T. Chu, M.D., Ph.D., Professor, Department of Pathology

Alejandro Soto-Gutierrez, M.D., Ph.D., Assistant Professor, Department of Pathology

Xinyan Tracy Cui, Ph.D., Professor, Department of Bioengineering

Johnny Huard, Ph.D., Professor, Department of Orthopedic Surgery (University of Texas)

Dissertation Director: Rocky S. Tuan, Ph.D., Distinguished Professor, Department of Orthopedic Surgery and Bioengineering

INDUCED PLURIPOTENT STEM CELL-DERIVED MESENCHYMAL PROGENITOR CELLS: PROMOTION OF NEURITOGENESIS AND AXON ELONGATION THROUGH NEUROTROPHIN AND CYTOKINE PRODUCTION

Rachel M. Brick, PhD

University of Pittsburgh, 2017

Adult bone marrow derived, multipotent mesenchymal stem cells (MSCs) have been shown to exhibit support nerve regeneration by secreting neurotrophic factors typically produced by Schwann cells. However, MSCs have limited expansion capacity, and therefore have limited lifespan and use.

Induced pluripotent stem cells (iPSCs) can potentially overcome this drawback—iPSCs are adult cells reprogrammed with pluripotency factors to become like embryonic stem cells. Thus, MSCs may be taken from a patient and reprogrammed into iPSCs, such that their expansion capacity is virtually unlimited. After expansion, the iPSCs can be differentiated once again into mesenchymally-derived induced mesenchymal progenitor cells (MiMPCs). This technology has the potential to yield an almost unlimited supply of MSC-like cells.

We report here that MiMPCs can be induced to produce neurotrophic factors (NTFs) such as brain-derived neurotrophic factor (BDNF) at levels comparable to those produced by MSCs. NTF production further increases when MiMPCs are induced in a simulated inflammatory environment. MiMPCs are also capable of producing multiple other factors and cytokines that have been shown to enhance nerve regeneration, including osteonectin and IL-6.

Our results show that treatment with conditioned medium derived from MiMPCs and MSCs resulted in enhanced neuritogenesis and extension lengths of cultures of chick embryonic dorsal root ganglia (DRG). MiMPC/DRG co-cultures grown on 2-dimensional electrospun nanofibrous biomaterial scaffolds are also comparable morphologically and physiologically to MSC/DRG scaffold co-cultures. In these cultures, neurite length is significantly decreased with the introduction of a Jak/STAT inhibitor, suggesting that secreted cytokines from the IL-6 family are required for neurite extensions. Complexity of these neurite extensions decreases, but is not abolished, when Trk-receptor inhibitors are applied, suggesting the involvement of other non-traditional neurotrophic factors in the MiMPC secretome in the enhancement of neuritogenesis.

Taken together, these results strongly suggest that MiMPCs may be a suitable clinical replacement for MSCs in nerve regeneration cell therapeutics. Future assessment of this therapeutic potential will include testing the efficacy of an MiMPC-seeded nerve conduit to repair peripheral nerve injury in an experimental animal model, such as the rat sciatic nerve transection model.

TABLE OF CONTENTS

LIST OF TABLES

LIST OF FIGURES

LIST OF ABBREVIATIONS

Abbreviation	Full term
48hr BCM	48 hour basal conditioned medium
αMEM	minimal essential medium eagle – alpha modification
β-ME	beta mercaptoethanol
BDNF	brain-derived neurotrophic factor
CD	cluster of differentiation
CNTF	ciliary neurotrophic factor
CM	conditioned medium
Ctrl	control
DRG	dorsal root ganglion
EGF	epithelial growth factor
FGF2	basic fibroblast growth factor
GDNF	glial cell line-derived neurotrophic factor
GM	growth medium
GM-MiMPCs	MiMPCs cultured under normal growth conditions
GM-MSCs	MSCs cultured under normal growth conditions
HBSS	Hank's buffered salt solution
HLA-D/R	human leukocyte antigen-antigen D related
IL	interleukin
iPSC	induced pluripotent stem cell
LIF	leukemia inhibitory factor
MiMPCs	Mesenchymally-derived induced mesenchymal progenitor cells
MSCs	mesenchymal stem cells
NGF	nerve growth factor
NI-MiMPCs	neurotrophically induced MiMPCs
NI-MSCs	neurotrophically induced MSCs
NIM	neurotrophic induction medium
hNRG	human neuregulin
NT-3	neurotropin-3
NTF	neurotrophic factor
ON/SPARC	Osteonectin/secreted protein acidic and rich in cysteine
PBS	phosphate buffered saline
PCL	poly-e-caprolactone
PDGF	platelet derived growth factor

PS	penicillin-streptomycin
PSF	penicillin-streptomycin/fungizone; antibiotic-antimycotic
RA	retinoic acic (all-trans)
siRNA	silencing RNA

PREFACE

Funding Acknowledgements

Commonwealth of Pennsylvania Department of Health

U.S. Department of Defense (W81XWH-10-2-0084, W81XWH-15-1-0600)

Scientific Acknowledgements

The work presented in this document would not have been possible without the dedication and contributions of my committee and my mentor, Rocky S. Tuan. The guidance and insights from my committee have been invaluable on this journey as well, and my deepest thanks go to Drs. Charleen Chu, Johnny Huard, Tracy Cui, and Alex Soto-Gutierrez for their enthusiasm and support. The following individuals, listed alphabetically, have provided indispensable teachings and advice: Dr. Peter G. Alexander, Karen L. Clark, Dr. Solvig Diederichs, Kelsey Gloss, Dr. Heidi Zupanc, Aaron Sun, and Dr. Jian Tan.

Personal Acknowledgements

First and foremost, my most heartfelt gratitude goes to Rocky for giving me a home at CCME and generously providing a means to explore my scientific interests. Your guidance and patience have been immeasurably valuable in teaching me effective practice and presentation of science.

A simple “thank you” to my friends and family is wholly inadequate to express my appreciation. You have been there for me every step of the way, pushing me and believing in me, encouraging me and patiently listening to me whine and rant through every setback and frustration.

To all my friends from A to Z: Peter Alexander, Natasha Baker, Danielle Cimafranca, Karen Clark, Thais Cuperman-Pohl, Solvig Diederichs, Kelsey Gloss, Riccardo Gottardi, Sasha Halim, Philip Hochendoner, Yangzi Jiang, Daniel Krieg, Alex Land, Brett Landy, Melanie LaVoie, Thomas “Tang Mian” Lozito, Soumya Nanda, Joseph Sherman, Aaron Sun, Jian Tan, Veronica “Vee” Ulici, Haruyo Yagi and Heidi Zupanc,. I’m sure there are plenty more that I’ve forgotten to mention, but please know that your love and support have been every bit as important.

To the many friends I’ve made in virtual communities these past few years—SoundCloud and Wattpad in particular—thank you for nurturing my love for the creative arts. These hobbies were an escape from the daily grind, and surely served to preserve my sanity. Though we come from all walks and stages of life, from all ethnicities, separated by distance and time zones, your support in both my scientific and creative endeavors have remained steadfast.

To my family, I am eternally grateful for your unwavering support and encouragement. To my mom and dad, Monica and Martin Brick, thank you for believing in me every day, and looking at the bright side all these years. I know how little you both started out with, and how hard you’ve worked to build a comfortable life for our family. I can’t imagine how many sacrifices you’ve had to make for me, but you’ve shown me that with hard work and perseverance, anything is possible.

To all, you have my eternal and most heartfelt gratitude.

1.0 INTRODUCTION

Peripheral nerve damage often accompanies and complicates limb injuries. Proper healing of nerve damage can be quite challenging, especially as the success of nerve regeneration is dependent upon the rate and quality of axon growth and myelination to bridge the gap across the injured area. Regeneration is mediated by Schwann cells, which secrete neurotrophic factors and migrate to form Bands of Büngner, a longitudinal tunnel that both guides the regenerating neuron towards its target and secretes neurotrophic factors to encourage nerve regrowth. However, this process is error-prone, and can often result in formation of painful neuromas [1]. Currently, the gold standard treatment for large nerve gaps include autologous nerve graft surgery at the sacrifice of other nerves from a donor site, but even the best treatment is limited—even with multiple surgeries, often times complete motor function is never fully regained, and the donor site is at least partially deinnervated [2].

An alternative to the autologous nerve graft is an autologous Schwann cell transplant to the injured site. While this method does not sacrifice a healthy nerve, it still risks damage to the nerve at the Schwann cell donor site. The patient thus risks similar donor site morbidities as those seen in autologous nerve grafts. Allogeneic Schwann cell transplants have also been attempted, but due to the immunogenic nature of Schwann cells, these transplants are quickly rejected by the host [3]. Because of these limitations, a more practical approach is needed. To answer this need, several studies have shown that bone marrow derived mesenchymal stem cells

(MSCs) have the ability to act as Schwann-like cells, given the proper induction environment, and can support nerve regeneration by secreting neurotrophic factors (NTFs) [4, 5].

While neurotrophically induced-MSCs (NI-MSCs) are capable of producing many of the same NTFs as Schwann cells, they have finite expansion capacity, and require invasive techniques to acquire, e.g., bone marrow aspiration. Induced pluripotent stem cells (iPSCs), derived by reprogramming adult somatic cells, including MSCs, that exhibit embryonic stem cell (ESC)-like pluripotency, represent a potential cell source that can overcome this drawback as iPSCs can grow indefinitely [6]. iPSCs are produced by reprogramming with four transcription factors and have a virtually unlimited expansion capacity. We and others have shown that after expansion, the iPSCs can be differentiated into MSC-like cells, which we have termed induced mesenchymal progenitor cells (MiMPCs). In this manner, this technology has the potential to yield an almost unlimited supply of MiMPCs. In this study, we aim to test if these MiMPCs, originally derived from MSCs, have the same ability to support neuronal regeneration as the parent MSC. With this capacity, MiMPCs may represent a potentially infinitely renewable cell source for the support of nerve regeneration and cell therapy. Our results show that MiMPCs can secrete neurotrophic factors after neuroinductive treatment and can produce factors to improve neurite outgrowth in a chick embryonic dorsal root ganglion (DRG) model. These findings suggest that neurotrophically induced-MiMPCs (NI-MiMPCs) may be considered a suitable substitute cell type to support nerve growth.

1.1 IMPACT AND INCIDENCE OF NERVE INJURY

Peripheral nerve injuries can result in the loss of sensory function, motor function, or both, and is a significant cause of morbidity and disability. Because of the close anatomic association between nerves and various subcutaneous tissues (such as blood vessel, bone and tendon), nerve injuries commonly accompany a number of limb injuries including dislocated, fractured or broken bones. For example, the most common form of upper extremity nerve injuries associated with fractures is radial nerve injuries resulting from humeral fractures [7]. Nerve injuries can also occur as a side effect of surgery. For example, the saphenous nerve is often injured during knee surgeries or autogenous hamstring tendon harvesting during anterior cruciate ligament (ACL) reconstruction [8, 9]. Shoulder surgeries can also result in iatrogenic damage to the nerve or the brachial plexus, which may then require further surgical treatment. In these cases, peripheral nerve repair may be more treatable than brachial plexus damage [10]. Surgical nerve injuries frequently result in the formation of a neuroma, although these can also occur after a crush or stretch injury. Neuromas form from disorganized nerve growth, typically by becoming trapped by scar tissue, or become swollen without any abnormal nerve growth. While generally benign (malignant nerve tumors are given other terms), these growths are very painful and can still affect functional use of the area by limiting motion and contact.

These types of injuries can have lasting effects on a patient, both in terms of quality of life and socioeconomic burden. Not only are surgical procedures costly, patients may also be taken out of the workforce, possibly for life, which incurs a burden upon the population as a whole in the form of lost labor production [11]. A Swedish study found that the healthcare cost of digital nerve injuries alone averaged slightly less than 3,000 Euros in terms of surgical or outpatient care (but came close to 6,000 Euros if tendons were involved). Taking into account

the value of lost workforce, the cost per patient could be as high as 9,000 Euros, depending on the type of work forfeited. The bulk of patients ranged from 21-40 in age, which makes up the primary population of the working force [12]. In the United States, nerve injuries cost the healthcare system approximately 150 billion dollars annually. They again occur primarily in young, otherwise healthy civilians and military officers who are the most at risk for traumatic injuries [13].

1.2 CLASSIFICATIONS AND TYPES OF NERVE INJURY

Seddon described in 1943 three classes of nerve injuries—neurapraxia, axonotmesis and neurotmesis. In 1951, Sunderland expanded these classifications into five stages.

Seddon	Sunderland	Definition
Neurapraxia	Stage I	Compression and conduction block No transection
Axonotmesis	Stage II	Axonal transection Wallerian degeneration occurs
—	Stage III	Axonal and endoneurium transection Possible intraneural fibrosis and neuroma formation
—	Stage IV	Perineurial and fascicle disruption Possible intraneural fibrosis and neuroma formation
Neurotmesis	Stage V	Complete nerve transection

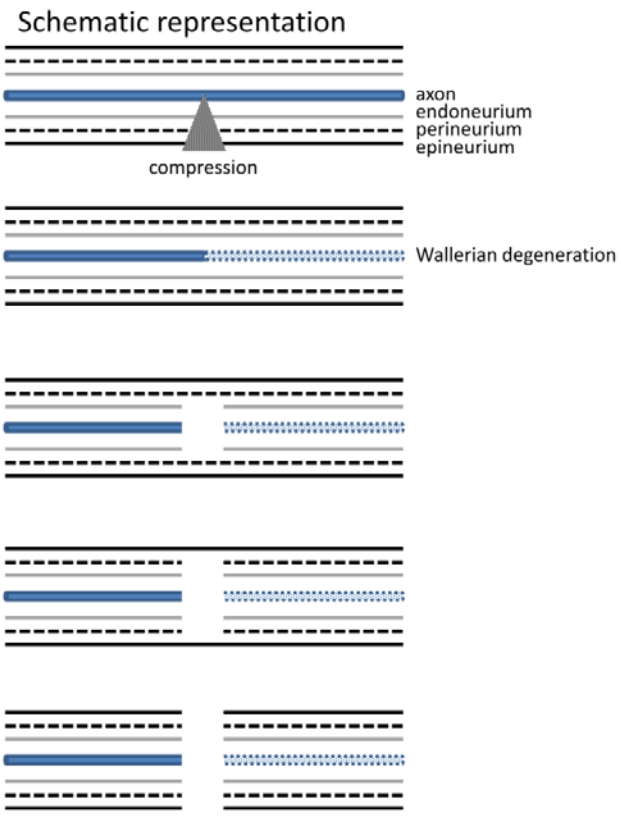

Figure 1. Seddon and Sunderland classifications of peripheral nerve injuries
Table and schematic diagrams summarizing Seddon's and Sunderland's classifications of peripheral nerve injuries.

1.2.1 Neuropraxia

Neuropraxia (Sunderland's Stage I) is caused by a mild neural lesion in the myelin sheath, which temporarily blocks nerve conduction [14-16]. The axon is not transected in these types of injuries and there is no degeneration of nerve fibers and no interruption in the surrounding connective tissues. However, if neuropraxia is caused by mechanical forces (as opposed to ischemia), localized degradation of the myelin sheath may occur. It is possible to fully recover from this type of injury without surgical intervention in as little as 1 day, or as long as 3 months when the myelin sheath is reestablished [15].

1.2.2 Axonotmesis

Axonotmesis (Sunderland's Stage II) occurs when the axon is transected, but the surrounding connective tissues, particularly the endoneurial tube, remains intact [14]. This type of lesion typically occurs as a result of a more severe crush injury than those causing neuropraxia. The distal end of the transected axon will degenerate via a process called Wallerian degeneration. As the structure of the endoneurial tube has not been compromised, these types of nerve injuries have a good prognosis (especially for short distances) because the endoneurial tube can act as a natural guide for nerve regrowth [15]. In these cases, motor neuron function is less likely to recover than sensory function because motor end-plates do not survive as long as sensory neurons following denervation [17].

Stages III and IV of Sunderland's classifications further expounds upon Seddon's axonotmesis by defining transection of the endoneurial tube, and destruction of nerve fascicle components except for the epineurium, respectively [16]. Both stages III and IV may experience

intraneural fibrosis, which impedes nerve regeneration, and may lead to neuroma formation as the guide for nerve growth is lost [15]. Without repair, functional recovery is poor as growing nerves generally become disoriented or are blocked due to fibrotic infiltration.

1.2.3 Neurotmesis

Neurotmesis (Sunderland's Stage V) is the most severe classification of nerve injury, where all sections of the nerve (axon, myelin sheath, endoneurium, perineurium and epineurium) are injured or completely transected. These commonly result from laceration or ischemic injuries. Wallerian degeneration also occurs in this case, but prognosis of functional recovery is poor. Surgical repair is necessary in this case, and depending on the length of the nerve gap, an autograft may be required.

1.3 NATURAL WOUND HEALING: CLASSIC ROLES OF SCHWANN CELLS AND NEUROTROPHINS

1.3.1 Wallerian degeneration

To heal, the nerve must follow a sequence of events, which typically begin 24-48 hours after nerve transection: Wallerian degeneration, axon regrowth, and end-target reinnervation [1]. Without these three events, effective nerve regeneration may not occur, and the patient may experience partial or total loss of motor-sensory function. Following peripheral nerve transection, the cell body undergoes a metabolic change and prioritizes the production of

structural components needed for cellular repair and axon regeneration, in lieu of neurotransmitter production [2]. Intracellular and extracellular stores of calcium activate calpain, a protease which degrades the cytoskeleton and begins granular disintegration of the axon. Axon degradation precedes further degeneration of other nerve components [18]. Calcium release also stimulates Schwann cell proliferation [19], as well as formation of new growth cones in the axon [20].

As mentioned in the previous section, Wallerian degeneration occurs in Sunderland's Stages III-V, generally after loss of membrane integrity and axon degradation [1]. The myelin sheath begins to break down and the axons become disorganized and begin to disintegrate. Macrophages and Schwann cells are recruited to the site of injury and begin to clear away myelin sheath debris. Only by clearing away the injured myelin sheath are Schwann cells able to proliferate and form the bands of Büngner to begin the axon regeneration process.

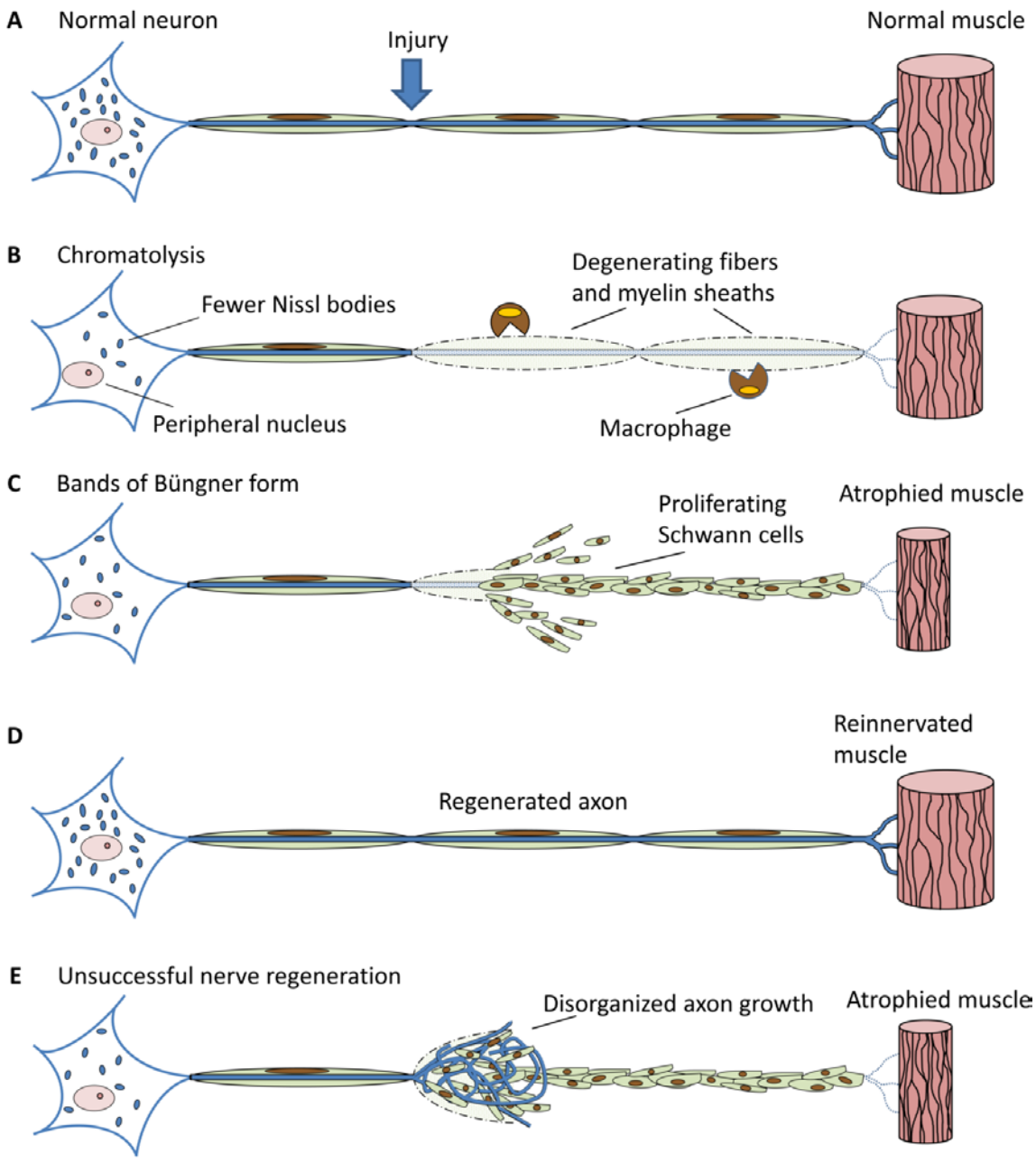

Figure 2. Stages of Wallerian degeneration

(A) Normal, healthy neuron with an intact axon that has been exposed to traumatic injury. (B) Upon injury, macrophages are recruited to the site and clear away the degenerating axon along with myelin sheath debris. The nucleus is displaced to the periphery of the neuron, along with disintegration of Nissl bodies during a process called chromatolysis. (C) Schwann cells proliferate to form the Bands of Büngner, engulfing the growing axon. Deinnervated target organ begins to atrophy. (D) A successfully regenerated axon reinnervates target organ. (E) Axon growth is disorganized and a neuroma forms. End target remains atrophied due to continued deinnervation, and loss of sensory or motor function may occur.

1.3.2 Schwann cells

In the peripheral nervous system, Schwann cells take on two forms: myelinating and non-myelinating. Myelinating Schwann cells wrap around the axon of the nerve to form an insulating myelin sheath, allowing for quicker conduction of nerve impulses. Non-myelinating Schwann cells wrap around smaller-diameter, C-fiber axons to form Remak bundles [21]. While non-myelinating Schwann cells do not provide insulation in the same sense that myelinating sheaths do, they organize the C-fiber axons by surrounding and separating each axon with cytoplasm [22]. Both are responsible for maintaining the health and survival, and promoting the regeneration of peripheral neurons.

When Schwann cells proliferate to form the bands of Büngner, they provide the basal lamina structure that will ideally guide the nerve towards the appropriate end-organ. Expression of other adhesion molecules, such as N-cadherins and other cadherins, or integrins are increased in the bands of Büngner. Some evidence suggests that the type of adhesion molecule expressed is dependent upon the type of axon (i.e., sensory or motor) that is regenerating, and that these adhesion molecules may help to organize axons and Schwann cells [20, 23]. In addition to physical support, they also secrete neurotrophins to encourage nerve survival and growth. It is toward these neurotrophins, and other classes of factors, that the growth cone end of the regenerating axon is attracted. The growth cone, which is an exploratory apparatus, can also respond to other molecules such as neurite-promoting factors (i.e., fibronectin and laminin) and matrix precursors (i.e., fibrinogen) [2].

1.3.3 Nerve growth factor

Nerve growth factor (NGF) is often considered the original neurotrophic factor as it was the first to be described [24]. It regulates the survival and maturation of developing peripheral nerves, particularly sensory and sympathetic nerves. In addition to trophic effects, such as survival and maintenance, it has also been demonstrated that NGF has chemotropic properties in that it can guide axon growth and promote branching and arborization [2, 25]. Because of these properties, many studies have investigated the possibility of applying NGF to nerve lesions in hopes of improving healing after nerve lesion [26-28]. These studies showed that when NGF was incorporated into constructs such as a fibrin glue [28], fibrin matrices [29], or a heparin-binding affinity-based delivery system [30], nerve regeneration across a gap defect was enhanced. Fiber count and density increased in the presence of NGF, and improved regeneration efficiency compared to controls, even when the nerve defect distance exceeded critical gap length (>15mm) [30].

However, while NGF has certainly proven to enhance nerve regeneration, other neurotrophic factors such as brain-derived neurotrophic factor (BDNF), neurotrophin-3 (NT-3), ciliary neurotrophic factor (CNTF), and glial-derived neurotrophic factor (GDNF) have also shown that they are capable of enhancing nerve regeneration and even act synergistically with extracellular matrix molecules, with Schwann cells, and with each other [31-34].

1.3.4 Brain-derived neurotrophic factor

BDNF has been shown to increase myelin formation [35], and restore motor function and nerve conduction velocity to crushed sciatic nerves in rats [36]. Wilhelm, et al showed that both BDNF

and Schwann cells had to be present for effective healing of cut peripheral nerves [34]. Increased levels of BDNF after injury can also indirectly activate the Jak/STAT pathway in Schwann cells by phosphorylating STAT3/STAT1, leading to increased Schwann cell cytokine production that promote neuritogenesis and nerve regeneration [37]. Bella, et al, also showed that BDNF can act directly on pelvic ganglion in rats, activating the Jak/STAT pathway to promote neurite growth, an effect which could be truncated with the application of Jak/STAT inhibitor AG490 [38]. Ataxic mice injected intrathecally with BDNF-producing mesenchymal stem cells also showed lowered apoptotic markers and decreased degeneration of axons, demonstrating the clinical potential for BDNF-producing stem cells not only in post-injury applications, but in neurodegenerative diseases as well [39].

1.3.5 Glial cell line-derived neurotrophic factor

GDNF promotes the survival of both sensory and motor neurons, and, like NGF, was also capable of increasing nerve fiber density and myelination. A 2006 study by Li, et al showed that when Schwann cells overexpressing GDNF was introduced at the site of injury in rat sciatic nerve, there was an increase in survival and function of motor neurons. Nerve regeneration was also improved over controls when conduits filled with GDNF-expressing Schwann cells were used to bridge a transection gap [40]. Unlike NGF, nerve injuries treated with GDNF regrew nerves with larger diameters, which indicated that GDNF was more capable of promoting nerve maturation [41]. Of particular importance is the role of GDNF in delayed nerve repair. If surgical repair is not possible immediately after nerve injury, chronic axotomy may occur where neurons are no longer able to innervate their end-target organs, which yields a high probability of poor nerve regeneration. However, a study by Wood et al showed that an implantable, slow-release

GDNF delivery system via microspheres can still enhance motor nerve regeneration even after nerve repair was delayed for 1 week [42].

1.3.6 Neurotrophin-3

A study focusing on neurotrophin-3 (NT-3) showed that when rats with dorsal root ganglia (DRG) avulsions were given intrathecal NT-3, they were able to regenerate the DRG through the dorsal root entry zone into the spinal cord, which promoted functional recovery [43]. NT-3 has also shown to be effective in improving both weight and functional use of muscle fibers containing heavy myosin, implying that NT-3 is not only capable of improving motor neuron deficits, it may potentially prevent atrophy of the type 2b subset of muscles fibers [44].

1.3.7 Ciliary neurotrophic factor

Similarly, CNTF administration to a sciatic nerve injury also promoted higher functional motor recovery as well as conservation of muscle mass when compared to NGF administration alone [45], indicating that aside from survival-promoting effects, CNTF also plays a role in survival and regeneration of motor neurons [46]. Unlike other neurotrophic factors, CNTF does not seem to be involved in neuronal survival, but rather only exerts its effects after nerve injury. This hypothesis is supported by the fact that newborn animals do not express CNTF, but if exogenous CNTF is introduced, motoneurons, which are highly susceptible to retrograde cell death following axotomy, are protected from degeneration [47]. In a progressive motor neuronopathy (pmn) mouse, the mutation causes disease and degeneration of motor neurons, resulting in death by the seventh or eighth week. However, Sendtner et al found that creating a lesion in the facial

nerves dramatically decreased the level of degenerated motor nerves due to endogenous release of CNTF by Schwann cells after injury. In pmn mice lacking endogenous CNTF, this protective effect was not seen [48].

Table 1. Neurotrophins and their receptors and functions

	Receptors	**Function**
Nerve growth factor (NGF)	Trk-A (high affinity); p75/NGFR (low affinity)	Guides axon growth; regulates nerve maintenance, survival and proliferation; promotes branching and arborization
Brain-derived neurotrophic factor (BDNF)	Trk-B (high affinity); p75/NGFR (low affinity)	Increase myelin formation; promote Schwann cell cytokine production; enhances neurogenesis and neuron sprouting
Glial-cell derived neurotrophic factor (GDNF)	RET; co-receptor GFRα1	Promotes survival of sensory and motor neurons; increases nerve fiber density; promotes myelination
Neurotrophin-3 (NT-3)	Trk-C (high affinity); TrkB; p75/NGFR (low affinity)	Survival and differentiation of neurons; encourages neurogenesis and synapse formation
Ciliary neurotrophic factor (CNTF)	CNTFR; IL6R; co-receptor gp130	Survival and regeneration of motor neurons; neuroprotective

1.4 ROLE OF INFLAMMATION AND OTHER NON-NEUROTROPHINS

1.4.1 The IL-6 cytokine superfamily

Aside from the classically studied neurotrophins, the roles of other cytokines (particularly those in the IL-6 cytokine superfamily) and growth factors in peripheral nerve injury have come to light. As LIF and CNTF are both part of the IL-6 cytokine superfamily, these two molecules share very similar actions on sensory neurons. These molecules were originally termed

hematopoietic regulators for their effects on myeloid cells, but have since been identified as having a role in cholinergic differentiation [49].

A number of diverse and seemingly contradictive functions have been found for leukemia inhibitory factor (LIF). When acting upon an embryonic stem cell, LIF inhibits differentiation and maintains pluripotency. However, in the presence of myeloid leukemic cells, LIF initiates terminal differentiation, and it is for this function that the cytokine is named [50]. A study in 2003 showed that over the span of 4 months, delivery of leukemia inhibitory factor (LIF) to a 1 cm nerve gap via a conduit significantly enhanced the regenerated axon distance when compared to plain nerve conduit controls [51]. Conversely, when LIF was knocked down via LIF-specific antisense morpholinos, STAT3 activation was markedly decreased, which resulted in a severe impairment in nerve healing and axon sprouting after injury, indicating that LIF signaling plays a beneficial role in functional recovery [52].

IL-6 is a cytokine widely known for both its pro- and anti-inflammatory properties. Among its role in the inflammatory response, studies have demonstrated an extensive variety of other functions for IL-6, including enhancing proliferation, maintaining stemness of MSCs, and protection from apoptosis [53]. It has been shown to play a positive role in nerve regeneration after traumatic nerve injury *in vivo* and that in the presence of increased IL-6 and overexpression of IL-6R, axotomized nerves regenerate quicker than their wild type counterparts [54, 55]. Exogenous IL-6, when delivered to the site of injury, can increase expression of growth-associated genes such as GAP-43 and small proline rich protein 1A (SPRR1A), and can signal through the gp130 receptor to activate the Jak/STAT3 pathway to overcome the actions of axonal growth-inhibitory myelin proteins [55, 56]. Studies have shown that both Trk and gp130

receptors can activate the Jak/STAT3 pathway, which plays an integral role in axon regeneration, and the inhibition of which can severely impede axon extension length [37, 57].

Schwann cells has also been found to produce the extracellular matrix molecule, osteonectin, also known as secreted protein acidic and rich in cysteine (SPARC) or BM-40 [58]. As the name might suggest, osteonectin was originally discovered as an osteoblast secretion and promotes bone formation and initiating mineralization. It does this by binding both collagen I and hydroxyapatite crystals, and linking and depositing calcium and phosphate from surrounding solution to the non-mineralized matrix tissue [59]. More recently, it has been shown that Schwann cells are also capable of secreting osteonectin, and that it may play a synergistic role with BDNF [32] and NGF [33] in terms of promoting nerve regeneration and axon elongation. These papers showed that when the actions of BDNF and NGF were inhibited via blocking the Trk receptors, nerve growth, while lessened, was not abolished. The study found that Schwann cell conditioned medium containing osteonectin were able to partially rescue the regeneration of nerve axons when Trk receptors were pharmacologically inhibited, but when osteonectin was removed from the conditioned medium, nerve regeneration was suppressed [32, 33].

Table 2. Non-neurotrophins and their receptors and functions

	Receptors	**Functions**
Interleukin-6 (IL-6)	IL6R (CD126); gp130 coreceptor	Anti-inflammatory (myokine); mediates fever; pro-inflammatory (cytokine)
Leukemia inhibitory factor (LIF)	LIFR (CD118); gp130 coreceptor	Inhibits differentiation (embryonic stem cells); induces differentiation (myeloid leukemic cells)
Osteonectin	Unknown	Binds calcium and collagen; cell-matrix interactions; bone mineralization

1.5 MODERN SURGICAL REPAIR METHODS

Timely surgical repair after traumatic nerve injury remains the best treatment method. If the nerve is transected, a direct end-to-end repair with no tension placed on the two nerve ends gives the best chance for functional recovery. However, when a tensionless, end-to-end repair cannot be performed, the current gold standard of repair for nerve injuries with a critical gap is surgical nerve autografting, a technique developed around World War II, and in the last 50 years, only minute improvements have been made in surgical techniques [13].

1.5.1 The nerve autograft

Typically, in a nerve autograft, characteristics of the nerve must be considered. Diameter, patterning and number of fascicles, length required, cross-sectional shape and area, and patient preferences must all be taken into consideration [60]. The surgeon will harvest a section of nerve from a healthy donor site on the patient's body that is deemed less vital and graft the donor section into the primary site of injury. Some of the more commonly used donor nerve sites include the sural nerve or saphenous nerve for upper body injuries. As with direct end-to-end repair, there should be no tension placed on host or donor nerve ends, so the harvested donor nerve should be approximately 25% longer than the gap distance [60]. The drawback to this approach remains the fact that a second site of injury will result from the surgical removal of a nerve section, which may risk the donor site suffering from the same morbidities as those seen in typical nerve injuries (i.e., neuroma formation, scarring, loss of sensation or function) [61]. Though this approach is deemed the gold standard when alternative approaches are

contraindicated, only up to 40-63% of patients experience functional recovery with nerve autografts depending on time elapsed, and severity and location of injury [60].

1.5.2 Nerve transfer surgery

Nerve transfer surgeries remain an alternative option to the autograft. This technique, first described by Tuttle in 1913 [62], has been developing over the past decades with reports of positive outcomes, particularly in cases of injuries to the upper extremities (upper arm or proximal forearm) and brachial plexus reconstruction [63-65]. In these cases, the surgeon will opt to use a redundant nerve in close proximity to the injured or avulsed nerve as a donor of neurons and axons in order to reinnervate the affected organ [63]. For example, the intercostal nerve can be transferred to help repair and reconstruct both sensory and motor brachial plexus nerve injuries [64]. Multiple nerve transfers may also be required in certain circumstances. In cases where restoration of elbow flexion is necessary, the most commonly performed procedure is a double fascicular nerve transfer, where median and ulnar nerves are coapted to the musculocutaneous nerve, reinnervating the bicep [63].

1.6 STEM CELLS IN TISSUE REPAIR

While various surgical methods yield moderate success in terms of functional recovery, many studies have investigated the possibility of applying stem cells from a myriad of sources towards nerve regeneration in a cellular therapy approach.

1.6.1 Neurotrophic potential

Among the most common sources of stem cells used were those derived from muscle [5, 66], bone marrow [4, 67-70], embryonic, neural and adipose tissues. Of particular interest is the ability of these cells to produce neurotrophic factors and act as replacements for Schwann cells in the event of traumatic nerve injury. Through exposure to environmental cues, studies have shown that cells can be differentiated *in vitro* toward a more neuro-supportive phenotype that enhances the secretion of neurotrophic factors and myelinating ability. This approach commonly exposes stem cells to β-mercaptoethanol, all-trans retinoic acid, IBMX, forskolin, and neuregulin [5, 68, 71]. While many studies have reported the benefits of differentiating stem cells [70, 72-74], other studies have shown that undifferentiated stem cells can be equally effective [39, 75]. The main appeal of the use of undifferentiated stem cells comes from cutting the time needed for cell treatment and differentiation, possibly making this approach more applicable in the clinic [76]. Further arguments for using undifferentiated stem cells come from reports stating that maintaining differentiation *in vivo* is difficult once environmental cues are removed, though contradictory findings have been published in other studies that show advantages for either differentiated or undifferentiated cells, or that there is no significant difference [76]. The findings presented in this body of work agree that there does not appear to be a significant difference between undifferentiated and differentiated stem cells when it comes to neuritogenesis or axon elongation in peripheral nerve regeneration.

1.6.2 Traumatized muscle cells

While traumatized muscle stem cells have been shown to secrete neurotrophic factors and boost axon elongation, these cells fit in a rather particular niche of usage, in that they are reasonably accessible after blast trauma. This makes muscle stem cells a viable source of cells taken from debrided injury zones from musculo-skeletal trauma. Stem cells taken from these injured tissues can produce neurotrophic factors such as BDNF, NT-3 and CNTF [77], and are capable of enhancing the extension of growing axons [5]. Lavasani, et al showed that the use of non-traumatized muscle progenitor stem cells also mitigated skeletal muscle atrophy typically found with nerve injury [66].

1.6.3 Mesenchymal stem cells

Mesenchymal stem cells (MSCs) sport several advantages as a candidate for cellular therapy in nerve regeneration. Since their discovery in the 1960s [78], they have been well studied and characterized such that we now have defined a minimum criteria for MSCs [79]. The use of these cells also carries little ethical implications compared to other sources like embryonic stem cells. Studies have shown that MSCs are less immunogenic, particularly by secreting high levels of cyclooxygenase-2 (COX2), a T-cell activation inhibitor [214], which lowers the risk of rejection in allogeneic transplants [80]. Many studies have shown that MSCs are readily able to produce various neurotrophic factors as well as cytokines that have a positive effect on nerve regeneration [68, 74]. The combination of the above factors makes them a promising therapy option in the short term, and transplantation studies have shown that MSCs, whether injected locally or systemically, are capable of enhancing nerve regeneration. For example, Xia et al showed that

MSCs introduced through the femoral artery to STZ-induced diabetic rats showed improvement in restores neuropathic morphology [207]. Marconi, et al similarly showed that systemically injecting adipose-derived MSCs into mice down-regulated inflammation and improved functional recovery in acute sciatic nerve crush [75]. Systemically injected MSCs are capable of homing in to the lesion site via chemotactic signals, though this approach typically requires a large quantity of cells as a substantial portion (90%) of injected cells will collect and form emboli in the lungs [213]. Local application of MSCs via scaffolds also requires vast numbers of cells, however, MSCs can be difficult to harvest from bone marrow, and their usage and lifetime is finite as they senesce after several passages in culture, which may subject the already injured patient to further invasive and painful procedures.

1.6.4 Embryonic stem cells

Embryonic and pluripotency stem cells are attractive alternatives to the typical sources of adult stem cells. Since Thomson described their isolation method in 1998 [81], human embryonic stem cells (hESCs) have taken a center stage in regenerative medicine. As these cells can theoretically be propagated infinitely, and can potentially be differentiated into any cell type given the appropriate environmental cues, many researchers have devised methods to differentiate hESCs into MSCs [82, 83] or neural lineage cells [84, 85]. There is great potential for these cells in regenerative medicine, but working with them comes with its own set of challenges. hESCs, as their name implies, are isolated from embryos at the blastocyst stage of development, a process that destroys the embryo. This fact has embroiled the use of hESCs in research in much controversy. Differentiated hESCs, when transplanted, risk immune rejection, but a study by Rong, et al showed that a knock-in of constitutively expressed CTLA4-Ig/PD-L1 into allogenic

hESCs provided a means of localized immune protection without resorting to systemic immune suppression [86]. While this approach seems promising, genetic modification of hESCs along this particular route is questionable as it opens up the potential for tumorigenic or viral-infected hESCs to escape immune detection.

1.6.5 Induced pluripotent stem cells

The method to reprogram induced pluripotent stem cells (iPSCs) from mouse fibroblasts was first discovered and described by Yamanaka and Takahashi in 2006 [87], for which a Nobel Prize was awarded. iPSCs are adult somatic cells, such as fibroblasts, that have been reprogrammed to an ESC-like state. The significance of this discovery cannot be overstated, as the scientific community now has the potential means to replace the controversial use of human embryonic stem cells in research, as well as a versatile tool to develop *in vitro* disease models for any genetic disease from which cells may be obtained from a patient.

1.6.6 iPSC development

The traditional Yamanaka iPSC-generation method includes using retrovirus to introduce four transcription factors into adult somatic cells: *Sox2*, *Oct3/4*, *Klf4*, and *c-Myc*. However, as retroviral reprogramming relies upon inserting genetic factors into the genome, this process risks causing genetic mutation and dysfunction. It is important to note that continued exogenous or ectopic expression of these reprogramming factors can lead to dysplastic lesions [88]; it is thus critical to optimize the transient expression of these reprogramming factors. Since Yamanaka's initial discovery, other viral methods, including lentivirus and adenovirus [89], have been used to

generate iPSCs. Adenovirus is an attractive alternative to retrovirus because their use can induce transient exogenous expression of genes without integration into the genome [90]. Recently, some studies have focused on alternative, non-viral methods to generate iPSCs. These include plasma transfections, and the use of the Piggybac transposon system [91]. Nuclear transfer has also been used to generate iPSCs from mouse fibroblasts [92], as well as transfection with multi-protein expression vectors [93]. There have been multiple reports that small molecules such as GSK3-β inhibitor and ascorbic acid [94], can increase reprogramming efficiency by acting as replacements for c-Myc (GSK3-β inhibitor CHIR99021) or Klf4 (GSK3-β inhibitor kenpaullone) [95, 96].

1.6.7 iPSC characteristics

To be considered an iPSC, the generated cell must maintain several characteristics. They must be positive for expression of pluripotency stem cell markers such as Sox2, Oct3/4, SSEA3, SSEA4, TRA1-60 and TRA1-81 [91]. Histological staining of cells implanted into NOD/SCID mice must show the formation of all three germ layers (mesenchymal, ectodermal and endodermal) in the gold standard teratoma assay in order to establish the pluripotency of the generated cells [97]. Germline competence can be achieved with selection for Nanog expression, as Nanog is highly associated with pluripotency, and is a target of Oct3/4 and Sox2. Subsequently, these Nanog-expressing iPSCs can integrate into embryos and contribute to form adult chimeras [90].

1.6.8 iPSC differentiation potential

As iPSCs can theoretically be differentiated into any cell type, given the appropriate environment, they are an attractive alternative to embryonic stem cells as they pose much less of an ethical quandary. Our laboratory has explored the use of iPSCs as a possible replacement for MSCs in terms of differentiation potential, proliferation rate, and phenotypic similarity. Our study found that while MSC-parentage induced iPSC-derived mesenchymal progenitor cells (MiMPCs) were a distinct population of cells regarding expression patterns of mesenchymal and pluripotency genes, they exhibited the morphologies typical of MSCs and fibroblasts, and were still capable of osteo-, adipo-, and chondrogenesis [98].

iPSCs have also been explored as a method to model nerve cultures, particularly Schwann cell cultures. Schwann cells and neurons are difficult to isolate and culture, but as iPSCs can be differentiated into both neurons and Schwann cells [99, 100], these cells may offer a new way for researchers to study nerve regeneration and translational medicine. These cells have the potential to be powerful research tools in regenerative medicine once reliable, standard differentiation protocols are established.

1.6.9 Key differences between MSCs and iPSC-derived MSC-like cells

Recently, mesenchymal-like cells have been differentiated from iPSCs in our laboratory, termed induced mesenchymal progenitor cells (iMPCs)[98]. iMPCs were characterized in terms of their likeness to MSCs, especially concerning similarities in cell surface markers and ability to differentiate along adipogenic, osteogenic, and chondrogenic lineages. Several cell types were examined—iMPCs differentiated from iPSCs reprogrammed from amniotic epithelial cells, and

from mesenchymal cells, termed AE-iMPCs and M-iMPCs repectively. As there is currently no standard protocol to differentiate human embryonic cells or iPSCs into mesenchymal-like cells, in addition to various cell types, different methods were used to differentiate iPSCs into iMPCs. Diederichs confirmed that iMPCs shared a similar morphology as those seen in MSCs and fibroblasts, and demonstrated that iMPCs expressed many of the same cell surface markers including CD73, CD44 and CD105.

As previously stated, there is no standardized protocol to differentiate iPSCs into iMPCs, resulting in difficult and varied characterization of the iMPC cell type. Diederichs, et al, examined which method would yield an iMPCs that would most closely resemble the well-defined MSC. Various methods were used to differentiate iPSCs into iMPCs, including embryoid body generation, spontaneous differentiation, indirect coculture with MSCs, and treatment with unconditioned MSC growth medium [98].

However, there were key differences that made iMPCs a distinct cell type from MSCs. While iMPCs were capable of limited differentiation, indicating that they were indeed MSC-like, there were fundamental differences at the gene expression level regarding in vitro trilineage differentiation. MSCs also out-performed iMPCs in terms of differentiation, and as iMPCs were only partially able to differentiate in vitro, the authors concluded that iMPC cultures actually form heterogeneous populations. However, iMPCs were capable of inducing ectopic bone formation in vivo, demonstrating again that a subset of the iMPC population are MSC-like. The authors state that iMPCs are an attractive MSC-like cell type, though their utility may be limited until they can be enriched to form a more homogenous population of truly MSC-like cells [98].

1.7 SYNTHETIC AND NATURAL SCAFFOLDS

Multiple studies have shown that topographical cues can affect adhesion, growth and differentiation of various cell types. For example, Embryonic stem cells can also be cultured on nanotopographical surfaces, and under these conditions, can be differentiated along mesenchymal lineages without the typical chemical induction treatments [82]. MSCs cultured on TGF-β1-loaded aligned electrospun nanofibrous scaffolds were more apt to differentiate toward myogenic lineages than MSCs grown on tissue culture polystyrene with TGFβ1-supplemented medium [101]. Yim et al. also found that when MSCs were given a nanotopographical surface along with biochemical cues, neural markers were significantly upregulated compared to when MSCs were cultured with biochemical cues alone [102]. Neurons too, can sense and respond to nanostructures, which ultimately affect adhesion, viability and axon pathfinding [103, 104]. Studies have found that in addition to directional guidance, these topographical structures can also decrease the number of neurites and branching [105, 106] and increase the length of neurite extensions [107, 108]. As important as it is for nerves to receive biochemical support, it is of equal importance to provide a physical guide so regenerating axons do not lose their way to the end target. The longer the distance required of the neuron to regenerate, the more likely a neuroma will form due to disorientation of extending neurites.

Various materials have been investigated for their potential usage in biological scaffold nerve guides. Natural polymers and extracellular matrix scaffolds have been constructed from collagen, hyaluronic acid, agarose, chitosan and fibrin gels. However, as these materials do not afford the mechanistic strength needed, or degrade too quickly, they are often combined with synthetic polymers to improve these qualities [109, 110]. Commonly used synthetic polymers

include poly-l-lactic acid (PLLA), poly-caprolactone (PCL), poly-lactic-co-glycolic acid (PLGA) and polyglycolic acid (PGA) [222].

1.7.1 FDA regulatory requirements

The first generation of synthetic nerve scaffolds were generally made of silicone which, while inert, were nonresorbable and often caused compression injury to nerves. They also required a secondary surgery for removal [111]. Today, to be considered a candidate for use as a nerve growth conduit, the FDA has required that nerve growth conduits be able to provide mechanistic support to regrowing axons, as well as prevent fibroblastic infiltrates, retain any secreted neurotrophic factors by nerve ends and Schwann cells, but remain permeable enough to allow for the efflux of waste and influx of nutrients and sufficient oxygen [112]. These requirements mean that the ideal pore size should range from 10-25 μm to allow for diffusion of molecules, but disallow the infiltration of fibroblasts and immune cells [113]. The material should ideally be flexible enough to accommodate movement of the limb, but still retain its shape so as not to cause further damage and compression to the injured nerve [114]. Scaffolds should also be biodegradable to eliminate the need for a secondary removal surgery, but should retain structural integrity until after the injury has healed.

1.7.2 Currently available scaffolds

There are several FDA-approved nerve conduits available on the market today. Many of these scaffolds are constructed from Type I collagen, PGA and PCL. In 2001, the first two collagen type I nerve conduits, NeuroMatrix and NeuroFlex, were approved for use by the FDA. Both

conduits are flexible and fully resorbable in 4-8 months in vivo. Nutrient perfusion is made possible by pores in the 0.1-0.5um range [115]. They are ideal for bridging gaps shorter than 2.5 cm. In 2004, another collagen type I conduit was approved, NeuraWrap. This conduit was designed to prevent neuroma formation and avoid compression of the nerve, with longitudinal slits that would provide more yield and minimize encapsulation and entrapment. According to the manufacturer, the porous outer membrane would offer mechanical resistance to compression by surrounding tissues [115]. NeuroMend is another collagen type I conduit that is similar to the others in that a semipermeable membrane allows the passage of nutrients while preventing infiltration from fibroblasts and inflammatory cells, but is unique in that it can be unrolled and curled to best fit the dimensions needed for the injured nerve [115].

Neurotube and Neurolac, composed of PGA and PLCL, respectively, have also been used in the clinic. Neurotube was the first synthetic scaffold to be approved by the FDA in 1999 [115]. It has had positive findings in the clinic when used in short deficits of 3 cm or less, but generally did not seem to yield significant improvements compared to nerve graft controls [116]. Use of Neurolac has likewise seen positive results in the clinic, and as this particular conduit is transparent, it offers the added advantage of monitoring the placement and suturing of nerve endings, as well as allowing examination of whether the conduit has become occluded by a blood clot or the like [117].

Decellularized natural scaffolds can also be used as a nerve conduit. While full allografts and xenografts can induce immune reactions and potential subsequent rejection without the use of immunosuppressant drugs, decellularized scaffolds can provide the enhanced regenerative properties of basal lamina and extracellular matrix without the immunogenic components [118]. Both chemical and physical methods have been applied to decellularize scaffolds. Commonly

used physical methods include lyophilization, freezing, pressure, agitation, and sonication to disrupt cell membranes, resulting in cell lysis [119]. Chemical methods can be used with or without physical treatments. Typically, chemical methods include enzymatic digestion or treatment with alkaline or acidic solutions, detergents, and hypotonic or hypertonic solutions.

AxoGen's Avance is a commercially available decellularized scaffold which uses a proprietary method with detergents and chondroitinases to strip cells away from the extracellular matrix. In the clinic, it has been successful in treating nerve gaps up to 3 cm in length [111]. Whitlock, et al, compared the results of Avance and NeuraGen (Type I collagen) in 14 mm gaps in the clinic and found that Avance promoted nerve regeneration as much as NeuraGen and autografts, and demonstrated no significant differences 12 weeks after implantation [120]. Clinical trials also showed that Avance implants of 0.5-30 mm in length were able to restore sensation after 9 months [115].

1.7.3 Scaffolds as a delivery system for neurotrophins

Scaffolds can also be used as a delivery system for neurotrophic factors to enhance regeneration. Sun, et al created a NGF-collagen-binding-domain fusion protein that could bind to collagen, showing that NGF could be concentrated and retained at the site of injury, enhancing peripheral nerve repair [121]. Kokai, et al, also developed a PCL scaffold as a means of slow-release and diffusion of growth factors and oxygen that was dependent upon parameters such as pore size, pore percentage, and wall thickness. They found that thicker walls and higher porosity allowed for both higher oxygen diffusion as well as higher rate of growth factor retention [112].

1.7.4 Scaffold filler materials and growth substrates

Gels are a remarkably versatile substrate in which to hold additional supplemental components to encourage axon elongation. These gels can typically be incorporated into the lumen of the scaffold, so that in addition to the physical support from the scaffold, the lumen filling may also provide trophic support. Gels can incorporate molecules such as neurotrophins (NGF, CNTF, VEGF, BDNF, NT-3), hyaluronic acid, and ECM proteins (i.e. laminin, collagen, and fibrinogen) [215]. Autologous Schwann cells and bone stromal cells have been suspended in Matrigel and introduced into the lumen of conduits. Studies of molecule incorporation into gels from Williams (fibrin [217]), Madison (collagen [216]), Rosen (collagen [218]), Rich (NGF [219]), Hadlock (NGF [220]) and Hobson (VEGF [221]), all showed that incorporating their respective molecules into hydrogel or Matrigel and including the gel into the lumen of a scaffold increased axon count and myelination, improved sprouting and the rate of axon regrowth, and improved functional recovery in animal models [215].

1.7.5 *In vitro* models for peripheral nerve injury

Human samples of compressed nerve tissue are extremely difficult to come by for peripheral nerve studies. What limited quantities are available are generally isolated from the median, ulnar, tibial and radial sensory nerves [122]. Animal models therefore have great utility in this field of study, providing an avenue for researchers to introduce a nerve injury, then follow up with monitored treatment methods. *In vitro* models can also provide invaluable information as they are isolated from extraneous factors and can offer a narrower window of study to develop treatment methods and examine the effects of any pharmacological agents. As they are generally

free from ethical implications, it is highly desirable to conduct nerve studies *in vitro* prior to any animal studies if possible.

Numerous cells and cell lines exist that are commonly used in *in vitro* nerve cell studies. Among these are PC12 cells, neuronal cell line 50B11, primary Schwann cell cultures, and adult rat dissociated dorsal root ganglion neurons. Nerve cell lines can be used to study cell signaling, the effects of drugs or molecules on cells, changes in cell behaviors as a result of external influences, and the compatibility of new biomaterials.

PC12 cells are a well-established cell line commonly used in exocytosis and neural differentiation studies. They were first isolated from a rat pheochromocytoma, in the adrenal medulla, by Greene and Tischer in 1976 [123], and were later developed into a clonal cell line. PC12 cells have also been used as a model for their non-malignant counterparts, adrenal chromaffin cells, as they exhibit many similar phenotypic properties. Their popularity in research is generally because they are easily cultured, and are versatile in pharmacological studies. PC12 cells have also been useful in the investigation of the mechanism of action of neurotoxins.

PC-12 cells differentiate in response to NGF into a neuronal phenotype. Upon exposure to NGF, they stop proliferating and will extend neural processes in which small vesicles will aggregate. A study by Zerby and Ewing demonstrated that while the location of exocytosis changed with differentiation and frequency of vesicle release decreased, the levels of catecholamine contents did not [124]. Signaling through NGF contributes to neurite outgrowth via the MAP kinase/ERK pathways [125], the effects of which could be reversed when MAP kinase and ERK inhibitors were used [126]. The state of PC12 differentiation could be assessed via levels of axonal growth associated protein 43 (GAP43)—levels of GAP43 increased during differentiation, but decreased when inhibitors were introduced into cultures.

Studies have shown that upon treatment with dexamethasone, PC12 cells differentiate into neuroendocrine chromaffin-like cells. The rate of endocytosis and exocytosis, as well as excitability and calcium channel coupling, is dramatically increased when PC12 cells have been treated for 5-7 days. This discovery was beneficial in allowing research to be performed on single cell modulation of neurotransmitter release, and in seeing the effects of pharmacological or toxic agents [127].

50B11 neuronal cells are an immortalized line of embryonic rat dorsal root ganglia, generated via transfection with SV-40 T antigen [128]. Although limited in lifespan and usage, 50B11 cells provide an *in vitro* model for nociceptive neuronal studies. Due to their ease of culture and differentiation, they are well suited for high-throughput assays for phenotypic and drug screens testing for neurotoxic and neuroprotective agents [129]. In the presence of forskolin, they are able to differentiate, form neurite extensions, express neural markers, and generate action potentials. However, as 50B11 cells are only able to survive for 72 hours after differentiation, they are not used for long-term studies, i.e., in myelination studies which require over 10 days in culture [128]. Melli, et al, proposed that while 50B11 cells could be used as a starting point in high-throughput assays and screens, primary DRG cultures should be used in follow-up validation studies [130].

The use of Schwann cell lines has also led to many discoveries in nerve signaling pathways. Armstrong, et al, determined that laminin activated the NF-κB pathway by showing increased NF-κB-p65 phosphorylation localized to the nucleus. However, upon inhibition of the NF-κB pathway, the benefits of laminin was abolished and neurite extension lengths were stunted, showing that the NF-κB signaling pathway plays an integral role in activating the neurotrophic potential of Schwann cells [131]. Schwann cells have also been used to determine

the origins of neurotrophic factors and neurotransmitters. For example, while it was known that gamma-aminobutyric acid (GABA), an inhibitory neurotransmitter, was present in the peripheral nervous system, it was not always known where GABA was synthesized. Using primary isolates of Schwann cells, Magnaghi, et al showed that GABA synthetic mechanisms and enzymes were present within the Schwann cell. Additionally, they demonstrated that GABA is synthetized and localized in Schwann cells, and that allopregnanolone, a GABA-A receptor modulator, can further stimulate GABA production [132].

Dorsal root ganglia (DRGs) are structures found immediately outside the spinal column, in the intervertebral foramina, which are small openings present between each pair of vertebrae. They are primarily composed of sensory neurons which serve to innervate peripheral organs. Rat and chicken embryonic DRGs are commonly used in primary nerve cultures. As these cells are longer lived than 50B11 cells, they are ideal for myelin formation studies. These types of cells are ideal for assessing what may happen *in vivo* in peripheral nerves, as primary cultures are typically naïve cells harvested from healthy tissues. However, as harvesting primary nerves (as well as Schwann cells) requires the dissection from target organs, it is inevitable that axons will be transected, therefore making it virtually impossible to culture uninjured primary nerves or Schwann cells. For this reason, these *in vitro* models may be a good way to evaluate physiological response or treatment methods for traumatic injury to peripheral nerves, and may provide a great avenue to optimize tissue engineered constructs [133].

DRG cultures are a promising way to assess survival, visualize neurite extensions and branching, and study neuron responses to drugs. When dissociated, DRGs or spinal cords can also be used to test responses and behaviors in both sensory and motor neurons. DRGs can also be directly co-cultured together with Schwann cells to mimic *in vivo* conditions where Schwann

cells provide myelination for axons. From these cultures, it was demonstrated that Schwann cells are capable not only of producing neurotrophic factors, but also various extracellular matrix proteins that greatly improve the survival and growth of neurite extensions [133, 134]. While direct Schwann/DRG cocultures can provide valuable information regarding the interaction between the two cell types, as well as how they may respond to pharmacological agents, the fact also remains that isolating Schwann cells requires injury of a healthy nerve, and therefore are difficult to obtain and culture in sufficient numbers. Of course, as these cultures are performed *in vitro*, observations in all studies should be further validated with *in vivo* models.

Cells and cell lines have their limitations in that not all behaviors observed in culture may be applicable to a living model. For this reason, animal models are also commonly used in nerve studies, whether the aim is regeneration or disease modeling and treatment.

1.7.6 *In vivo* models of peripheral nerve injury

A number of injury models in animals are used for *in vivo* studies related to nerve regeneration, including inducing crush injuries, lacerations, and compression. Short and long term injuries have been studied, commonly using the rat sciatic nerve. Researchers typically utilize behavioral observations, nerve conduction/electromyograms, and histology to evaluate and monitor their studies.

Nerve banding is ideal for modeling chronic compression injuries, and is a technique developed by Susan Mackinnon, a leader in peripheral nerve surgery. It is performed by surgically exposing the sciatic nerve and applying constrictive tubing around the nerve to compress the diameter. Varying degrees of compression can be applied, allowing for flexibility in the study to determine effects of “tight” (diameters of 0.6 and 0.9 mm) or “loose” (diameters

of 1.1 and 1.5 mm) compressions. In her paper, Mackinnon discovered that at 1 month, rats with 0.6 and 0.9 mm compressed sciatic nerve exhibited gross signs of Wallerian degeneration, and at 3 months, nerve regeneration appeared to have occurred around the tubing [135, 136]. Meanwhile, rats in the 1.1 and 1.5 mm compression group showed very little necrosis, though some nerve swelling did occur.

Mackinnon's model was frequently used by other researchers. In his study with rats, Dellon, et al, showed that this method significantly lowered the amplitude and slowed conduction velocity, and that this effect was especially pronounced in diabetic rats, indicating that hyperglycemia made nerves particularly prone to compression injuries [137]. Gupta and Steward also used Mackinnon's model to examine the effects of compression on Schwann cells. In their studies, they used a tube with an inner diameter of 1.3 mm. In accordance with Mackinnon's observations, Gupta and Steward did not observe Wallerian degeneration with this looser compression—however, they did find that this level of compression disrupted the myelin sheath and prompted Schwann cell proliferation, particularly at the 2 and 4-week time points. Their study supports the hypothesis that Schwann cells can be induced to proliferate given mechanical stimuli [138].

The effects of ischemia have also been studied via pneumatic balloon compression. Rydevick, et al observed that 60-80 mmHg pressure was sufficient to cut off blood flow to the nerve. The study also showed that 3-7 days after acute ischemia, induced with 400 mmHg pressure over 2 hours, nerves still did not recover normal blood flow, and that the previously compressed area received slow or stagnant circulation [139]. The authors concluded that compressive injury to blood vessels decreased intraneural microcirculation, and that varying degrees of pressure can result in blood flow changes.

One disadvantage of these compression models is the introduction of foreign material into the body, which may lead to an inflammatory reaction and confound the results of the study. Thus, while these compression models are useful in studying varying degrees of injury, other models have been developed that result in a pure nerve lesion.

Crush injuries are more serious than compression, and almost always lead to Wallerian degeneration. Rat sciatic nerve is widely used to simulate this injury, generally to evaluate pain and effect on motor function. Mouse models are also valuable due to the wide variety of transgenic lines, which allow for a more detailed examination of the roles of any critical molecule in nerve regeneration [140]. Typically, nerve crush injuries are simulated via angled forceps, chilled forceps, hemostatic forceps and vascular clamps. While this model generally does not seem to offer flexibility in degree of injury, this model has proven to be consistent and reproducible, making it a valuable model for clinically relevant injuries.

Sciatic nerve is not the only nerve used in crush injury models. Burgette, et al describe a crush model that uses the intracranial facial nerves in rats [141]. Studies using this model are clinically relevant for patients undergoing microsurgery of the skull base for tumors or lesions. Disruption of facial nerves can impact the patient both psychologically and socially. While developing this model, Burgette used sham surgeries as controls and determined that the surgical procedures were safe, and that the only cause of nerve damage was the 1-minute crush to the facial nerve. Rats in the crush injury group exhibited complete facial paralysis, which included loss of blinking reflex and lack of whisker movement [141].

Partial or full nerve transections have also been utilized as a model for nerve injury and pain. This has served as a great model for examining the efficacy of surgical repair and suturing nerve ends, as well as other methods. For example, in Brushart's initial studies with rats in 1990,

he found that motor neurons will preferentially reinnervate a distal motor branch, even if there are sensory nerves mixed in, demonstrating a staggered regenerative process, and the presence of a mechanism that promotes specificity between sensory and motor nerves. It appeared that initial regeneration during the first 2 weeks post-injury, neuron regeneration was random where motoneurons projected indiscriminately to sensory and motor neurons. However, in follow up time points, the authors noticed a continuous decrease in random projections, where motoneurons increasingly matched up with distal motor branches, and collateral sensory axons were “pruned” out [142].

Further studies in by Al-Majed and Brushart, et al, showed that the application of 20 Hz of electrical stimulus accelerated the onset of motor axon regeneration, but ultimately did not increase the overall rate of regeneration. However, as the electrical impulse gave the regenerating axons a push at the beginning, the authors observed that 3 weeks of regeneration with an electrical impulse was equivalent to regeneration seen after 5-8 weeks without stimulus [143].

Repetitive motion models, while difficult and time consuming to perform, can provide an invaluable model for simulating prevalent human conditions that damage nerves such as carpal tunnel syndrome. Carpal tunnel syndrome is the most common form of work-related nerve inflammation, and causes the highest rate of lost work days, with almost half of all cases resulting in 31 days or more of work loss. It is caused by repetitive motion of the wrists and hands, leading to compression of the median nerve as it passes through the wrist by flexor tendons and interstitial fluid. It is characterized by pain, tingling and paresthesia in the fingers and hands, and may extend up the arm. This may lead to muscle weakness and functional deficiencies.

Cohort studies for carpal tunnel syndrome are time consuming and costly, and difficult to control, as repetitive motions may vary from person to person in the workplace or home. There is also no method to measure the force exerted or pressure placed on the carpal tunnel by each person in the study as they go about their daily activities. This prompted Clark et al to describe a repetitive rat model with fully described and controlled repetitive motion. The rats were placed into a chamber within a custom designed apparatus and trained to reach outside the chamber to pull on a bar for a specified time to obtain food. Over time, the authors measured significant decreases in the rats' grip strength, nerve conduction velocity, and reach rate. Macrophage infiltrates and fibrosis increased in and around the medial nerve. From this model, the authors concluded that the repetitive tasks were the cause of the exhibited elements of carpal tunnel syndrome [144].

1.8 HYPOTHESIS AND SPECIFIC AIMS

Ongoing research suggests that a multitude of stem cell sources can be used to enhance peripheral nerve regeneration. While studies have shown that iPSCs can potentially be differentiated into functioning nerves themselves, there is little literature on the utility of iPSCs promoting nerve regeneration of the patient's own nerves. Our laboratory has previously studied the characteristics of iPSC-derived MSC-like cells, termed MiMPCs, and found that while they are a distinct population of cells, they resemble MSCs in terms of cell surface markers and trilineage differentiation. Because MiMPCs are derived from iPSCs, they are virtually unlimited in terms of availably supply, and represent a unique source of cells for regenerative medicine.

However, the therapeutic potential of MiMPCs in traumatic peripheral nerve injury has yet to be evaluated.

The overarching hypothesis is that MiMPCs are capable of neurotrophic activity that can be influenced by chemical cues, and provide clinically-relevant enhancements to regeneration of peripheral nerves after trauma. The following specific aims were designed to test this hypothesis:

Specific Aim 1: Determine the optimal line of starting iPSCs and method of differentiation to yield the an MSC-like population that closely resembles a nerve lineage phenotype, and optimize medium treatment method to elicit the highest neurotrophic potential from MiMPCs.

Specific Aim 2: Determine the components of the MiMPC secretome critical for neurite extension branching and length via use of key signaling pathway inhibitors.

Specific Aim 3: Develop a nerve guide that incorporates the benefits of MiMPCs, either with conditioned medium or with cell co-culture.

The following chapters feature a detailed account of results for each specific aim.

2.0 MESENCHYMALLY-DERIVED INDUCED MESENCHYMAL PROGENITOR CELLS DERIVED FROM INDUCED PLURIPOTENT STEM CELLS MAINTAIN APPROPRIATE NEURAL MARKERS AND SECRETOME

2.1 INTRODUCTION

Using the technology described by Yamanaka and Takahashi in 2006, where mouse fibroblasts were reprogrammed using transcription factors KLF4, Oct3/4, Sox2 and c-Myc, any adult somatic cell can theoretically be induced into a pluripotent stem cell (iPSC) state, mimicking the utility of the human embryonic stem cell (hESC). Like the hESC, iPSCs can be differentiated into any cell type, given the appropriate environmental cues. The advantage of iPSCs in research lies in 1) their relative ease of acquisition, 2) the fact that they are not derived from embryos entails significantly fewer ethical implications in their use and 3) that in vitro modeling of human cells no longer required invasive procedures to acquire a particular cell type.

Mesenchymally-derived induced mesenchymal progenitor cells (MiMPCs) can potentially be indefinitely differentiated from iPSCs. Their similarities to the well-defined mesenchymal stem cell (MSC) make them an attractive alternative, as MSCs may require invasive procedures to acquire and isolate, such as bone marrow aspiration or adipose tissue biopsies.

Previous work in the laboratory has shown that MiMPCs are a heterogeneous population that contain a subpopulation positive for typical MSC markers CD105, CD73 and CD44, and negative for pluripotent markers CD45, TRA-1-60, and HLA-D/R (human leukocyte antigen-antigen D related). While capable to a lesser extent than MSCs of chondrogenic, adipogenic, and osteogenic trilineage differentiation, their neurotrophic potential has yet to be evaluated.

Epigenetic memory inherent in iPSCs is a fundamental difference between iPSCs and hESCs. This phenomenon can influence gene expression via DNA methylation, a process that results in the epigenetic modification of DNA in somatic cells. Residual DNA methylation can remain even after reprogramming. The possibility of epigenetic memory playing a role was taken into consideration during this previous characterization work. Deiderich's study was designed using iPSCs derived from amniotic epithelial cells (AEiPSCs) similarly differentiated toward induced mesenchymal progenitor cells (AEiMPCS) as controls. The results showed no significant difference between MiMPCs and AEiMPCs, indicating that epigenetic memory did not play a role as far as MSC-likeness.

As no previous work had been done with MiMPCs in a nerve regenerative capacity, the question remained if the source of the parental cell for the iPSCs was critical for performance in a neurotrophin supportive manner. The results presented below showed that MiMPCs differentiated from iPSCs derived from MSCs were much more adept than AEiMPCs at producing BDNF, and thus, we selected MiMPCs for further characterization in terms of neuroinduction and comparison to Schwann cells.

2.2 METHODS

2.2.1 Culturing feeder-free induced pluripotent stem cells (iPSCs) in mTeSR medium

Two lines of induced pluripotent stem cells (iPSC) were piloted in this study—the first were reprogrammed from human amniotic epithelial cells, and was a generous gift from Dr. Gerald Schatten's laboratory at the University of Pittsburgh. The second iPSC line tested was reprogrammed via lentivirus from human bone marrow mesenchymal stem cells (MSCs) by University of Pittsburgh's Stem Cell Core.

Preparing iPSC culture substrate. Feeder-free iPSC were cultured on Matrigel coated 6-well tissue culture plates (all from Corning Incorporated, Corning, NY). Plates were coated only 1 day prior to, or immediately before use and never allowed to dry. To coat the plates, Matrigel was thawed on ice before use. The tube containing Matrigel aliquot remained sterile and stayed on ice for the duration of the coating process. A tube of sterile DMEM (Thermofisher, Waltham, MA) was cooled on ice. Once thawed, Matrigel was mixed into the cold DMEM at a concentration of 11.6 µl of Matrigel per 1 ml of DMEM. 1 ml of Matrigel/DMEM mix was used per well to coat wells in a 6-well plate. The Matrigel/DMEM mix was allowed to coat the plate for 1-2 hours at room temperature, or overnight at 4˚C. Prior to seeding cells, Matrigel/DMEM coating mix was aspirated and immediately replaced with warmed mTeSR medium (Stemcell Technologies, Vancouver, Canada).

Thawing and culturing iPSCs. iPSCs were thawed, washed with DMEM, centrifuged at 1.0g for 5 minutes, and gently pipetted with large-bore pipette tips for tissue culture. One vial of frozen cells was thawed and plated per well for a 6-well plate. Culture medium used was mTeSR1 (Stemcell Technologies), which was prepared according to manufacturer's instructions

and supplemented with 1x penicillin-streptomycin/fungizome (PSF; Thermofisher), and changed daily.

Undifferentiated iPSC culture maintenance. Even with all precautions taken, spontaneous differentiation of iPSCs can still occur, determined by morphological changes. Undifferentiated iPSCs are typically small in size and grow in tight-knit colonies with a clearly defined edge. Once differentiated, cells generally appear enlarged and spread out across the culture growth surface. To maintain an undifferentiated iPSC population in culture, these cells must be removed via manual dissection under a microscope in sterile conditions. A sterile, flame-drawn glass Pasteur pipette was used as a tool for manual removal of these cells.

Passaging iPSC cultures. Confluence of iPSC colonies was determined by morphological observation with phase contrast microscopy using an Olympus CKX41 microscope (Olympus Corporation, Shinjuku, Tokyo, Japan). As iPSCs did not grow in monolayer, the size and apparent depth of the colony was used to gauge confluency. Colonies were deemed confluent when the centers of the colony became more refractive, taking on a brighter, "shiny" appearance under the microscope, indicating a change in depth, and thus, a change in the thickness of the colony. iPSCs were passaged enzymatically, with 1 mg/ml Dispase (Stemcell Technologies) for 7 minutes at 37° C.

iPSCs must be washed with 1x phosphate buffered saline (PBS; ThermoFisher) before Dispase could be applied. 1 ml of Dispase was added per well in a 6-well plate and allowed to incubate at 37˚C for 7 minutes. After gently washing with 1xPBS, mTeSR medium was added to the well and a cell lifter (Corning Incorporated) was used to scrape colonies into suspension. Cells were pipetted gently with large-bore pipette to break up colonies and centrifuged at 1 g for 5 minutes before evenly distributed into fresh Matrigel-coated wells.

2.2.2 Differentiation of amniotic epithelial- and mesenchymal- parentage iPSCs

Two different methods of iPSC differentiation were used: embryoid body (EB) formation, or treatment with mesenchymal growth medium (MGM).

To form embryoid bodies, iPSCs were first grown to confluent colonies in mTeSR medium (Stemcell Technologies) supplemented with 1x penicillin-streptomycin-fungizone (PSF; ThermoFisher). Once confluent, colonies were enzymatically digested with 1 mg/ml Dispase (Stemcell Technologies) for 7 minutes at 37°C. Cells were then washed with 1x PBS (ThermoFisher), and manually scraped off the plate with a cell lifter (Corning Incorporated, Corning, NY). Aggregated cell colonies were placed into suspension culture in non-tissue culture treated plates (Corning Incorporated) and cultured with EB medium (Dulbecco's modified Eagle's medium [DMEM], 20% KnockOut serum replacement, 2 mM L-glutamine, 1x MEM non-essential amino acid solution [all from ThermoFisher], and 0.1 mM β-mercaptoethanol [BME; Sigma-Aldrich, St. Louis, MO]).

Six-well plates are coated with gelatin (Stemcell Technologies) for 20 minutes. EBs were grown for 3 days, then collected and transferred to the gelatin-coated plates with MSC-differentiation medium (DMEM, 10% fetal bovine serum [FBS; ThermoFisher], 2 mM L-glutamine, 1 μM all-trans retinoic acid [RA; Sigma-Aldrich], and 1x PSF) for another 8 days. After 8 days, EB outgrowths were trypsinized and filtered through a 40 μm mesh. Cells were collected and plated onto gelatin-coated tissue culture plastic (TCP) with DMEM and 5% FBS, and incubated at 37° C for 1 hour. Cells were washed twice with 1x PBS and the remaining adherent cells were cultured in normal MSC growth medium (αMEM, 10% FBS, 1x PSF [all from ThermoFisher], and 1 ng/ml basic fibroblast growth factor [FGF2; RayBiotech, Norcross, GA]).

Treatment with mesenchymal growth medium (MGM) was as follows: when iPSC cultures were confluent and ready for differentiation, mTeSR medium was aspirated, cells were washed with 1xPBS, and then medium was replaced with fresh mesenchymal stem cell (MSC) growth medium (minimum essential medium α [α-MEM; ThermoFisher], 10% FBS, 1 ng/ml FGF2, 1xPSF). They were incubated for 7 days with one intermittent medium change. MiMPCs were trypsinized and seeded onto gelatin-coated flasks. Cells were passaged and expanded following conventional methods for MSCs.

2.2.3 Neuroinductive treatment of MiMPCs and MSCs

MiMPCs and control MSCs were plated at approximately 3,000 cells/cm^2 on gelatin-coated flasks and maintained in MSC GM until the cultures reached 70% confluency. To develop optimal neuroinductive treatment of MiMPCs and MSCs, three different protocols were assessed.

Each of the following treatment protocols was preceded by this pre-treatment method: For the first 24 hours of the neurotrophic induction, cells were cultured with αMEM supplemented with 10% FBS, 1x PSF (all from ThermoFisher), and 1 mM β-mercaptoethanol (BME; Sigma-Aldrich). The following 48 hours of pre-treatment included all of the aforementioned reagents, and 35 ng/ml retinoic acid (RA; Sigma-Aldrich).

For 7 days following pre-treatment, MiMPCs and control MSCs were treated with neurotrophic induction medium (NIM), consisting of Dulbecco's MEM (DMEM)/Ham's F-12 medium (ThermoFisher) supplemented with 5% FBS, 0.5 mM 3-isobutyl-1-methylxanthine (IBMX; Sigma-Aldrich), 10 uM forskolin (Sigma-Aldrich), 20 ng/ml epidermal growth factor (EGF; Peprotech, Rocky Hill, NJ), 5 ng/ml platelet derived growth factor (PDGF; Peprotech), 50

ng/ml recombinant human neuregulin-beta 1/heregulin 1-beta EGF domain (hNRG1; R&D Systems, Minneapolis, MN), 10 ng/ml FGF2, 6 μg/ml RA, 10 ng/ml IL-1β and 2% v/v B-27 Supplement (ThermoFisher). The MiMPCs and MSCs remained in NIM medium for 7 days, with one intermittent medium change after 3 days in culture

Table 3. Neuroinductive medium treatment protocol

Name	Steps	Reagents
Pre-treatment	24 hours	αMEM, 10% FBS, 1mM BME, PSF
	48 hours	αMEM, 10% FBS, 1mM BME, PSF, 35 ng/ml RA
NIM	Days 0-3 Days 4-7	DMEM/F12, 5% FBS, PSF, 0.5 mM IBMX, 10 uM forskolin 20 ng/ml EGF, 5 ng/ml PDGF, 50 ng/ml hNRG1, 10 ng/ml FGF2, 6 ug/ml RA, 10 ng/ml IL-1β, B-27 supplement

Table 3 illustrates the neurotrophic induction treatment method used here, indicating protocol timeline and regents used. Henceforth, all references to NIM will refer to the medium described in the above protocol, and all NI- notations will refer to cells that have been treated with NIM. All GM- notations will refer to control cells cultured in growth medium that did not receive treatment.

2.2.4 Collecting conditioned medium from MiMPCs and MSCs

After the 7-day induction in NIM, the MiMPCs and MSCs were cultured in a basal medium (DMEM-F12, 5% FBS, insulin-transferrin-selenium-X [ITS-X], pen-strep; all reagents obtained

from ThermoFisher) for 48 hours, at which point the medium samples were collected, filtered, and designated as 48-hour basal conditioned medium (48hr BCM) for use in DRG co-culture experiments (see below). As a control, media conditioned by uninduced MiMPCs and MSCs were designated as (48hr BCM).

2.2.5 Detection of BDNF production from MiMPCs and MSCs

Pre-treatment medium was aspirated and discarded. Conditioned medium (CM) was collected during each medium exchange during the NIM treatment period—The CM from the first NIM medium exchange was labeled as “Day 3” upon collection, and the final NIM medium exchange was labeled as “Day 7” upon collection. 48hr BCM was also collected from cells. These conditioned media were assayed for BDNF production using ELISA kits against BDNF (R&D Systems). Each ELISA was performed according to manufacturer’s instructions, using Costar 96-well EIA/RIA, high binding, flat bottom plates (Corning Incorporated).

2.2.6 Cell marker characterization with immunocytochemistry

The culture medium was aspirated from the MiMPC, MSC, and Schwann cell control cultures (cell line sFN92.6, obtained from ATCC, Manassas, VA), and cells were washed with phosphate buffered saline (PBS; ThermoFisher). Cells were fixed with 4% paraformaldehyde (Electron Microscopy Sciences, Hatfield, PA) for 20 minutes, washed, and treated for 1 hour with hot 10 mM sodium citrate (Sigma-Aldrich) in 10% ethanol for antigen retrieval. After blocking with 5% FBS for at least 1 hour at room temperature, the cultures were incubated with primary antibodies for at least 4 hours at room temperature, or overnight at 4°C.

Immunofluorescence was carried out to localize the following cell markers on MiMPC, MSC, and Schwann cell cultures both before and after neurotrophic induction treatment: Schwann markers – GFAP (chicken IgY; cat. ab4674), P75/NGFR (rabbit IgG; cat. ab8874), S100B (rabbit monoclonal IgG; cat. ab52642); pluripotency markers - Sox2 (rabbit IgG; cat. ab97959), SSEA4 (mouse IgG; cat. 560307), and Oct3/4 (mouse IgG; cat. 560308); and MSC markers - CD44 (mouse monoclonal IgG; cat. MAB7045), CD73 (mouse monoclonal IgG; cat. ab81720) and CD105 (goat IgG; cat. AF1097). Primary antibodies were diluted in block buffer per manufacturer's instructions. Samples were incubated with secondary antibodies, diluted in block buffer per manufacturer's instructions, for 1 hour at room temperature. All cells were nuclear-counterstained with 4',6-diamidino-2'-phenylindole dihydrochloride (DAPI; ThermoFisher) for approximately 1 minute. SSEA4 and Oct3/4 antibodies were obtained from BD Biosciences, Franklin Lakes, NJ. CD44 and CD105 antibodies were obtained from R&D Systems. All other antibodies were purchased from Abcam (Cambridge, MA). Secondary antibodies used were AlexaFluor 488 conjugates from ThermoFisher (rabbit anti-goat IgG [cat. A27012], goat anti-mouse IgG [A10680], goat anti-chicken IgY [A11039], donkey anti-rabbit IgG [A21206]).

2.2.7 Gene expression analysis with real time RT-PCR

RNA was isolated from induced MiMPCs using RNeasy Plus Mini Kit (Qiagen, Valencia, CA) according to manufacturer's protocol. cDNA was synthesized using Invitrogen's SuperScript III First-Strand kit (ThermoFisher). Real time RT-PCR was performed using SYBR Green PCR Master Mix from Life Technologies (ThermoFisher) and a StepOnePlus Real Time PCR machine (ThermoFisher). All gene expression levels were normalized to that of 18S rRNA as the control housekeeping gene. Primers for BDNF, GDNF, CNTF, and 18S rRNA were

obtained from Qiagen, and the primer for NGF was obtained from Integrated DNA Technologies (Coralville, IA).

RT^2 Profiler PCR Arrays (Qiagen) were used to assay for expression of human neurotrophins and receptors, and inflammatory cytokines and receptors. Arrays were run using RT^2 SYBR Green ROX qPCR Mastermix (Qiagen) as per manufacturer's protocols. PCR data analysis and heat map generation was done via Qiagen's online RT^2 Profiler PCR Array Data Analysis (version 3.5; http://pcrdataanalysis.sabiosciences.com/pcr/arrayanalysis.php).

2.2.8 Statistical analysis

At least three independent experiments were conducted with three replicate samples per set of conditions were performed for each assay. All quantitative data are presented as a mean ± standard deviation. Significance of results was determined via Student's T-test, or Tukey's post-hoc analysis as appropriate. All statistical analysis was performed in Microsoft Excel.

2.3 RESULTS

2.3.1 BDNF production by MiMPCs differentiated from iPSCs

To determine the most advantageous parental-lineage of iPSCs and differentiation method toward a mesenchymal-like cell type that would yield the highest production of BDNF, MiMPCs and AEiMPCs were differentiated using either the mesenchymal growth medium (MGM) or embryoid body formation (EB) methods, as outlined above. Upon completing NIM treatment,

Day 7 conditioned medium (CM) was collected from each group, and BDNF production was confirmed with sandwich ELISAs as previously described.

Day 7 CM showed that BDNF production, measured in pg/ml BDNF produced per 10^6 cells, was highest in neurotrophically induced MiMPCs (NI-MiMPCs) generated via the MGM method (Figure 3A). BDNF levels from NI-MiMPCs were significantly higher than those seen in any group of AEiMPCs generated using either the MGM or EB methods.

From these results seen in Figure 3A, we concluded that MiMPCs were significantly superior to AEiMPCs in terms of neurotrophic support, so all the following characterizations and studies in this and subsequent chapters utilize MiMPCs differentiated from iPSCs of mesenchymal parentage.

2.3.2 Progression of BDNF production by MiMPCs over time

Figure 3B shows ELISAs against BDNF that are focused more closely on the secretory pattern of MiMPCs. Cells were neurotrophically induced, and conditioned medium from Days 3 and 7, and 48-hour basal conditioned medium (48hr BCM) were assayed for BDNF production. BDNF production by MiMPCs was enhanced with NIM treatment. Conditioned medium assayed by ELISA during and after the induction period showed a consistent increase in BDNF concentrations compared to growth controls. The most marked increase in BDNF production by MiMPCs occurred at day 7 ($p<0.05$), with an approximately 5-fold increase in BDNF levels compared to GM-MiMPCs. Although this enhanced production of BDNF tapered off after the inductive medium was removed, conditioned medium collected 48-hours after induction still showed a 2-fold increase in BDNF concentration. While MSCs also showed a significant increase in BDNF production at Day 7 ($p<0.05$), the concentration was well below the levels

detected in the MiMPC conditioned medium. The significant increase in BDNF production did not persist in conditioned medium taken from either MiMPCs or MSCs 48-hours after induction (48hr BCM).

2.3.3 Morphological comparison of MiMPCs to MSCs

Phase contrast microscopy showed that iPSCs grew in feeder-free colonies of small, undifferentiated cells (Figure 4A), and were able to differentiate into MiMPCs that exhibited an MSC/fibroblastic morphology (Figure 4B) comparable to control MSCs (Figure 4C). All microscopy fields shown in Figure 4 are representative of the cultures.

2.3.4 MiMPCs express the same cell surface markers as MSCs and Schwann cells

As previously stated, MiMPCs (induced mesenchymal progenitor cells derived from mesenchymal-lineage iPSCs using the MGM differentiation method) were chosen for all subsequent experiments. Through their usage and numerous passages, iPSCs retained expression of pluripotent markers SSEA4, Oct3/4 and Sox2 (Figures 5A). We further characterized the MiMPCs for neuronal lineage, as earlier work had only characterized these cells in terms of MSC tri-lineage differentiation and MSC-likeness (Figures 5B and 6).

First, we showed the transition of surface markers from pluripotency to MSC and Schwann markers. Feeder-free iPSCs were grown to confluency and differentiated into MiMPCs. On the third day of the differentiation period, a group of MiMPCs were set aside, paraformaldehyde-fixed and stained for mesenchymal (CD44, CD105 and CD73), Schwann (GFAP, S100B and p75/NGFR), and pluripotent markers (SSEA4, Oct3/4 and Sox2). On day 3,

it was shown that MiMPCs expressed mesenchymal markers CD44 and CD105, but was only weakly positive for CD73. MiMPCs were positive for all Schwann cell markers, and were positive for Sox2, faintly positive for Oct3/4, and negative for SSEA4 (Figure 5B). This gave us reason to extend the differentiation period in the protocol out to 7 days total, in order to give the cells more time to fully differentiate into a mesenchymal-like cell. With a 7-day differentiation protocol, cells were strongly positive for all mesenchymal markers, and negative for all pluripotent markers (Figure 6).

These cells have been shown to be a distinct population of cells that express mesenchymal cell markers, such as CD44, CD73 and CD105, and are capable of behaving similarly to MSCs in that they can be differentiated along osteogenic, as well as adipogenic and chondrogenic lineages [98]. Immunohistochemistry also showed that MiMPCs, like MSCs and Schwann cell controls, expressed mesenchymal markers (CD44, CD105 and CD73) and neurologically relevant cell markers (GFAP, S100B and p75-NGFR), the expression of which was not affected upon neuroinductive treatment (NI-MiMPCs and NI-MSCs). Similarly, non-induced MiMPCs and MSCs grown in growth medium (GM-MiMPCs and GM-MSCs) were also positive for mesenchymal and Schwann cell markers (Figure 6).

2.3.5 Changes in gene expression after neurotrophic induction

Analysis of gene expression using PCR array panels for neurotrophins and inflammatory cytokines showed an upregulation in genes relevant to nerve regeneration, including IL-6, LIF, IL-1B, and osteopontin (SPP1) in NI-MiMPCs, compared to GM-MiMPCs and to MSC groups (Figure 7). ELISA results confirmed that the upregulated genes correlated with increased,

corresponding protein levels in cell culture supernatant. We did not conduct an ELISA to detect IL-1β, as 10 ng/ml of IL-1β was included in the neuroinductive medium.

As there is only approximately a 40% correlation between mRNA upregulation and protein production [145-147], we used ELISAs to confirm the production of each of the aforementioned factors.

2.3.6 Production of non-neurotrophins by MiMPCs after neurotrophic induction

Our previous ELISA data show that under normal growth medium conditions, control MSCs produced low levels of BDNF. Following neurotrophic induction, NI-MSCs produced significantly higher levels of BDNF. Although MiMPCs exhibited many of the same characteristics seen in MSCs, our results showed that GM-MiMPCs were able to produce small amounts of BDNF; in fact, BDNF production levels from GM-MiMPCs were comparable to those seen from induced MSCs. However, our ELISAs detected significantly higher BDNF production from MiMPCs after treatment with NI medium (Figure 3).

Other cytokines have previously been shown to improve nerve regeneration after injury, among them IL-6 [54, 55], LIF [51, 148], osteopontin, clusterin [149], and osteonectin [32, 33, 58]. Interestingly, the cytokine ELISA results on medium samples conditioned by NI-MiMPCs and NI-MSCs also demonstrated marked increases in the concentration of these factors (Figure 8).

We assayed conditioned medium collected at days 3 and 7 of the NI medium treatment, as well as basal medium conditioned for 48-hours after the NIM treatment period was over. The ELISA data in Figure 8 show that IL-6 and osteonectin production remained relatively constant throughout and after the induction period (Figure 8A, C and E), but there was a significant

decrease in osteopontin and LIF production during and after the NIM treatment period (Figure 8B and D). Since osteopontin and LIF concentration levels were low in the NI-MiMPC conditioned basal medium, we focused on BDNF, IL-6 and osteonectin for the set of experiments investigating the effects of MiMPCs and MSCs of neurite extension in DRG cultures in the following chapter.

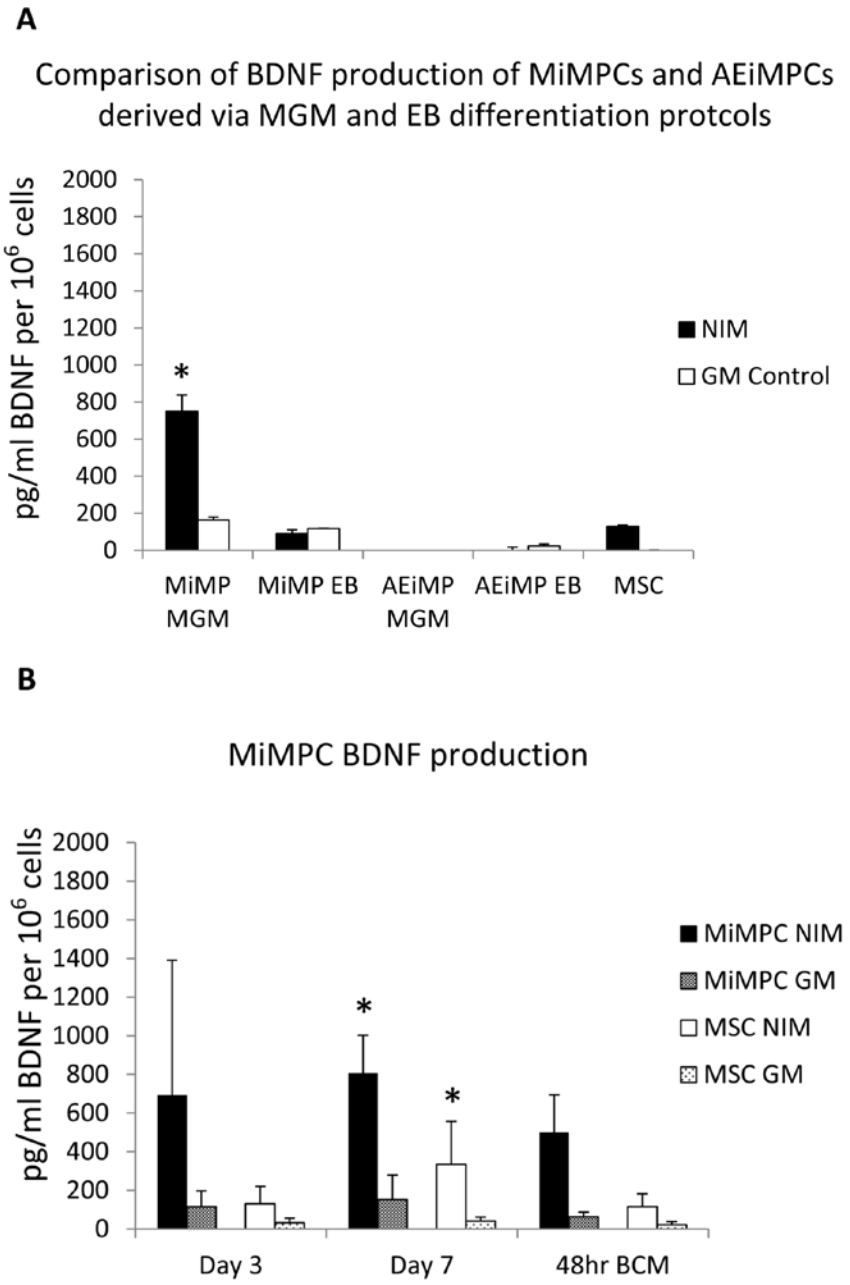

Figure 3. Production of BDNF by NI- MiMPCs, AEiMPCs, and MSCs quantified by ELISAs

(A) Comparison of conditioned medium taken from Day 7 of induction cultures from MiMPCs and AEiMPCs, differentiated via the mesenchymal growth medium method (MGM), or embryoid body formation method (EB). Neurotrophically induced MiMPCs (NI-MiMPCs) differentiated from iPSCs via the mesenchymal growth medium (MGM) treatment method showed significantly enhanced ($p<0.05$) BDNF production compared to all other groups. **(B)** Conditioned neuroinductive media taken from days 3 and 7 of induction culture, and conditioned basal medium taken from cultures 48 hours post-induction (48hr BCM), were assayed for levels of BDNF. Groups marked with a * indicate a significant difference ($P<0.05$) compared to growth medium control (GM) groups. All ELISAs are expressed in pg/mls produced per million cells.

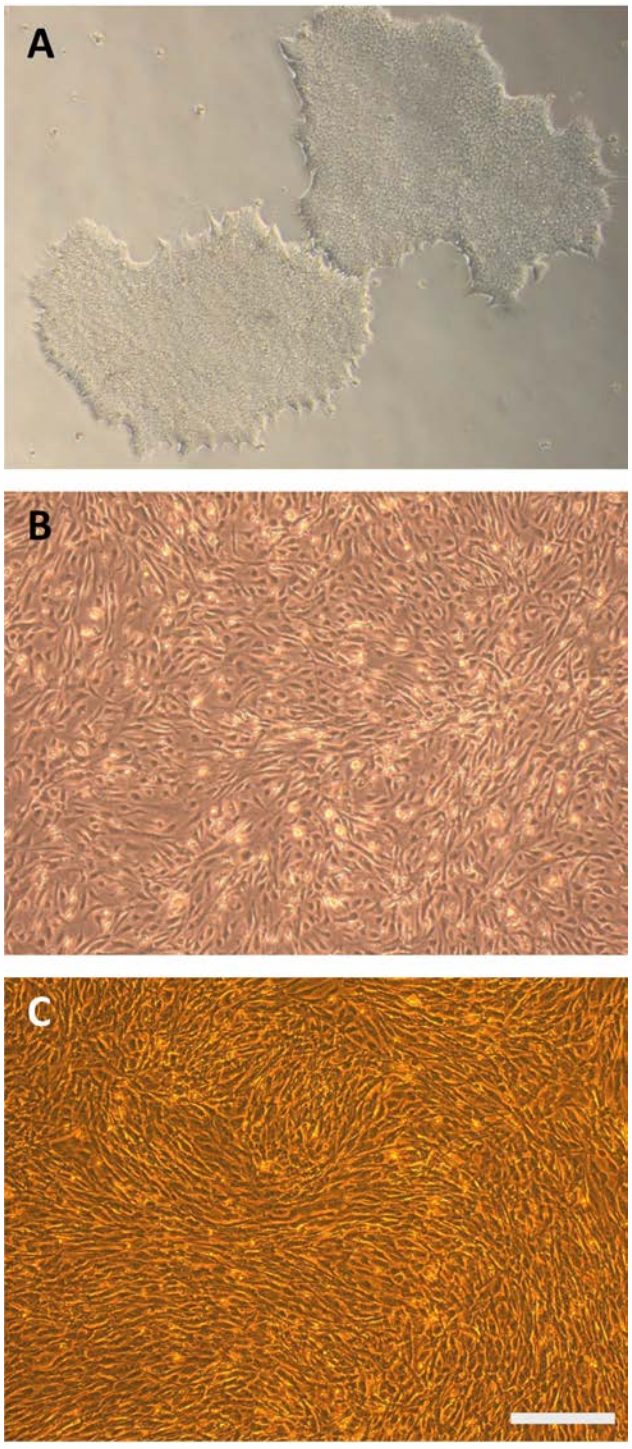

Figure 4. Morphology of MiMPCs and MSCs examined by phase contrast microscopy
(A) Undifferentiated colonies of human iPSCs reprogrammed from human bone marrow MSCs [98]. Cells grew to confluent colonies on Matrigel, in feeder-free culture. **(B)** Confluent MiMPC cultures differentiated from iPSCs. All MiMPC cultures resembled MSCs in morphology, with no remaining iPSC morphology. **(C)** Confluent control MSCs isolated from human bone marrow (passage 5). Images taken at 4x. Bar = 560 µm.

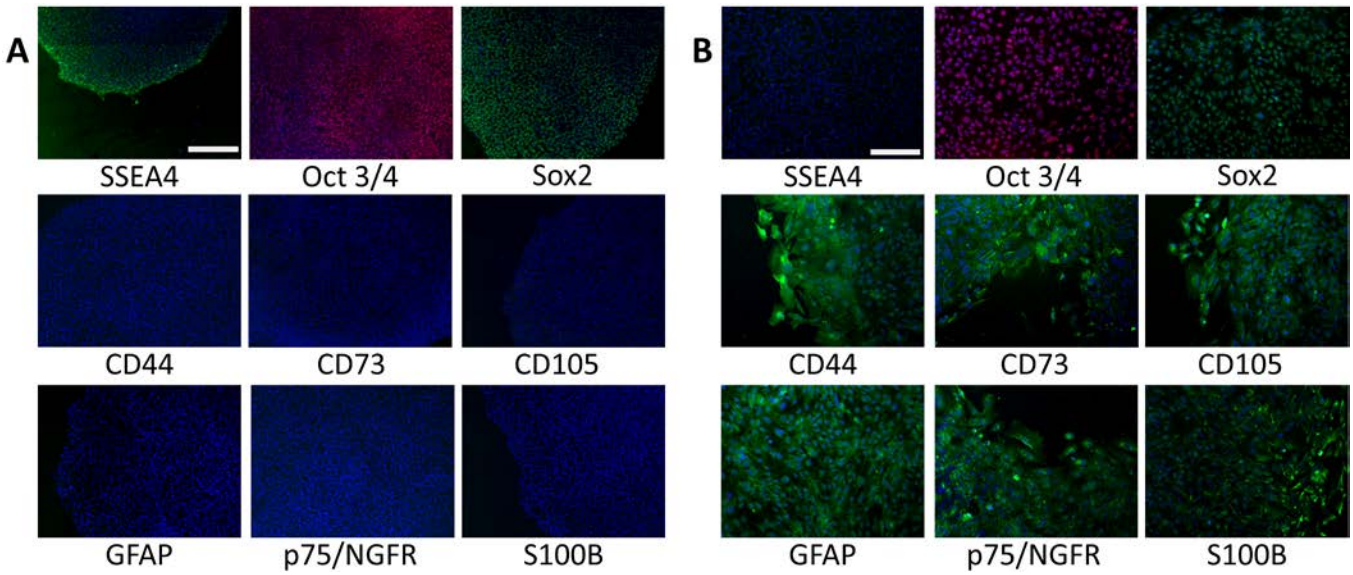

Figure 5: Expression of various stem cell markers during conversion of iPSCs to MiMPCs detected by immunofluorescence

MiMPCs were fixed and immunofluorescently stained on the third day of differentiation; colonies of confluent iPSCs served as controls. Cells were stained for MSC markers (CD44, CD73, and CD105), Schwann cell markers (GFAP, p75/NGFR, and S100B), and pluripotent stem cells markers (Sox2, SSEA4, and Oct3/4). All cells were counterstained with DAPI. **(A)** iPSCs were negative for MSC and Schwann cell markers, but stained positively for pluripotent markers, indicating the maintenance of stemness throughout culture and passaging. **(B)** MiMPCs cells were strongly positive for CD44 and CD105, and weakly positive for CD73. MiMPCs also stained positive for all Schwann cell markers, positive for Sox2, weakly positive for Oct3/4, and negative for SSEA4, showing their transition and demonstrating the need for long differentiation period. All cells were imaged at 10x magnification. Bar = 220 µm.

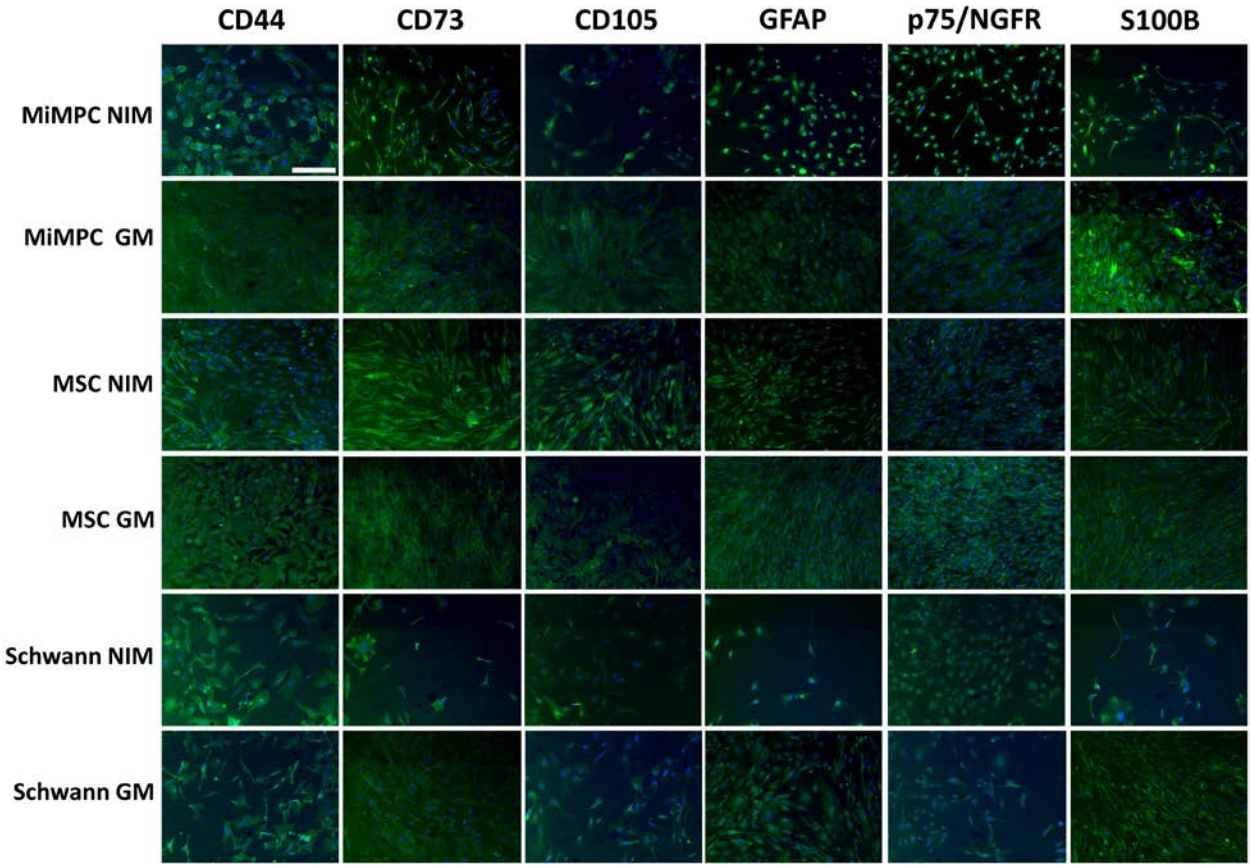

Figure 6: Expression of neurological and mesenchymal cell markers in MiMPCs and MSCs during neurotrophic induction examined by immunofluorescence

MiMPCs and MSCs were cultured in neurotrophic induction medium (NIM) or growth medium (GM). Neurotrophically induced MiMPCs and MSCs were fixed and stained with antibodies against MSC markers (CD44, CD73, CD105) and Schwann cell markers (GFAP, p75/NGFR, and S100B). Neurotrophically induced and non-induced MiMPC and MSC cultures stained positive for all MSC and Schwann cell markers. Schwann cells were stained as a control, and were positive for all markers. All cells were counterstained with DAPI. All images were taken at 10x magnification and are representative of all fields. Bar = 220 µm.

(A) Changes in human neurotrophins and receptor genes in NI-MiMPCs

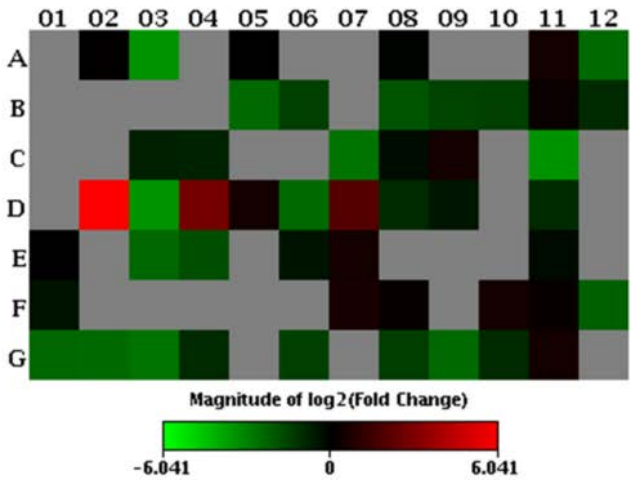

Layout	1	2	3	4	5	6	7	8	9	10	11	12
A	ADCYAP1R1	ARTN	BAX	BCL2	BDNF	CBLN1	CCKAR	CD40	CNTF	CNTFR	CRH	CRHBP
	1.42	1.03	-11.39	1.42	1.01	1.42	1.42	-1.06	1.42	1.42	1.37	-5.64
B	CRHR1	CRHR2	CX3CR1	CXCR4	FAS	FGF2	FGF9	FGFR1	FOS	FRS2	FRS3	FUS
	1.42	1.42	1.42	1.42	-5.69	-2.85	1.42	-3.98	-3.02	-2.82	1.16	-1.99
C	GALR1	GALR2	GDNF	GFRA1	GFRA2	GFRA3	GMFB	GMFG	GRPR	HCRT	HSPB1	IL10
	1.42	1.42	-1.7	-1.77	1.42	1.42	-6.67	-1.23	1.37	1.42	-11.28	1.42
D	IL10RA	IL1B	IL1R1	IL6	IL6R	IL6ST	LIF	LIFR	MAGED1	MC2R	MEF2C	MT3
	1.42	65.86	-11.28	6.76	1.37	-5.73	4.01	-1.99	-1.41	1.42	-1.97	1.42
E	MYC	NELL1	NF1	NGF	NGFR	NGFRAP1	NPFF	NPFFR2	NPY	NPY1R	NPY2R	NR1I2
	1.01	1.42	-5.57	-3.55	1.42	-1.4	1.39	1.42	1.42	1.42	-1.18	1.42
F	NRG1	NRG2	NRG4	NTF3	NTF4	NTRK1	NTRK2	NTSR1	PNOC	NPY4R	PSPN	PTGER2
	-1.37	1.42	1.42	1.42	1.42	1.42	1.48	1.16	1.42	1.4	1.14	-4.77
G	STAT1	STAT2	STAT3	STAT4	TACR1	TFG	TGFA	TGFB1	TP53	TRO	UCN	VGF
	-5.53	-5.77	-6.7	-1.97	1.42	-2.81	1.42	-2.8	-5.64	-2.01	1.37	1.42

(B) Changes in inflammatory cytokines and receptor genes in NI-MiMPCs

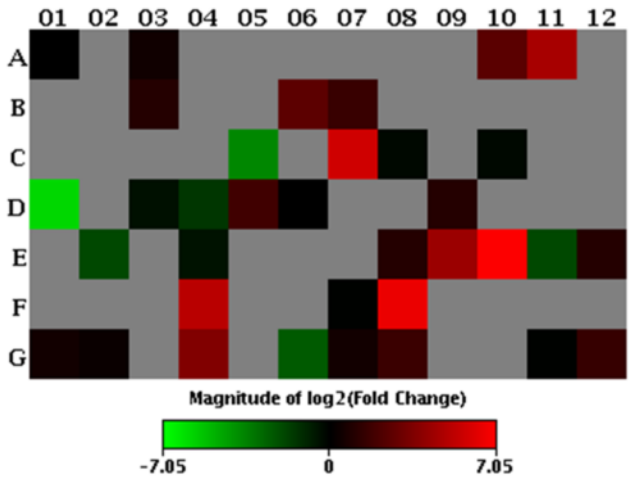

Layout	1	2	3	4	5	6	7	8	9	10	11	12
A	AIMP1	BMP2	C5	CCL1	CCL11	CCL13	CCL15	CCL16	CCL17	CCL2	CCL20	CCL22
	1.01	2.02	1.34	2.02	2.02	2.02	2.02	2.02	2.02	5.7	24.6	2.02
B	CCL23	CCL24	CCL26	CCL3	CCL4	CCL5	CCL7	CCL8	CCR1	CCR2	CCR3	CCR4
	2.02	2.02	2	2.02	2.02	5.86	2.97	2.02	2.02	2.02	2.02	2.02
C	CCR5	CCR6	CCR8	CD40LG	CSF1	CSF2	CSF3	CX3CL1	CX3CR1	CXCL1	CXCL10	CXCL11
	2.02	2.02	2.02	2.02	-13.36	2.02	54.54	-1.17	2.02	-1.17	2.02	2.02
D	CXCL12	CXCL13	CXCL2	CXCL3	CXCL5	CXCL6	CXCL9	CXCR1	CXCR2	FASLG	IFNA2	IFNG
	-63.47	2.02	-1.38	-2.81	3.45	1.01	2.02	2.02	1.96	2.02	2.02	2.02
E	IL10RA	IL10RB	IL13	IL15	IL16	IL17A	IL17C	IL17F	IL1A	IL1B	IL1R1	IL1RN
	2.02	-4	2.02	-1.4	2.02	2.02	2.02	1.99	20.07	132.49	-3.97	1.96
F	IL21	IL27	IL3	IL33	IL5	IL5RA	IL7	CXCL8	IL9	IL9R	LTA	LTB
	2.02	2.02	2.02	34.7	2.02	2.02	-1.03	90.64	2.02	2.02	2.02	2.02
G	MIF	NAMPT	OSM	SPP1	TNF	TNFRSF11B	TNFSF10	TNFSF11	TNFSF13	TNFSF13B	TNFSF4	VEGFA
	1.43	1.21	2.02	11.86	2.02	-5.59	1.39	3.07	2.02	2.02	-1.05	2.84

Figure 7: Heat maps of PCR gene expression assay analysis of NI-MiMPCs
MiMPCs and MSCs were cultured in neurotrophic induction medium (NIM) or growth medium (GM). PCR arrays targeting **(A)** human neurotrophins and receptor genes; and **(B)** human inflammatory cytokines and receptor genes were performed and heat maps were generated using Qiagen's online RT2 Profiler PCR Array Data Analysis tool (version 3.5). For both heat maps, mRNA levels in NI-MiMPCs were normalized against GM-MiMPCs and GM-MSCs control groups. Among the neurotrophins and receptor genes **(A)**, upregulation was detected in mRNA levels of IL-1B, IL-6 and LIF, with fold changes of 65.86, 6.76, and 4.01, respectively. Among the inflammatory cytokines and receptor genes **(B)**, upregulation in mRNA levels was detected for genes relevant to nerve regeneration, including a 11.86 fold increase in SPP1.

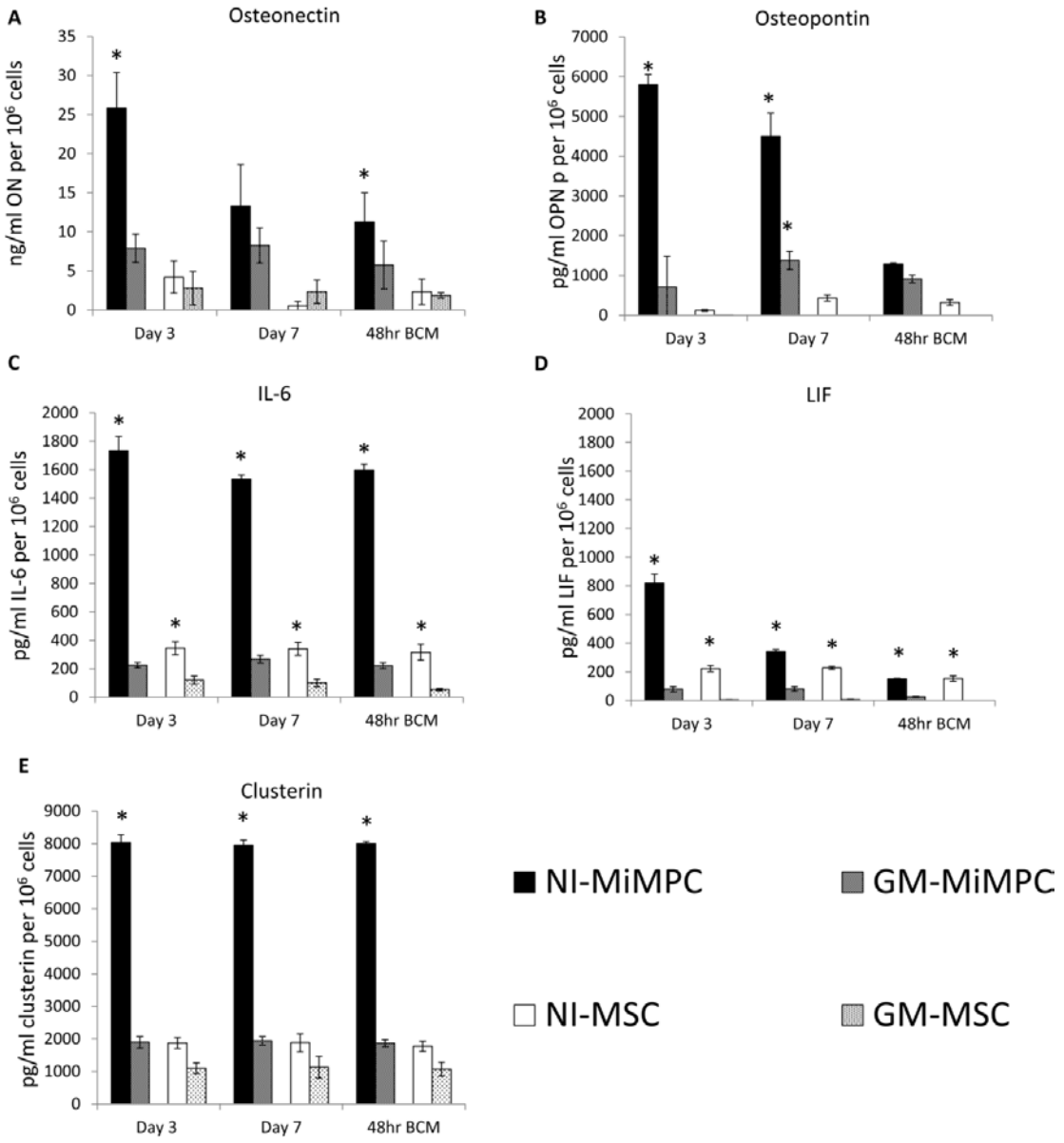

Figure 8: Production of factors by NI- MiMPCs and MSCs, quantified via ELISA
MiMPCs and MSCs were cultured in neurotrophic induction medium or growth medium. Conditioned media taken from days 3 and 7 of induction culture, and basal conditioned medium taken from cultures 48 hours post-induction (48hr BCM). The conditioned media assayed include those from MiMPCs (induced, NI-MiMPCs; uninduced, GM-MiMPCs), and from MSCs (induced, MI-MSCs; uninduced, GM-MSCs), as well as basal medium (controls). Medium was assayed for levels of **(A)** Osteonectin, **(B)** Osteopontin, **(C)** IL-6, **(D)** LIF, and **(E)** clusterin. All ELISA results are expressed in pg/ml or ng/ml produced per million cells. Medium taken from NI-MiMPC cultures contained high levels of all assayed factors compared to GM-MiMPCs, NI-MSCs, and GM-MSCs. Osteonectin, IL-6, and clusterin exhibited relatively constant secretion levels, while osteopontin and LIF showed decreased expression levels during induction treatment and the 48-hour post-induction period. *, $p < 0.05$, denotes significance of NI groups of each cell type compared to their respective GM controls.

2.4 DISCUSSION AND CONCLUSIONS

No defined protocol exists for the majority of iPSC differentiations. Multiple literature sources describe their own novel protocol for differentiation along various lineages including mesenchymal stem cells, cardiomyocytes, and hepatic cells [83, 98, 150-153]. In our past studies, it was assumed that published protocols for human embryonic stem cell (hESC) differentiation will have the same effect on iPSCs. While this can add flexibility to a study and provide leeway in terms of optimization, it should be noted that different methods could cause a difference in cell function or differentiation capability, even if the desired phenotype is expressed (i.e., morphology, expression of cell markers) [92]. For this reason, this study begins with characterization and comparison of MiMPCs and AEiMPCs in the context of neurotrophic potential, even though both cells have been previously characterized in earlier work by Diederichs in the context of adipogenic, chondrogenic, and osteogenic differentiation capabilities [92].

While EB formation has previously been reported as a viable way to generate MSC-like cells from either hESCs or iPSCs, our studies show that EB formation, as far as BDNF production, is not a favorable method to generate MiMPCs. The MGM method, however, has proven to be amenable to BDNF production. It is possible that since embryoid body formation inherently implies that not all cells (i.e. cells in the inner portion of EBs) will be exposed to the same chemical microenvironment, the MiMPCs generated from the EB method are thus more heterogeneous, and perhaps differ more drastically in their ability to produce BDNF. It may be an interesting future study to detail the differences between these two methodologies and how it may influence the secretome of the MiMPC, particularly as related to neurotrophic support. Because neurotrophin production capacity is of utmost importance for nerve regeneration, this

parameter has been chosen to determine which cell type (MiMPCs or AEiMPCs) and which differentiation method (MGM or EB) was most suitable for this purpose.

Our results indicated that NI-MiMPCs were capable of producing far more BDNF than NI-AEiMPCs, when neuroinductive treatment protocol was used (Figure 3). However, it did not seem that the neuroinductive protocol was capable of promoting production of CNTF, NGF, NT-3 or GDNF. Initial trials of ELISAs appeared to detect trace levels of CNTF and NGF from both NI- MiMPCs and MSCs, but the results could not be reliably reproduced. Multiple literature sources have stated that MSCs can produce detectable levels of neurotrophins including CNTF, NGF and GDNF [5, 71, 154]. It is possible that our control MSCs are not producing all the expected neurotrophins due to factors beyond our control, such as the age of the patient from whom the cell was isolated (60-year-old male), environmental exposures, and any pre-existing condition that may have demanded an orthopedic surgery from the patient in the first place. Although the MSCs from which our iPSCs were reprogrammed were isolated from a middle-aged patient, and the iPSC karyotype showed no abnormality after 13 passages [98], there is a possibility that this resistance to producing certain neurotrophic factors is due to epigenetic factors that we have not accounted for.

The MiMPCs are capable of producing physiologically relevant levels of BDNF. Under normal conditions, NGF is typically expressed in the peripheral nerve, and BDNF synthesis is highest in the central nervous system, however, post-injury, BDNF mRNA and BDNF activity increase in peripheral nerves and Schwann cells, reaching up to 10 times the levels seen from NGF [155]. Therefore, it may be more physiologically relevant for MiMPCs to secrete high levels of BDNF compared to other neurotrophins.

It is noteworthy that parametric cyclic-AMP assays on conditioned medium did not yield results from any cell type (data not included). Adenosine cyclic monophosphate (cAMP) is a ubiquitous secondary messenger molecule in eukaryotic cells. Multiple studies have shown that elevated levels of cAMP can increase both myelin production by Schwann cells as well as axonal regeneration in nerves [156]. Although data on the effect of extracellular cAMP on nerve regeneration are limited, what little information there is seems to indicate that cAMP can have neurotrophic effects and enhance nerve regrowth [157]. However, neither induced nor non-induced MiMPCs or MSCs produced detectable cAMP into conditioned medium from either day 3, day 7 or 48-hours post-NIM treatment. It is likely that due to the presence of forskolin and IBMX in the NI-medium, cAMP levels were indeed elevated in day 3 and day 7 conditioned medium at the very least, but could have remained undetectable due to either the retention of cAMP within the cell, or degradation of the molecule despite immediate freezing upon sample collection. Furthermore, the published literature has reported that BDNF itself can increase cAMP levels by activating the ERK pathway, which leads to inhibition of phosphodiesterase4, which hydrolizes cAMP [158]. As BDNF production was high in NI-MiMPCs and NI-MSCs, there is further reason to believe that intracellular cAMP levels were elevated. Both renal[159] and muscle[160] cells have mechanisms to regulate the efflux of cAMP-adenosine to their respective extracellular matrices, though clearly it is a specialized process that the MiMPCs and MSCs do not possess.

A simple, morphological comparison showed that the MiMPCs differentiated from iPSCs resembled typical MSC cultures, while the original iPSC colonies did not resemble MSCs or MiMPCs. iPSC colonies were negative for all mesenchymal and Schwann cell markers, but were positive for pluripotent markers SSEA4, Sox2, and Oct3/4. Previous data from our lab confirmed

that the iPSCs used here were true pluripotent cells [98]. From this, we can ascertain that our iPSCs retained desirable qualities and remained pluripotent throughout their usage. Characterization of MiMPCs showed positive staining for many of the same cell surface markers as both MSCs and Schwann cells, including CD44, CD73, CD105, GFAP, S100B, and P75/NGFR.

The expression of p75/NGFR should be noted. A study by Bentley et al. (2000) showed that the lack of p75/NGFR was linked to a deficit in Schwann cell migration and coverage, as well as a substantial reduction in nerve bundle and axon formation. However, there have also been reports stating the negative effects of p75/NGFR after injury, and that it may have a role in axon apoptosis and death signaling pathways [161, 162]. While the majority of this study utilizes conditioned medium taken from these cells to use in DRG culture, we can include these cells in future *in vivo* studies along with a p75/NGFR inhibitor to prevent any potentially negative effects of p75/NGFR signaling. It does not appear that the literature related to p75/NGFR can confirm whether or not the presence of p75/NGFR is helpful or harmful in terms of axon regeneration after injury, although some data suggest that a p75/NGFR antagonist can have neuro-protective effects on retinal ganglion [163]. Therefore, it may be beneficial in future studies to knock down the expression of p75/NGFR in MiMPCs when co-culturing the cells with DRGs in electrospun scaffolds.

MiMPCs and MSCs are also capable of producing factors shown in previous works by other groups to enhance nerve regeneration, such as osteonectin, osteopontin, IL-6, LIF and clusterin (Figure 8). Osteonectin is a secreted matricellular protein that plays a role in bone mineralization by binding calcium to collagen [164]. Previous studies have shown that osteonectin can also play a role in promoting neural cell survival and initiating extension

outgrowth [33, 58]. It has also been suggested that osteonectin and BDNF may work synergistically to promote neurite outgrowth [32].

Multiple studies have already shown the benefits of having angiogenic factors present during nerve regeneration [69, 71, 210], and that angiogenesis and restoration of blood supply improves functional recovery. Man, et al showed that the presence of VEGF-overexpressing MSCs transplanted *in vivo* increased neurite extensions and Schwann cell proliferation [69]. At sites of injury, Mohammadi showed that local administration of exogenous VEGF would improve functional recovery in rats [211].However, VEGF is unlikely to be playing a role in our studies, as VEGF production is a point of difference between the secretomes of MiMPCs and MSCs. While MSCs are fully capable of secreting VEGF regardless of neuroinductive treatment, MiMPCs can secrete VEGF only when incubated in neuroinductive medium—no VEGF production was apparent in the GM or any basal conditioned medium (BCM) groups (Figure 19). In addition, DRGs were cultured only in BCM collected from cells. Furthermore, osteonectin is present in high quantities in the conditioned medium, and work by Kupprion et al suggests that osteonectin is able to bind VEGF and prevent its interaction with its receptor [165]. It is therefore likely that even if trace VEGF levels were present in MiMPC basal conditioned medium and escaped detection in the ELISAs, the effects of such minute levels would be inhibited by the comparatively high levels of secreted osteonectin. As MiMPCs will not be in NI medium when transplanted *in vivo*, it is likely that MiMPCs may not be able to support angiogenesis, and thus supplying exogenous VEGF or MiMPC transfection with VEGF-expressing plasmids may be required.

Osteopontin is a cell adhesion molecule that is expressed on a wide variety of cell types, and has been implicated in cell survival and inflammatory regulation [166]. There have been a

limited number of studies to suggest that osteopontin also plays a role in nerve regeneration, although there seems to be more of an association between osteopontin and motor neuron outgrowth rather than sensory neuron outgrowth [149, 167].

Clusterin is another commonly expressed glycoprotein found in most tissues [168]. As it is a commonly found molecule, many studies have found various roles for clusterin. It has been implicated in the pathogenesis of Alzheimer's [169], while another study found that clusterin alleviated peripheral neuropathy in rats [170]. Other studies have found that mRNA levels of clusterin were increased after peripheral nerve injury, and as clusterin is involved in lipid recycling, it suggests that the presence of this molecule at the site of injury aids Wallerian degeneration and Schwann cell proliferation [171, 172]. Meanwhile, clusterin may signal through the megalin receptor, a pathway which has been shown in the DRG to selectively promote sensory neuron outgrowth [173, 174].

It is well established that cytokines of the IL-6 superfamily, which includes IL-6 and LIF, are able to activate the Jak/STAT3 pathway, an important signaling pathway in neurite axon extension [175, 176]. Our ELISAs showed that higher concentrations of only certain growth factors and cytokines were maintained both during and after the neuroinductive treatment period had concluded, including IL-6, but not LIF. While it is likely that the increased concentration of IL-6 means that this cytokine will play more of a role than LIF, studies have shown that LIF is more potent than IL-6, and may be able to exert the same effects at a lower concentration [177]. However, the potency of LIF versus IL-6 was assessed on microvascular and endothelial cells, so it may still be premature to assume that LIF is having the same effect in nerve regeneration.

Taken together, it is probable that these properties of the MiMPC may have a positive influence on nerve regeneration, possibly superior to those seen from MSCs. If the conditioned

medium from NI-MiMPCs can be collected, or if the cells themselves can be harvested, it is conceivable that this medium or the cells can be used in procedures that enhance nerve regeneration.

3.0 NEUROTROPHICALLY INDUCED MIMPCS ENHANCE COMPLEXITY OF DORSAL ROOT GANGLION NEURITE EXTENSIONS INDEPENDENTLY OF NEUROTROPHIN SIGNALING

3.1 INTRODUCTION

It is well established in the literature that classic neurotrophins, such as BDNF, NT-3, NT-4/5 and NGF, play major roles in neuronal survival, maintenance, and repair. In the peripheral nervous system, Schwann cells are the main providers of such neurotrophins in addition to forming the myelin sheath.

Neurotrophins and extracellular matrix (ECM) proteins also play a part in neuritogenesis, a complex process where neurite extension processes grow out from the main body of the nerve cell. Neurites form from localized lamella collapse around microtubules, and their distal growth cones form from uncollapsed lamella. These growth cones and microtubules extend the neurite away from the cell body. These nascent neurite processes later mature into axons and dendrites [178].

The aforementioned neurotrophic ligands signal through the tropomyosin receptor kinases (Trk receptors), located in the plasma membrane of nerve cells. Three types of Trk receptors are found in human nerve cells—TrkA, TrkB, and TrkC. Typically, NGF is specific for TrkA, NT-4/5 and BDNF signal through TrkB, and NT-3 signals through TrkC. However, the

specificity of the ligands for their respective Trk receptor can depend upon the Trk isotype present. Various signaling pathways through Trk receptors are responsible for a multitude of functions, including differentiation, regulation of synaptic strength, plasticity, ion channel activity, neurotransmitter receptors, and modulates exo- and endocytosis of synaptic vesicles [179].

While the Trk receptor mediate a variety of nerve-related functions, they have been implicated in both neurogenic and non-neurogenic tumor growth, especially when they form oncogenic gene fusions. These chimeric Trk proteins are typically constitutively active, or have hyperactive kinase function, resulting in oncogenic potential. Although these oncogenic fusions were originally discovered in 1982, renewed interest in these chimeric proteins did not occur until recently, as personalized medicine and targeted therapies related to Trk receptors were not possible until the recent discovery of NTRK1, NTRK2, and NTRK3 gene fusions. For this reason, pharmacological blockers against the Trk receptor have been synthesized, some of which are in or approaching clinical trials.

One such drug is GNF5837, a potent pan-Trk receptor antagonist. It is an oxindole urea inhibitor with high binding affinity to TrkA, TrkB, and TrkC that targets the ATP binding cleft and an adjacent hydrophobic pocket. It has highly anti-proliferative effects and has been found to reduce tumors in mammals [180].

Cyclotraxin-B is a selective, potent cyclical peptide that allosterically modulates the action of TrkB receptors by altering the conformation of TrkB. Both BDNF-dependent and -independent activities were inhibited. It has been shown to have anxiolytic effects in mice without anti-depressant activity, thereby demonstrating its ability to cross the blood-brain barrier.

Due to these properties, cyclotraxin-B may be useful as a tool both for examining the effects of BDNF and as a potential treatment for brain disorders [181].

BDNF, IL-6 and LIF, previously established to be produced by MiMPCs, are also capable of activating the Janus kinase/signal transducer and activator of transcriptions (Jak/STAT) pathway to promote nerve regeneration after axotomy [37, 182]. In the peripheral nerve, phosphorylated STAT3 is increased following lesions. Cytokines in the IL-6 superfamily (i.e., IL-6 and LIF) facilitate this response by activating the receptor/gp130 complex which signals downstream through STAT3 [176]. STAT3 is associated with neuron regeneration, as it co-localizes with survival markers in nerves post-injury, and knockout models have exhibited deficiencies in neuronal function and survival after axotomy [182]. Lin et al showed that BDNF promoted neurite growth through the Jak/STAT pathway in mice pelvic ganglion by administering an inhibitor AG490 and confirming that BDNF-enhanced neurite growth was truncated [38].

The previous chapter showed enhanced BDNF production from NI-MiMPCs compared to GM-MiMPCs or MSCs. We hypothesize that based on the neurological studies found in the literature and the characterization of our MiMPCs, the conditioned medium from NI-MiMPCs will be able to enhance neuritogenesis from dorsal root ganglion (DRG) cultures. This effect was assessed in embryonic DRGs cultured on tissue culture plastic. In order to tease apart the MiMPC secretome and determine if secreted BDNF was truly the effector molecule, conditioned medium was supplemented with Trk receptor inhibitor drugs.

3.2 METHODS

3.2.1 Tissue culture plate preparation

100ng/ml poly-D-lysine solution was prepared and dispensed into each well of a 12-well plate. Polylysine was allowed to coat the plate for 3 days at 4˚C on a rocking platform, after which it was aspirated from wells, and wells were washed with sterile 1xPBS. 10 μg/ml laminin was prepared and used as a supplemental coating, and was allowed to coat the plate for 3 days at 4˚C on a rocking platform. Both poly-D-lysine and laminin were purchased from Sigma-Aldrich (St. Louis, MO).

3.2.2 Isolation of dorsal root ganglia (DRGs)

DRGs were harvested from day 9 chick embryos, using a previously described protocol [183]. The isolated DRGs were plated one per well on a 12-well plate coated with poly-d-lysine and laminin as previously described.

The DRGs were allowed to adhere to the substrate in medium consisting of DMEM-F12 and 5% FBS, further supplemented with 10 ng/ml each of basic fibroblast growth factor (FGF-2), epithelial growth factor (EGF) and nerve growth factor (NGF). After a 3-day settlement period, medium on DRGs were exchanged for 48-hour basal conditioned medium (48hr BCM) collected from either (1) NI-MiMPCs, (2) GM-MiMPCs, (3) NI-MSCs, or (4) GM-MSCs. Control DRGs were cultured in unconditioned basal medium consisting of DMEM-F12, 5% FBS, ITS-X, and pen-strep. All DRGs were cultured for 5 days. Cultures were then immunostained as outlined previously. Briefly, DRGs were fixed with 4% paraformaldehyde, incubated in hot sodium

citrate for antigen retrieval, blocked in 5% FBS and incubated with anti-heavy neurofilament primary antibody (Abcam, Cambridge, MA) diluted to 1:10,000 overnight at 4°C. Secondary antibody AlexaFluor 488 conjugate (ThermoFisher, Waltham, MA) was allowed to incubate for 1 hour at room temperature at a 1:300 dilution with blocking buffer. Neurite outgrowth quantitatively assessed via Sholl analysis (see below).

3.2.3 Optimizing Trk receptor inhibitor drug studies

DGRs were isolated as previously described, and plated on polylysine/laminin coated 12-well tissue culture plates. DRG growth control medium was supplemented with 10 ng/ml each of NGF, EGF and FGF. For the BDNF growth control, 20 ng/ml of BDNF was added to DRG control medium in addition to the aforementioned growth supplements. Negative growth control cultures consisted only of basal medium (DMEM-F12, 5% FBS, ITS and PSF). DRG cultures were separated into groups that were additionally supplemented with 100 nM, 500 nM, and 1 μM of cyclotraxin-B (ThermoFisher), a selective Trk-B inhibitor; and 12 nM and 24 nM of GNF5837, a selective and potent pan-Trk receptor inhibitor (Sigma-Aldrich). Sholl analysis [184] was used to determine optimal drug and concentration use for decreasing number of neurite extensions.

3.2.4 Trk receptor inhibition

To assess the involvement of Trk receptor-mediated neurotrophin signaling, the Pan-Trk inhibitor, GNF-5837 (Sigma-Aldrich), was used at a concentration of 24 nM, which exceeded IC_{50} values (7 – 11 nM for TrkA, TrkB, and TrkC) reported in the literature [180]. GNF-5837

was supplemented to 48 h BCM from NI-MiMPCs and control MiMPCs, and NI-MSCs and control MSCs, which were subsequently used to culture chick DRGs for 4 days. Cultures were paraformaldehyde-fixed and immunostained for heavy neurofilament, and branching complexity of neurite outgrowth was assessed.

3.2.5 Jak/STAT inhibition

To assess the involvement of JAK/STAT3-mediated signaling, cucurbitacin I, an inhibitor of the JAK2/STAT3 signaling pathway that suppresses the levels of tyrosine phosphorylated STAT3 [185], was used at a concentration of 60 nM. Cucurbatacin-I was supplemented to 48h BCM from NI-MiMPCs and control MiMPCs, and NI-MSCs and control MSCs, which were subsequently used to culture chick DRGs for 4 days. Cultures were paraformaldehyde-fixed and immunostained for heavy neurofilament, and branching complexity of neurite outgrowth was assessed (see below).

3.2.6 Immunofluorescent staining of DRG cultures

DRG/MiMPC co-cultures were fixed in buffered 4% paraformaldehyde and permeabilized with 10 mM sodium citrate in 10% ethanol heated to just under boiling temperature in the microwave for 1 hour. After blocking in 5% FBS, cultures were incubated with mouse anti-heavy neurofilament (1:500; Abcam, Cambridge, MA) in block buffer overnight at 4°C. After rinsing, cultures were then incubated with fluorescently labeled secondary antibodies (1:300; AlexaFluor 488 goat IgG, IgM; Invitrogen, Carlsbad, CA) for 1 hour at room temperature. Co-cultures that

included MiMPCs/MSCs were also nuclear-stainted with DAPI (1:10,000; Invitrogen, Carlsbad, CA) according to the supplier's protocol.

3.2.7 Quantitation of neurite branching complexity

Fluorescent DRG image tiles were processed with MetaMorph (Molecular Devices, Sunnyvale, CA), and digitally stitched together using open source software Fiji/NIH ImageJ (developed at the NIH, Bethesda, MD) [186]. All greyscale images were thresholded to create binary bitmap images. Neurite extension densities were measured using the Sholl analysis plugin function within Fiji. The algorithm automatically retrieves data from 2D or 3D images to perform a regression analysis and generate the metrics for Sholl-based dendrite arborization [187]. Fiji Sholl plugin was set such that each radius step consisted of 50 pixels with each radius being sampled 3 times. Critical values (Cvs; the measurement of the Sholl analysis that corresponds to the point of maximum branching density, see Figure 20 for a representative example of a Sholl analysis graph) were taken from each Sholl measurement and averaged to generate bar graphs. It should be noted that the graph in Figure 20 is only representative, and that the maximum number of neurite extensions may occur at different radii depending on the sample. All images were taken at 4x magnification using an inverted microscope (Olympus IX81) with a motorized stage controlled through MetaMorph, and the scale used was 620 pixels = 1 mm.

3.2.8 Statistical analysis

All data were presented as means ± standard deviation, unless otherwise stated. Statistical significance was determined by Student's T-test, Levene's test and Games Howell post-hoc tests as appropriate.

3.3 RESULTS

3.3.1 Morphological comparison of dorsal root ganglion (DRG) neurite extension complexity

All DRGs were dissected from 9-day old chick embryos. We evaluated the effect of neurotrophically induced cells on nerve growth by culturing DRGs with conditioned medium from NI-MiMPCs and NI-MSCs (Figure 9).

A morphological examination of immunofluorescence staining showed that DRGs cultured with both conditioned medium from NI and GM-MiMPCs appeared to have significantly improved neurite outgrowth, compared to either control cultures or those cultured with conditioned media from NI-MSCs (Figure 9A-E). DRGs cultured in conditioned medium from GM-MSCs also exhibited significantly enhanced neurite outgrowth. This demonstrated that MSCs and MiMPCs, particularly the latter, were producing factors that enhanced nerve growth. DRG neurite extension complexity was evaluated by Sholl analysis using ImageJ to quantitatively confirm these morphological findings.

3.3.2 Sholl analysis shows enhanced neurite branching complexity of DRGs grown in MiMPC conditioned medium

Sholl analysis confirmed that conditioned medium from both NI-MiMPCs and GM-MiMPCs yielded significantly enhanced neurite branching complexity in DRG cultures compared to controls. Complexity increased 2.1 and 2.3 times that of controls when DRGs were cultured in conditioned medium from NI-MiMPCs and GM-MiMPCs respectively. Sholl analysis also confirmed that DRGs cultured in conditioned medium from GM-MSCs but not NI-MSCs exhibited significantly enhanced neuritogenesis. Conditioned medium collected from GM-MSCs similarly increased neurite complexity by about 2.3 times that of controls. However, DRGs cultured in NI-MSC conditioned medium showed only 1.7 times the branching complexity compared to controls, and thus was not statistically significantly different from controls (Figure 9F-G).

3.3.3 GNF5837 reduced neurite branching in Trk-receptor inhibition DRG cultures

In our pilot studies to determine optimal drug and concentration use, we compared the Sholl results between DRGs treated with pan-Trk receptor inhibitor GNF5837 and TrkB-receptor inhibitor cyclotraxin B. With both drugs, we found an inverse relationship between the number of neurite extensions and the drug concentration used. The decrease in neurite extension complexity was most pronounced in DRG cultures containing 1uM cyclotraxin-B or 24nM GNF5837 (Figure 10). In these cultures, neurite extensions were significantly decreased from those seen in positive growth control cultures supplemented with 10ng/ml of each NGF, EGF, and FGF, and 20ng/ml of BDNF.

3.3.4 Conditioned medium from neurotrophically induced MiMPCs enhance DRG neurite complexity in the presence of GNF5837

The involvement of BDNF was tested by examining the effect of inhibiting the action of the neurotrophin Trk-receptor on DRG neurite outgrowth. The pan-Trk receptor inhibitor drug, GNF5837 (24 nM), was co-administered to the MiMPC conditioned medium treated DRGs. As shown in Figure 11A-E, DRG growth appeared to be only slightly reduced in complexity and size. The Sholl analysis results showed that, upon GNF5837 co-treatment, all conditioned medium treated groups, except for medium collected from NI-MiMPCs, experienced a marked decrease in neurite extension density (decreases of 45-60% measured branching density, as opposed to only a 10% decrease in measured branching density in cultures containing NI-MiMPC conditioned medium) (Figure 11F-G). Furthermore, as our cells did not produce detectable levels of the neurotrophins, NGF, NT-3, CNTF or GDNF, with the latter two not acting through the Trk receptors, this observation suggested that additional non-neurotrophic factors were likely being produced by NI-MiMPCs that were capable of initiating neurite extensions, acting independently of the Trk-receptors.

3.3.5 Presence of cucurbitacin-I in conditioned medium from neurotrophically induced MiMPCs does not abolish neurite outgrowth

As multiple published investigations have suggested a role for IL-6-type cytokines in nerve regeneration [55, 56, 176], and as our results suggested that BDNF was unlikely to be the only factor involved in enhancing neurite extension density, we sought to block the effects of IL-6 to determine if neurite density would be affected. As IL-6 signals through the Jak/Stat pathway, we

targeted the inhibition of this pathway with a pharmacological blocker, cucurbitacin-I [185]. The most immediate observable effect from cucurbitacin-I administration was the truncation in neurite extension length. However, a morphological examination did not make it obvious whether neuritogenesis had also suffered (Figure 12A-E).

Results from the Sholl analysis showed that treatment with cucurbitacin-I decreased neurite complexity to the extent that the effects of the conditioned medium from non-induced cells was no longer significantly different from that seen in control cultures. However, conditioned medium from NI-MSCs still enhanced complexity of DRG neurite extensions compared to controls (Figure 12F-G). While statistical analysis determined that CM from NI-MiMPCs no longer yielded a significant improvement, the average DRG culture still exhibited increased neuritogenesis compared to controls. The more pronounced effect of the addition of cucurbitacin-I to the DRG cultures, however, was the decrease in observed neurite extension length, which could not be accurately measured on tissue culture plastic due to the disorganized growth patterns typical of DRGs cultured on tissue culture plastic (TCP).

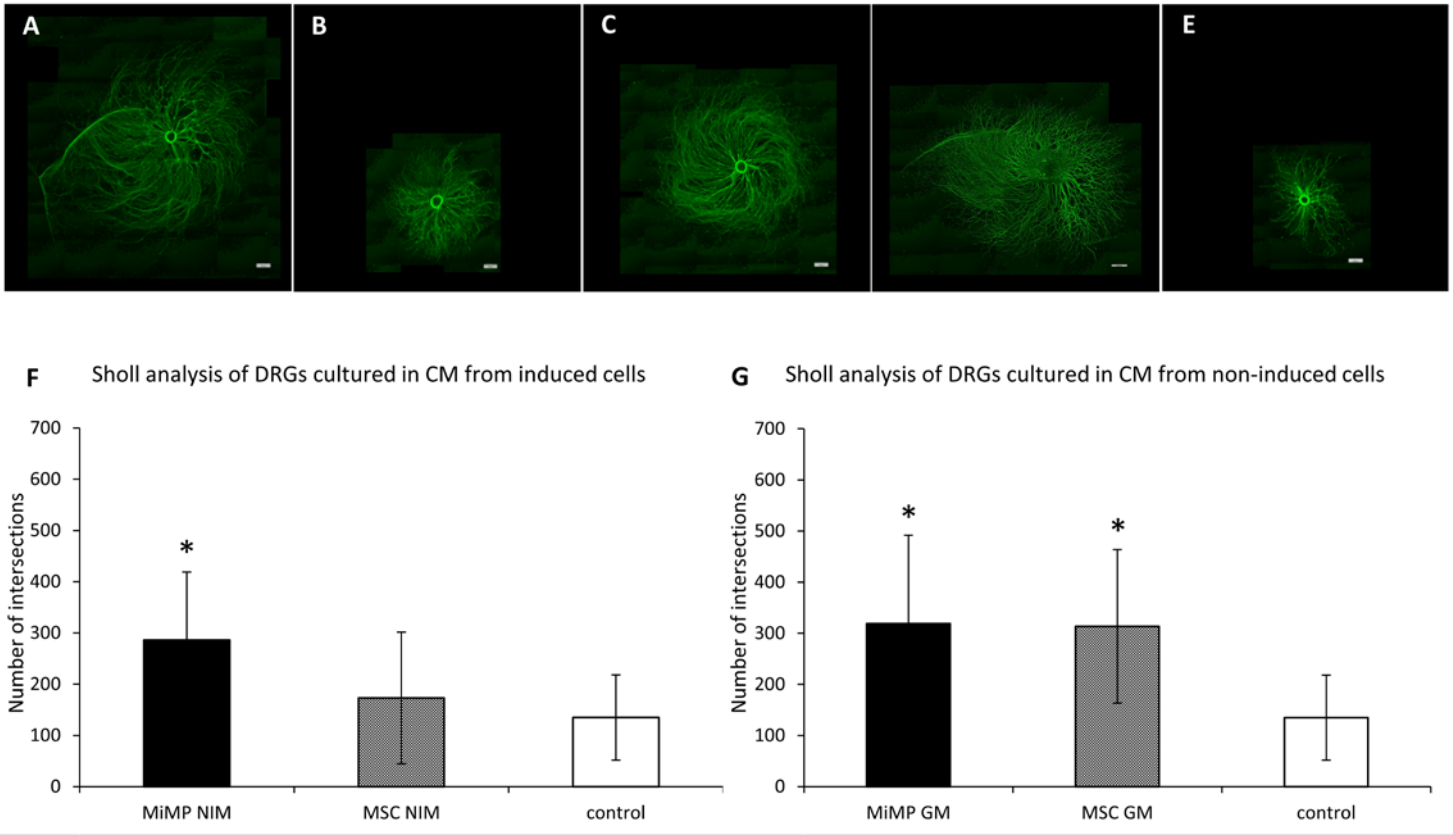

Figure 9: Morphological and quantitative comparison of DRG neurite extension branching complexity

Dorsal root ganglia (DRGs) are cultured for 5 days in medium conditioned for 48 hours by **(A)** NI-MiMPCs, **(B)** NI-MSC, **(C)** GM-MiMPCs, or **(D)** GM-MSCs. Controls in **(E)** show DRGs cultured for 5 days in unconditioned basal medium. All DRGs were stained with anti-heavy neurofilament antibody, an intermediate filament found in neurons, and imaged. **(F)** Sholl analysis on DRGs show that conditioned medium (CM) collected from NI-MiMPCs significantly enhanced neuritogenesis over controls, but DRGs cultures in CM from NI-MSCs did not show improvement. Sholl measuring radii ranged from: 4.52-9.11mm (MiMP NIM), 2.03-6.135mm (MSC NIM), and 4.12-6.22mm (controls) **(G)** Sholl analysis measures the number of intersections, and therefore, the number of neurite extensions, on images, which show that GM-MiMPCs and MSCs significantly enhance neuritogenesis ($p<0.05$) compared to controls. Sholl measuring radii ranged from: 1.06-10.00mm (MiMP GM), 3.88-8.39mm (MSC GM) and 4.12-6.22mm (controls). All images were taken at 4x, and scale bars represent 560 µm. Statistics for all groups were compared to controls using Games-Howell test.

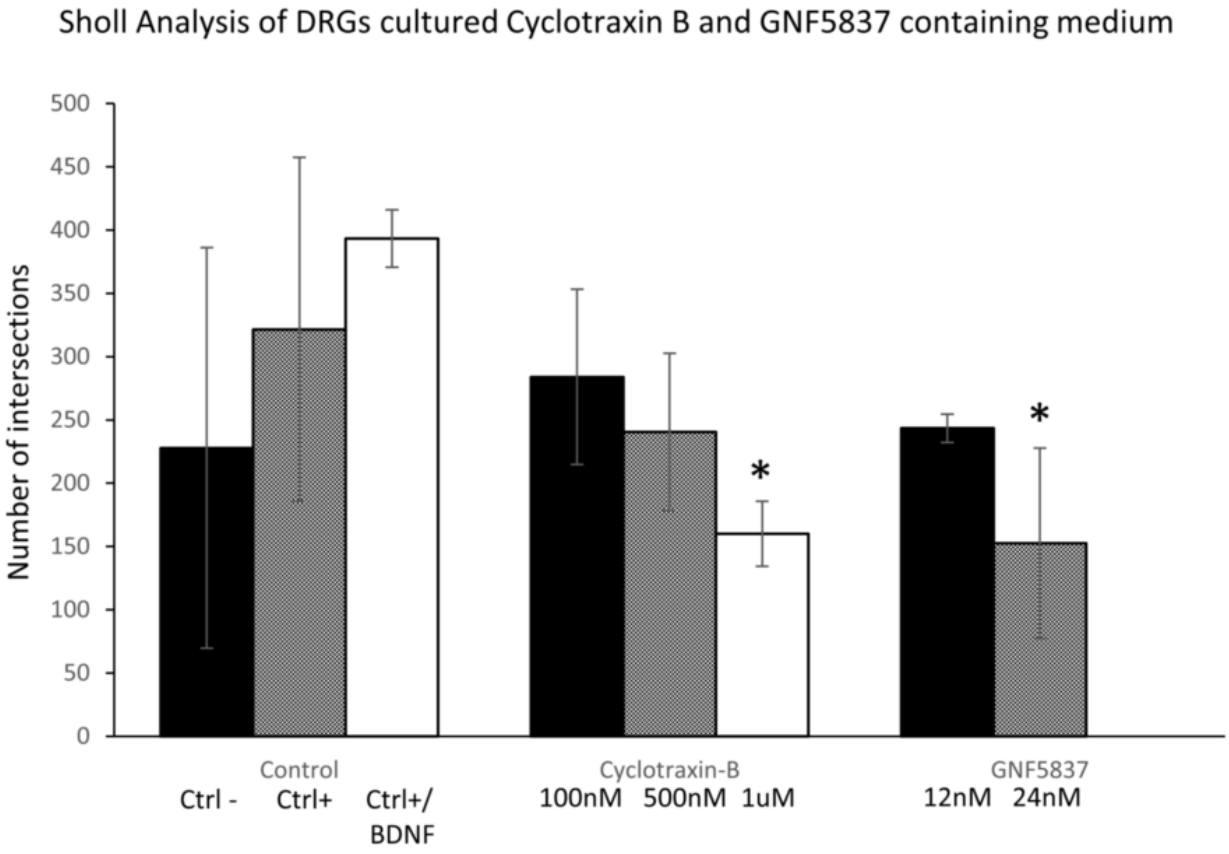

Figure 10: Effect of Trk-receptor inhibitor drugs quantified via Sholl analysis
Pilot study of the effect of different concentrations of cyclotraxin-B (selective TrkB receptor inhibitor) and GNF5837 (pan-Trk receptor inhibitor) on DRG neuritogenesis. Control (Ctrl) cultures included Ctrl- (basal medium; DMEM/F12, 5% FBS, ITS-X and pen-strep), Ctrl+ (basal medium, 10 ng/ml of each NGF, FGF and EGF) and Ctrl+/BDNF (Ctrl+, and 20 ng/ml of BDNF). Sholl analysis showed that medium supplemented with 1µM of cyclotraxin-B or 24 nM of GNF5837 significantly suppressed the number of neurites compared to Ctrl+/BDNF ($p<0.05$), and were comparable or slightly further suppressed compared to Ctrl- cultures. Number of neurites in cultures with 1µM of cyclotraxin-B or 24 nM of GNF5837 were suppressed compared to Ctrl+ cultures, but not significantly so. * denotes significant decrease of neurite extensions ($p<0.05$) of marked groups compared to Ctrl+/BDNF control cultures, determined via Student's T-test.

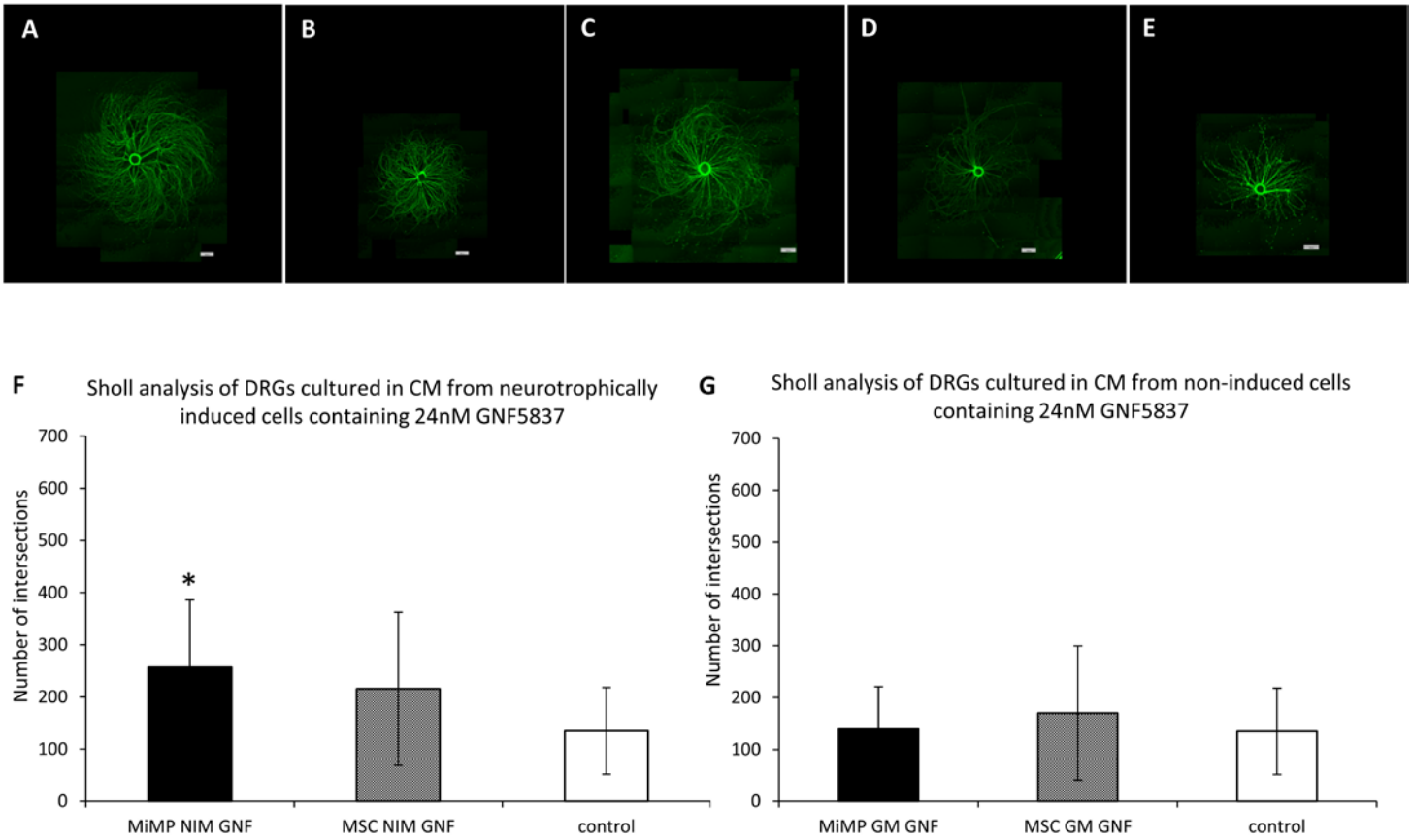

Figure 11: Morphological and quantitative comparison of DRG neurite extension branching complexity in the presence of GNF5837

Dorsal root ganglia (DRGs) were cultured for 5 days in medium conditioned for 48 hours by **(A)** NI-MiMPCs, **(B)** NI-MSC, **(C)** GM-MiMPCs, or **(D)** GM-MSCs. 24nM of pan-trk receptor inhibitor drug GNF5837 was added to each medium group in **A-D** and used to culture DRGs. Controls in **(E)** show DRGs cultured for 5 days in unconditioned basal medium. All DRG cultures were stained with anti-heavy neurofilament, an intermediate filament found in neurons. **(F)** Sholl analysis on DRGs show that conditioned medium (CM) collected from NI-MiMPCs significantly enhanced neuritogenesis over controls even in the presence of GNF5837, but DRGs cultures in CM from NI-MSCs did not show improvement. Sholl measurement radii ranged from: 1.63-8.23mm (MiMP NIM GNF), 2.83-7.50mm (MSC NIM GNF) and 3.16-5.00mm (controls) **(G)** Sholl analysis performed on images with NIH ImageJ measures the number of intersections, and therefore, the number of neurite extensions, which show that neuritogenesis of cultures in conditioned medium from GM- MiMPCs and MSCs are comparable to controls in the presence of 24nM of GNF5837. Sholl measurement radii ranged from: 1.87-9.36mm (MiMP GM GNF), 4.61-7.10mm (MSC GM GNF) and 3.16-5.00mm (controls). All DRGs were stained with anti-heavy neurofilament antibody and imaged. Images of conditioned medium cultures show a substantial increase in size and complexity of neurite outgrowth compared to controls. All images were taken at 4x magnification, and scale bars represent 560 µm. Statistics for all groups were compared to controls using Games-Howell test, and significant differences ($p<0.05$) are marked with a *.

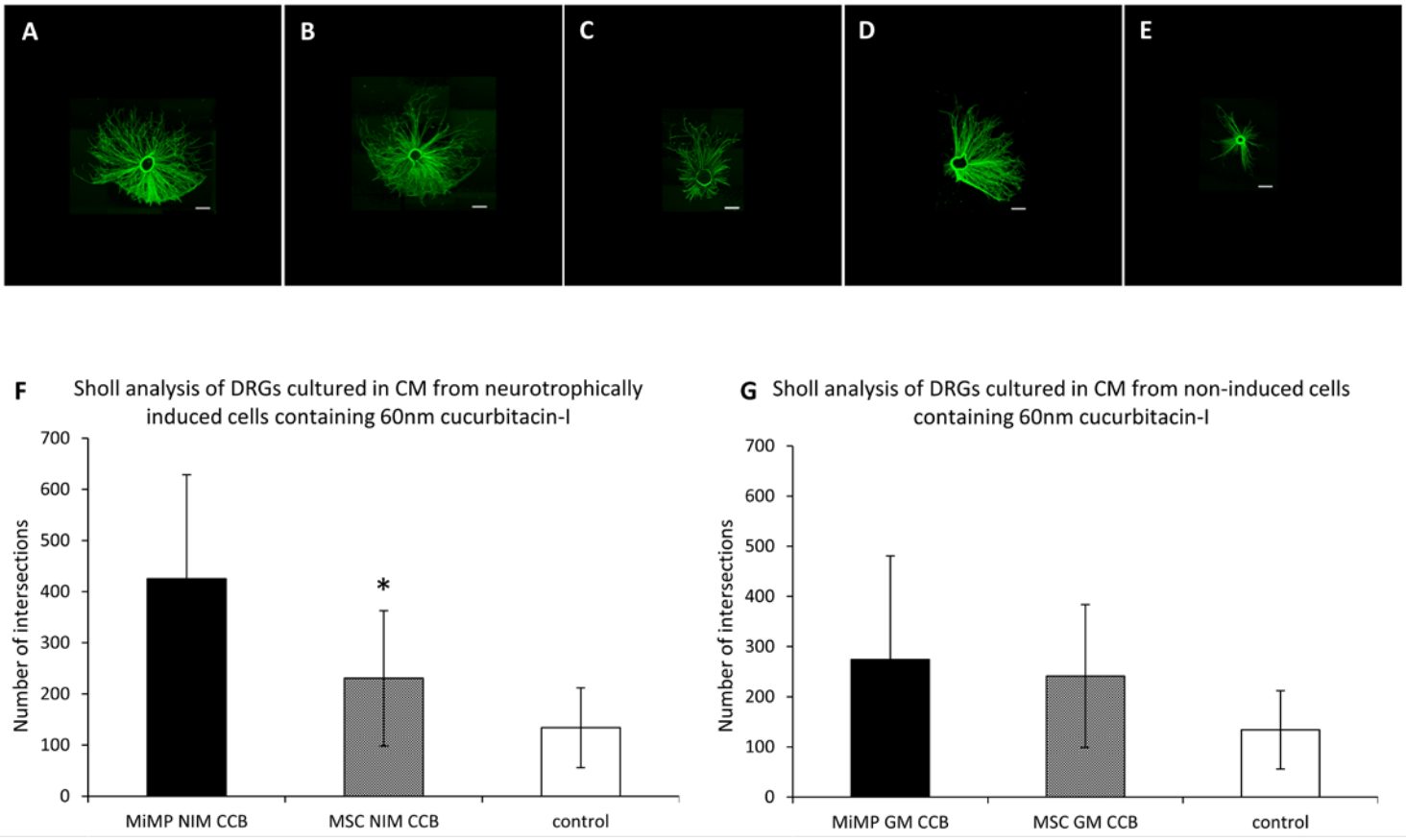

Figure 12: Morphological and quantitative comparison of DRG neurite extension branching complexity in the presence of cucurbitacin-I

Dorsal root ganglia (DRGs) were cultured for 5 days in medium conditioned for 48 hours by **(A)** NI-MiMPCs, **(B)** NI-MSC, **(C)** GM-MiMPCs, or **(D)** GM-MSCs. 60 nM of Jak/STAT inhibitor drug cucurbitacin-I was added to each medium group in **A-D** and used to culture DRGs. Controls in **(E)** show DRGs cultured for 5 days in unconditioned basal medium. All DRG cultures were stained with anti-heavy neurofilament, an intermediate filament found in neurons. **(F-G)** Sholl analysis performed on images via NIH ImageJ measures the number of intersections, and therefore, the number of neurite extensions. These showed that only neuritogenesis of DRGs cultured in conditioned medium from NI-MSCs showed improvement. All other CM groups were comparable to neuritogenesis measured in controls. Sholl measurement radii ranged from: 2.64-4.60mm (MiMP NIM CCB), 1.77-4.70mm (MSC NIM CCB), 2.48-4.83mm (MiMP GM CCB), 3.09-5.02mm (MSC GM CCB) and 2.88-6.14mm (control). All DRGs were stained with anti-heavy neurofilament antibody and imaged. Images of conditioned medium cultures show a substantial increase in size and complexity of neurite outgrowth compared to controls. All images were taken at 4x magnification, and scale bars represent 560 µm. Statistics for all groups were compared to controls using Games-Howell test, and significant differences ($p<0.05$) are marked with a *.

3.4 DISCUSSION

The previous chapter established that neurotrophic induction of MiMPCs enhances their ability to produce factors such as BDNF, IL-6 and LIF, which are able to support and enhance nerve regeneration. This chapter sought to create a functional bioassay to assess the utility of the MiMPC secretome in terms of neurite growth.

Conditioned medium (CM) taken from NI- MiMPCs and MSCs were used to culture dorsal root ganglia (DRGs) on polylysine/laminin coated tissue culture plastic (TCP). Sholl analysis quantitatively measured neurite density, and showed that CM from both NI- and GM-MiMPCs were able to significantly enhance neuritogenesis. By contrast, while CM from GM-MSCs improved neurite outgrowth, the results of treatments with CM from NI-MSCs were comparable to controls, once again indicating that although MiMPCs are similar to MSCs in terms of cell markers and morphology, there are key differences that make them a distinct stem cell population. The difference in secretomes between MiMPCs and MSCs is particularly impactful as observed from the effects on neurite outgrowths in DRG cultures. While it appeared that under normal growth conditions, MiMPCs and MSCs provide the same benefits toward neurite extensions, MiMPCs and MSCs clearly alter their secretomes differently in response to a neuroinductive environment.

Regardless of type, Trk receptors are responsible for neuronal survival and differentiation. Although cyclotraxin-B is a selective TrkB-receptor inhibitor, it was still able to decrease the number of neurite extensions found in DRG cultures supplemented with both NGF and BDNF neurotrophins. Control cultures that contained NGF but not BDNF also did not produce as many neurite extensions. Therefore, it is possible that BDNF plays a larger role than NGF when it comes to neuritogenesis. We chose GNF5837 over cyclotraxin-B as the Trk-

receptor inhibitor drug because while there was no evident production of NGF or NT-3 detectable in ELISAs, it was preferable to block action from all Trk receptors to avoid confounding results. BDNF was by far the most prominently produced neurotrophin, however, a multitude of other studies had shown that MSCs, at the very least, were capable of producing other neurotrophins (i.e., NGF). While we do not believe that either our MiMPCs or MSCs were producing any neurotrophins besides BDNF, there was the possibility that any low-level production may have degraded prior to the assays being performed. To ensure that no possible remnants of neurotrophins would result in activation of Trk receptors that would present with similar effects as BDNF and skew our results, we treated the cultures with the pan-Trk receptor inhibitor GNF5837. As no glial-derived neurotrophic factor (GDNF) or ciliary neurotrophic factor (CNTF) was detected in ELISAs, we did not pilot any studies with inhibitors against their receptors (CNTFR or GFRA1, respectively).

While both our MiMPCs and MSCs are capable of producing BDNF and osteonectin whether or not they have gone through neurotrophic induction (Figure 3B, 6), it seems that the positive effects of cell-conditioned medium on DRG outgrowth can be lessened, but not completely abolished, with the addition of GNF5837 for all conditioned medium groups except NI-MiMPC. In addion, while both GM- MiMPCs and MSCs were able to enhance neuritogenesis, only the conditioned medium from NI-MiMPCs was able to rescue neuritogenesis in the presence of GNF5837. It is possible that dosage of both BDNF and osteonectin are important, or that osteonectin is operating through a yet unknown receptor pathway as a major osteonectin-mediated signaling pathway has not yet been found [32]. Taking all this information together, it is likely that osteonectin production by our NI-MiMPCs are

causing increased neuritogenesis, and therefore, higher neurite extension density compared to controls, even in the presence of GNF5837.

To confirm this hypothesis, several attempts were made to reduce the amount of osteonectin present in CM via anti-osteonectin antibodies in the manner previously reported by Ma et al [32, 33]; however, the level of reduction we achieved was insignificant (data not shown). Our next immediate step will be to use siRNA targeting osteonectin to knock down expression. We will subsequently use the osteonectin-knockdown CM together with GNF5837 to determine if osteonectin and BDNF are enhancing DRG neuritogenesis.

Previous studies have shown that IL-6-type cytokines, such as IL-6 and LIF, are able to enhance peripheral nerve regeneration by activating the Jak/STAT3 pathway [175, 176]. Our ELISAs showed that higher concentrations of only certain growth factors and cytokines were maintained both during and after the neuroinductive treatment period had concluded, including IL-6, but not LIF. By blocking the activation of the Jak/STAT3 pathway with the pharmacological inhibitor, cucurbitacin-I, we observed that our conditioned medium could not rescue the neurite extension complexity, and exhibited a marked decrease in length of neurite extension, regardless of whether the conditioned medium was taken from induced or non-induced cells. From this, it is likely that the superior lengths of neurite extensions found in conditioned medium cultures are a result of these cytokines, particularly IL-6, produced by the cells and activating STAT3. We cannot rule out that LIF may play a role as LIF is a more potent cytokine than IL-6, and may be able to exert the same effects at a lower concentration [177]. However, the potency of LIF versus IL-6 was assessed on microvascular and endothelial cells, so it may still be premature to assume that LIF is having the same effect in nerve regeneration.

While TCP cultures can offer valuable data regarding the ability of the conditioned medium to promote neuritogenesis, TCP is hardly a practical medium to examine the effect of NI-MiMPC CM on nerve regeneration in a more clinically relevant study. In addition, obtaining true neurite length measurements from DRGs cultured on TCP was extremely difficult with little reliability, due to the highly disorganized neurite growth patterns exhibited. In our attempts to trace neurite lengths in these cultures, we could not accurately determine which path the neurite took, so in order to avoid unintentional inaccuracies in length measurements, we did not measure neurite elongation lengths on TCP cultures, instead examining this parameter only on aligned scaffold cultures. However, qualitative morphological observation clearly showed that axon extension lengths and sizes of DRG cultures were markedly decreased. This phenomenon could also be concluded simply from the fact that only a fraction of imaging tiles were needed to fully image the entire DRG culture at the same magnification compared to cucurbitacin-free cultures.

We examined the length parameter only when DRGs were cultured on aligned nanoscaffolds. As scaffolds are commonly used in the clinic to repair nerve gaps, the electrospun nanoscaffolds used offer a meaningful construct in which to examine the effect of NI-MiMPC conditioned medium in a more physiological and clinically relevant manner. As biomaterials technologies advance, it may be feasible to engineer a single scaffold construct to house both injured nerves and stem cells.

4.0 NEUROTROPHICALLY INDUCED MIMPCS ENHANCE LENGTH OF DORSAL ROOT GANGLION NEURITE EXTENSIONS IN ELECTROSPUN SYNTHETIC NANOSCAFFOLD CULTURES

4.1 INTRODUCTION

Successful surgical treatment of peripheral nerve injury greatly depends on the mechanism of injury and time to treatment. The current gold standard treatment for traumatic nerve injury is the nerve autograft. Allograft transplants and blood vessel conduits are also favored methods in surgical intervention. However, these treatment methods are fraught with limitations—in the case of a nerve autograft, harvesting a donor nerve is invasive and damages otherwise healthy nerves and tissues, possibly with associated donor site morbidities, in a patient already suffering from the initial injury. Generally, autograft donor sites are primarily sensory nerves, which is a further limiting factor because it precludes proper treatment of motor nerves (tibial) or motor-sensory (sciatic) [188]. Regeneration in mismatched nerve types may be due to differences in size, alignment, axonal size and distribution [189].

Nerve allografts and autologous blood vessel transplants can offer a solution that doesn't require a secondary injury, but is limited in that the surgeon must be able to match both the diameter and length required in the case of blood vessels, and alignment, axonal size and

distribution in the case of nerve allografts. Synthetic scaffolds are an option in the clinic as well; however, the use of biodegradable scaffolds is not associated with a high recovery rate [190].

Electrospun fibrous scaffolds offer a candidate substrate for nerve repair. Ideally, such scaffolds should be flexible enough to allow for movement, yet remain mechanically stiff enough to provide the needed support. They should be highly customizable and able to take any shape necessary [191] for a tensionless repair.

Commercially available nerve conduits are hollow tubes that aim to provide structural support for the regenerating injured nerve. These nerve guides aim to emulate the natural topographical microenvironment that would typically form during the natural healing process. For example, synthetic scaffolds can be electrospun with aligned strands to mimic the bands of Büngner, formed by proliferating Schwann cells. Unlike traditional approaches, the advancement of biomaterials and electrospinning technology allows for fine-tuned control over various parameters such as material, rate of degradation, length and diameter. Poly-ε-caprolactone (PCL) is a biodegradable polymer that can be easily prepared and electrospun. Due to its high biocompatibility and slow degradation rate, it may be well suited for *in vivo* transplantation [192]. An added advantage to PCL is that it has already been approved for clinical use, which potentially lessens regulatory hurdles [193].

Synthetic materials can be combined with other structural supportive materials, such as gels, sponges, or films, which can enhance the biochemical support capacity of the nerve guide and more closely imitate the function of Schwann cells and the bands of Büngner. One such example is gelatin. Gelatin is denatured collagen, and has been used extensively in the food, pharmaceutical and cosmetic industries. The fact that it is relatively inexpensive and can be

completely resorbed *in vivo* without immunogenic reactions makes it an ideal candidate for use in tissue engineering [194].

Gelatin can be chemically modified for photocrosslinking by UV light in the presence of a photoinitiator to form a hydrogel, allowing for cell encapsulation [191]. The ability to interface cellular therapy with biomaterials is important for applying these scaffolds in tissue engineering. The incorporation of live cells into nerve scaffold constructs may provide a biochemical support system for the regenerating nerve in addition to physical support. However, many limitations still exist that prevent live cell seeding on scaffolds during fabrication (i.e., organic solvents used to dissolve photoinitiators are cytotoxic, and cellular DNA damage results from UV light crosslinking), and cells are therefore frequently seeded after scaffold fabrication, which results in incomplete and inefficient cell distribution, and subsequent uneven tissue regeneration [191, 195].

The design and materials used in our scaffold circumvents the aforementioned limitations of typical nerve constructs. Lin, et al developed a composite scaffold incorporating polycaprolactone (PCL) with methacrylated gelatin. The authors used visible light and a visible light-activated initiator, allowing seeded cells to survive the photocrosslinking and encapsulation process [191]. PCL lent structural support, while the “sacrificial” gelatin fibers served three purposes—when the gelatin fibers contact water, the gelatin melts and coats the PCL fibers, creating an adherent surface for cells in the scaffold lumen. The gelatin also acts as a glue that holds the PCL fibers together, allowing the creation of a multilayered PCL scaffold that has the strength to retain sutures. Finally, the gelatin can encapsulate cells within the scaffold wall, providing a biocompatible structure for cells [191].

Our goal is to interface this technique of photocrosslinkable gelatin with scaffolds to encapsulate live cells and provide both a biochemical and structural support for nerve axon regeneration. Extrapolating from the enhanced growth measured in the previous chapter, we hypothesize that MiMPCs will have a positive effect on DRG/scaffold cultures, and that with aligned electrospun nanoscaffolds, we will be able to quantitatively determine meaningful length measurements of axon extensions.

4.2 METHODS

4.2.1 Synthesis of Photoinitiator LAP

The visible-light sensitive initiator lithium phenyl-2,4,6-trimethylbenzoylphosphinate (LAP) was synthesized as described by Fairbanks et al [196].

4.2.2 Preparation and photocrosslinking of methacrylated gelatin (mGelatin)

mGelatin was prepared by reacting gelatin (type B) (Sigma-Aldrich) with methacrylic anhydride using our recently published protocol [191]. Photocrosslinking was initiated using the visible-light sensitive initiator lithium phenyl-2,4,6-trimethylbenzoylphosphinate (LAP) [196].

Briefly, 15 g gelatin (type B) (Sigma-Aldrich) was dissolved in 500 mL water and placed in a 37° C shaker at 106 rpm for 2h or until dissolved. Subsequently, 12 mL methacrylic anhydride (Sigma-Aldrich) was added to the solution and it was placed back into the shaker

overnight. The resulting solution was dialyzed against deionized water using 2000 NMWCO dialysis tubing (Sigma-Aldrich) for a total of 3 days with at least 10 water changes. This was then lyophilized to obtain a foamy solid.

4.2.3 Fabrication of Electrospun Scaffolds

To create electrospun scaffolds, two separate solutions of (1) 14.0% w/v PCL (80 kDa; Sigma-Aldrich) in 2,2,2-trifluoroethanol (Sigma-Aldrich) and (2) 18% methacrylated-gelatin (mGelatin) in 95% 2,2,2-triflurorethanol in water. To fabricated aligned scaffolds, a custom-designed electrospinning device was utilized to generate a 40:60 composite scaffold consisting of mGelatin and PCL fibers. Two 10-mL syringes were separately filled with the PCL and mGelatin electrospinning solution, and they were fitted with a stainless steel 22G blunt-ended needle that served as a charged spinneret, and directed at a single central rotating mandrel (surface velocity of 10 m/s). The speed of the mandrel was sufficiently fast to align the collected fibers in a single direction. A flow rate of 2 mL/h was maintained with a syringe pump (Harvard Apparatus, Holliston, MA). A power supply (Gamma High Voltage Research, Inc., Ormond Beach, FL) applied a +15-20 kV potential difference between the needles and grounded mandrel to obtain a taylor cone for mGelatin and a +7-10 kV potential difference for PCL. Additionally, two aluminum shields charged to +5kV were placed perpendicular to and on either side of the mandrel to better direct the electrospun fibers toward the grounded mandrel. The distance between the mandrel and the needle was 15 cm for mGelatin fibers and 15 cm for the PCL fibers. The composite electrospun scaffold was generated with a final thickness of 100μm. The procedure was the same for creating randomly aligned scaffolds, except that the mandrel surface

velocity was 0.75 m/s. Scaffold alignments (random or aligned) were assessed via scanning electron microscopy.

4.2.4 Preparation of medium infused scaffold and seeding of DRG

A culture medium-mGelatin solution was prepared by combining concentrated 48hr BCM (concentrated using 3kD centrifugal filter tubes from Millipore [Billerica, MA], and spinning at 3800g for 20 minutes) with 40%w/v methacrylated gelatin in Hank's Balanced Salt Solution (HBSS; ThermoFisher) in a 3:1 ratio of 450 μL to 150 μL, to which 1.8 mg of photoinitiator LAP was added to achieve a 0.3% w/v concentration of the photoinitiator. A 3.0 x 5.5 cm sheet of composite scaffold consisting of either aligned or random fibers prepared as described above was wetted with 540 μL of the medium-mGelatin solution. Following this, each scaffold was folded lengthwise (along the 5.5 cm side) into thirds. The remaining 60 μL of the medium-mGelatin solution was then evenly applied on top of the folded random scaffold, and then the folded aligned scaffold was placed on top of that. The 6-layered construct was then exposed to visible light for 3 minutes (1.5 minutes on each side) to photopolymerize the construct. After construction of the completed multilayer scaffold, five cylinders of 8 mm diameter were punched out with a punch biopsy.

In cell-containing scaffolds, cells were trypsinized and combined with the condensed culture medium-mGelatin solution and applied to scaffolds at 1 million cells per scaffold construct. All scaffolds (with and without cells) were prepped the same day as DRG isolations and kept in basal medium (DMEM-F12, 5% FBS, ITS-X and pen-strep; all from ThermoFisher) until needed. DRGs were seeded via the following: upon isolation from the chick embryo, DRGs were individually pipetted, and pipette tips were held above the scaffold and below the level of

medium in the well. To ensure more accurate placement on the scaffolds, DRGs were allowed to descend out of the pipette via gravity, rather than being actively pipetted.

4.2.5 Live/Dead staining

Cells were encapsulated in mGelatin and seeded onto the random fibers side of electrospun scaffolds. They were cultured for 24 hours prior to staining with Live/Dead assay (ThermoFisher). Cell viability was assessed via fluorescence microscopy images.

4.2.6 MTS assay

Cells were encapsulated in mGelatin and seeded onto randomly aligned electrospun fibers. All cells were cultured in normal growth medium. 3-(4,5-dimethylthiazol-2-yl)-5-(3-carboxymethoxyphenyl)-2-(4-sulfophenyl)-2H-tetrazolium (MTS [CellTiter96 Aqueous one solution cell proliferation assay]; ThermoFisher). MTS reagent was diluted 1:5 with FluoroBrite DMEM medium (ThermoFisher) and 1.25 mL was incubated with scaffold cultures for 1.5 hours each, at days 0 (5 hours after initial seeding), 3 and 7 timepoints. After 1.5 hours, MTS/FluoroBrite reagent was collected from the scaffolds and absorbencies read at 480 nm wavelengths.

4.2.7 Quantitation of neurite extension lengths

Neurite extension lengths were quantified based on images of DRGs cultured on 2-dimensionally aligned nanofibrous poly-ε-caprolactone (PCL) scaffolds prepared by

electrospinning (see below). All images for scaffold cultures were taken at 10x using the inverted Olympus scope (IX81). Extension lengths were traced using Fiji/NIH ImageJ. Tracings were converted from pixel length into μm measurements using the scale of 1245 px = 800 μm.

4.2.8 Statistical analysis

All quantitative data are presented as means ± standard deviation, unless noted otherwise. Statistical differences and p-values ($p<0.05$) are denoted with a * and are determined by Levene's and Tukey's tests.

4.3 RESULTS

4.3.1 Random and aligned electrospun fibers

Electrospun scaffolds were imaged using scanning electron microscopy (SEM) to show the dual surfaces of the PCL-mGelatin composite scaffold. On one side, fibers are aligned (Figure 13A-B) while the opposing side shows random fibers (Figure 13C-D). By combining aligned and randomized fibers into a single scaffold construct, we have created optimal surfaces for both cell adherence and growth and guidance of DRG axon extensions. SEMs of the composite scaffolds show thin bands of mGelatin that crosslink to form a multilayered construct with integrated layers of PCL (Figure 13A, C).

4.3.2 Medium conditioned by neurotrophically induced MiMPCs enhance dorsal root ganglia (DRG) neurite extension lengths

We next determined the influence of NI-MiMPCs on DRG neurite length. This was carried out using embryonic chicken DRGs cultured on electrospun 2D aligned nanofibrous PCL/gelatin scaffolds, which afforded more consistent and reliable measurements of neurite length (Figure 14), as the aligned fibers helped to better organize neurite outgrowth, and allowed visualization and more accurate measurements of axonal distance covered. However, as aligned fibers organized DRG axonal growth, Sholl analysis to determine neurite density was not possible, and not included in the results of this chapter.

In doing so, we found that culturing DRGs in conditioned medium from any cell group significantly increased the length of neurite extensions compared to controls, although there was no difference between conditioned medium taken from any cell group (maximum length achieved with conditioned medium was 2,650 μm, while control lengths averaged 1,389 μm, an increase of 47.6%) (Figure 14 F-G).

4.3.3 TrkB receptor does not play a part in enhancing DRG axonal extension lengths

Again, we co-administered 24 nM of GNF5837 to determine if any factor acting through the Trk receptors played a role in altering length of the extensions. It has been reported that BDNF, acting through TrkB, is capable of activating STAT3, which is essential in axon extension [37]. However, the addition of the pharmacological blocker to conditioned medium did not result in a difference in neurite extension lengths when groups were compared to each other (Figure 15). All NI- and GM- conditioned medium groups significantly promoted axonal

extension lengths compared to controls, even with 24 nM GNF5837 supplemented. GM-MiMPCs and MSCs enhanced axonal length 1.93 and 1.62 times, respectively, compared to controls. NI- MiMPCs and MSCs similiarly enhanced axonal lengths 1.82 and 1.86 times, respectively, compared to controls (Figure 15 F-G).

These results led us to conclude that BDNF was unlikely to be the sole factor produced by the NI- or GM-MiMPCs that contributed to neurite extension length, suggesting the action of another signaling pathway.

4.3.4 IL-6 produced by MiMPCs contribute to DRG axon extension length

In the previous chapters, PCR and ELISA data confirmed that NI-MiMPCs produced and maintained a high level of IL-6 compared to uninduced cells (Figures 7 and 8), so our next set of experiments focused on the possible involvement of IL-6 on neurite extension length of DRGs cultured on 2D scaffolds. In addition, we also observed an apparent decrease in axon extension lengths in TCP cultures, but again, was unable to accurately measure length with such disorganized growth.

To test the possible involvement of IL-6 in neurite extension lengths, we chose the drug cucurbitacin-I to inhibit the Jak/STAT3 pathway [185]. Upon administration of cucurbitacin-I (60 nM) to the conditioned media, a dramatic decrease in neurite extension length of DRG cultures was once again observed (Figure 16). However, unlike results obtained in chapter 2, where axonal growth was merely truncated, DRG axon extensions were abolished on 2D scaffold cultures. This indicated that the actions of the Jak/STAT3 pathway and, by implication, the action of IL-6, was critical to neurite length, particularly in a setting of organized axon growth.

Since there were no observable extensions from the cucurbitacin-I treated group, these measurements were not included in Figure 16. As the complex, aligned topography is likely to be more relevant to tissue architecture *in vivo*, these results are consistent with an important role of IL-6 signaling through the Jak/STAT pathway in mediating the improvement of the length and complexity of neurite extensions by the MSC/MiMPC conditioned media.

4.3.5 Cells survive the process of being encapsulated in gelatin on scaffolds

To determine if our cells could survive the encapsulation process, we performed Live/Dead staining of the cells after seeding the cell/gelatin mixture onto the randomly aligned side of the 2D scaffolds. The fluorescent image in Figure 17 is representative of Live/Dead staining of the scaffold, showing that at least 50% of the seeded cells survived after 24-hours of culture, determined via manual count.

To determine if the surviving cells were sufficient for enhancing DRG axonal outgrowth, cells and DRGs were co-cultured on the scaffolds. Our MTS assay showed that MSCs proliferated between days 0, 3 and 7 in 2D scaffold cultures. MiMPCs maintained a steady level of metabolic activity, but did not seem to increase in number.

4.3.6 Incorporating cells in 3D scaffolds enhances DRG neurite extension growth

NI- or GM- cells were encapsulated in mGelatin and seeded on the random fibers side of the scaffold. These were co-cultured with DRGs (seeded on the aligned fibers side) on the scaffolds, and axon extension lengths were measured. Control DRG culture scaffolds were not seeded with cells. To assess if cells alone could continue producing necessary factors for nerve growth, only

basal medium, and no conditioned medium, was used in all co-cultures. Measurements were significantly higher in co-cultures containing NI- or GM- MiMPCs and MSCs when compared to cell-free controls. Encapsulated NI-MiMPCs and NI-MSCs promoted axonal extensions that were 2.03 times and 2.17 times longer than controls, respectively. GM- MiMPCs and MSCs offered similar benefits (1.88 and 1.65 times longer than controls) (Figure 18 F-G). There was no significant difference in lengths of axons measured between DRGs cultured with encapsulated induced and non-induced cells, or between MIMPC and MSC groups (Figure 18).

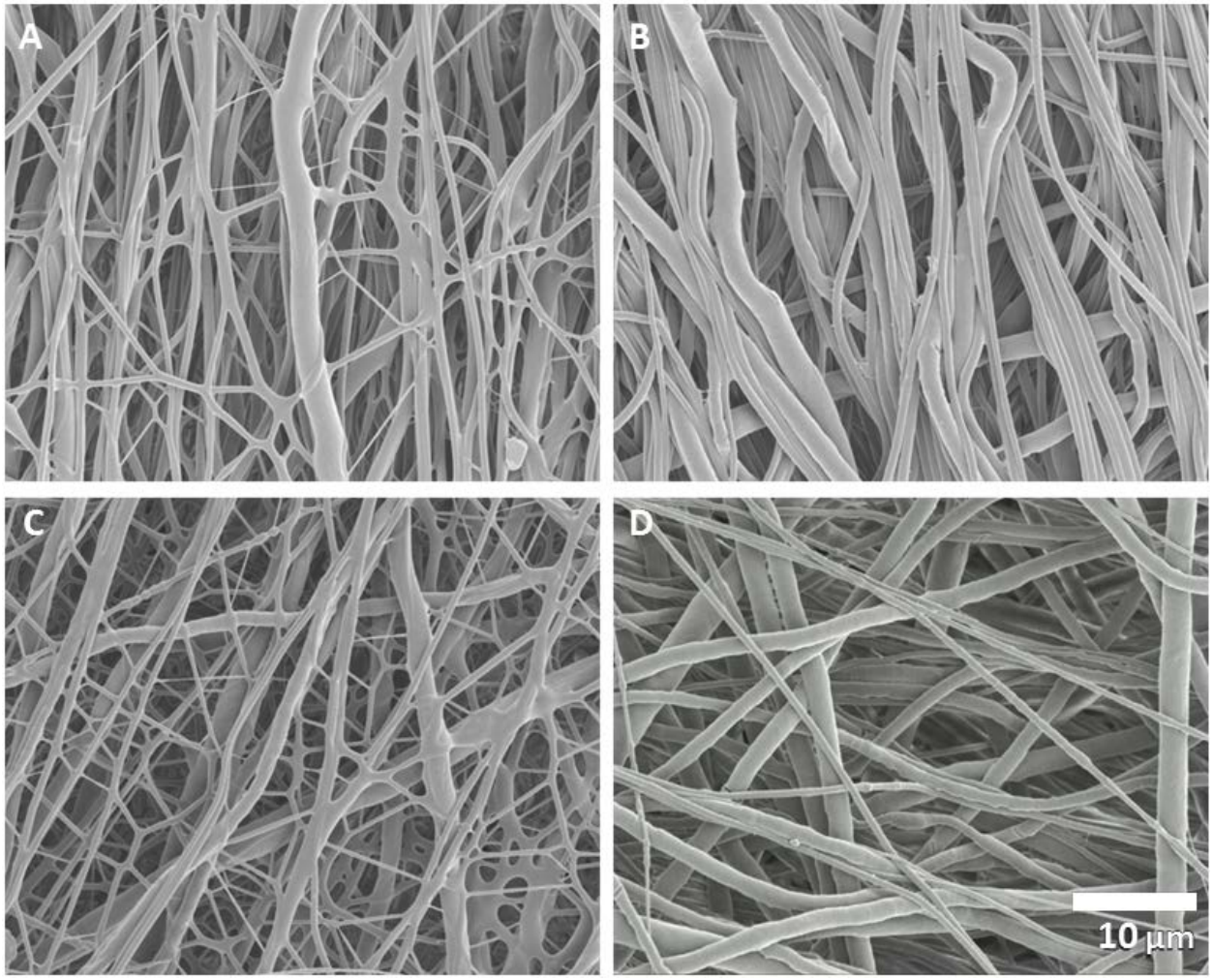

Figure 13: Scanning electron microscopy images of polycaprolactone/mGelatin composite scaffolds

SEM images of (A) Aligned PCL/mGelatin composite scaffold, (B) aligned PCL scaffold, (C) random PCL/mGelatin composite scaffold, and (D) random PCL scaffold. SEM of scaffolds with mGelatin revealed thin crosslinking structures that form a multilayered PCL scaffold.

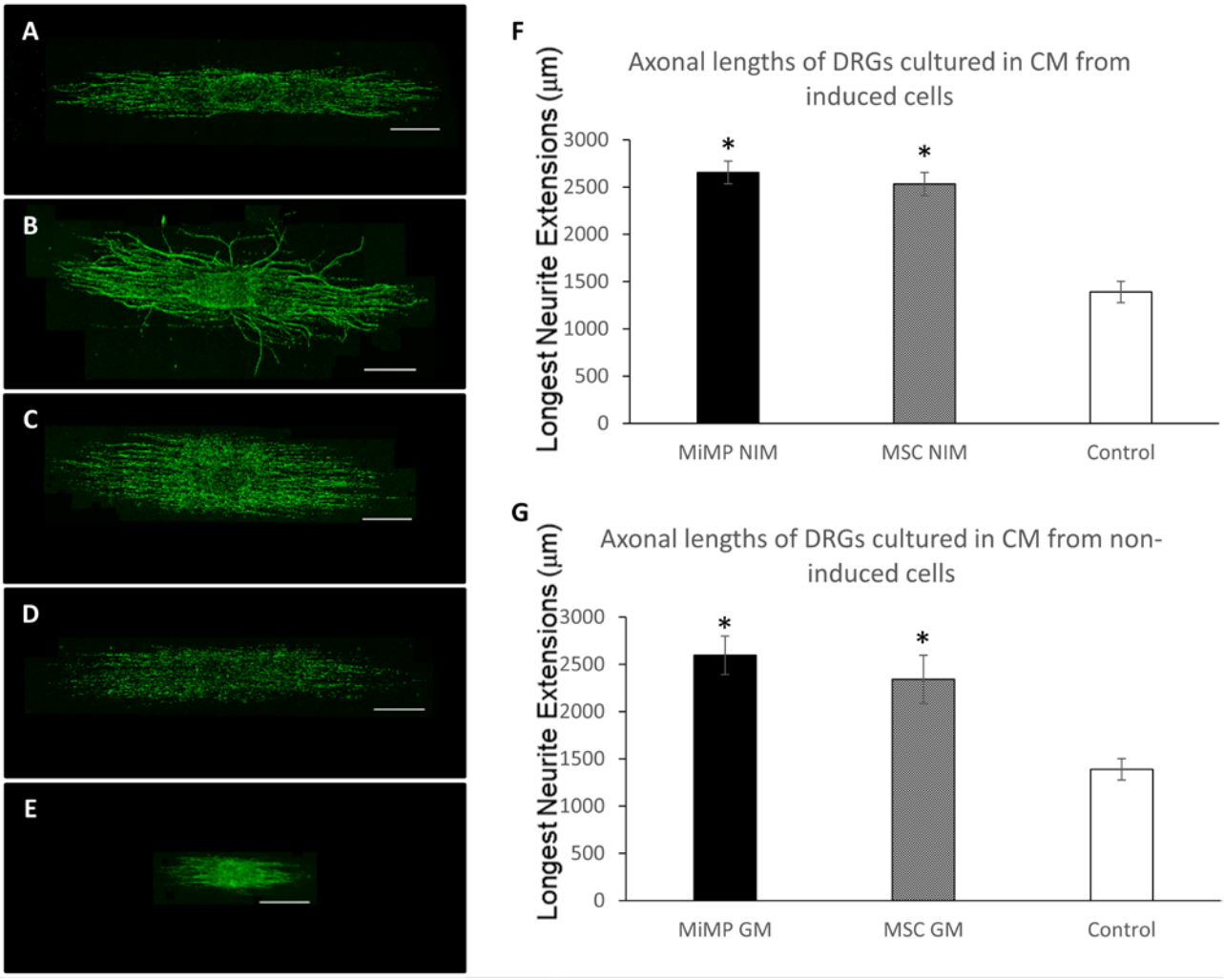

Figure 14: Morphologic and quantitative comparison of DRG axonal outgrowth
Dorsal root ganglia (DRGs) were cultured for 5 days on aligned electrospun scaffolds in medium conditioned for 48 hours by **(A)** NI-MiMPCs, **(B)** NI-MSC, **(C)** GM-MiMPCs, or **(D)** GM-MSCs. Controls in **(E)** show DRGs cultured for 5 days in unconditioned basal medium. All DRGs presented in this figure are representative cultures, and were stained with anti-heavy neurofilament antibody and imaged via fluorescent microscopy. Morphological observation of DRGs in images **A-D** show an increase in axon extension lengths compared to controls. **(F)** Axonal extension tracings on DRGs show that conditioned medium (CM) collected from both NI- MiMPCs and MSCs significantly enhanced neurite extension lengths over controls. **(G)** The 10 longest axonal extensions were traced in ImageJ and averaged, and show that conditioned medium from GM- MiMPCs and MSCs significantly enhance neurite extension outgrowth ($p<0.05$) compared to controls. All images were taken at 10x, and scale bars represent 800 µm. * denotes a significant difference ($p<0.05$) as compared to controls, determined by Tukey's HSD test.

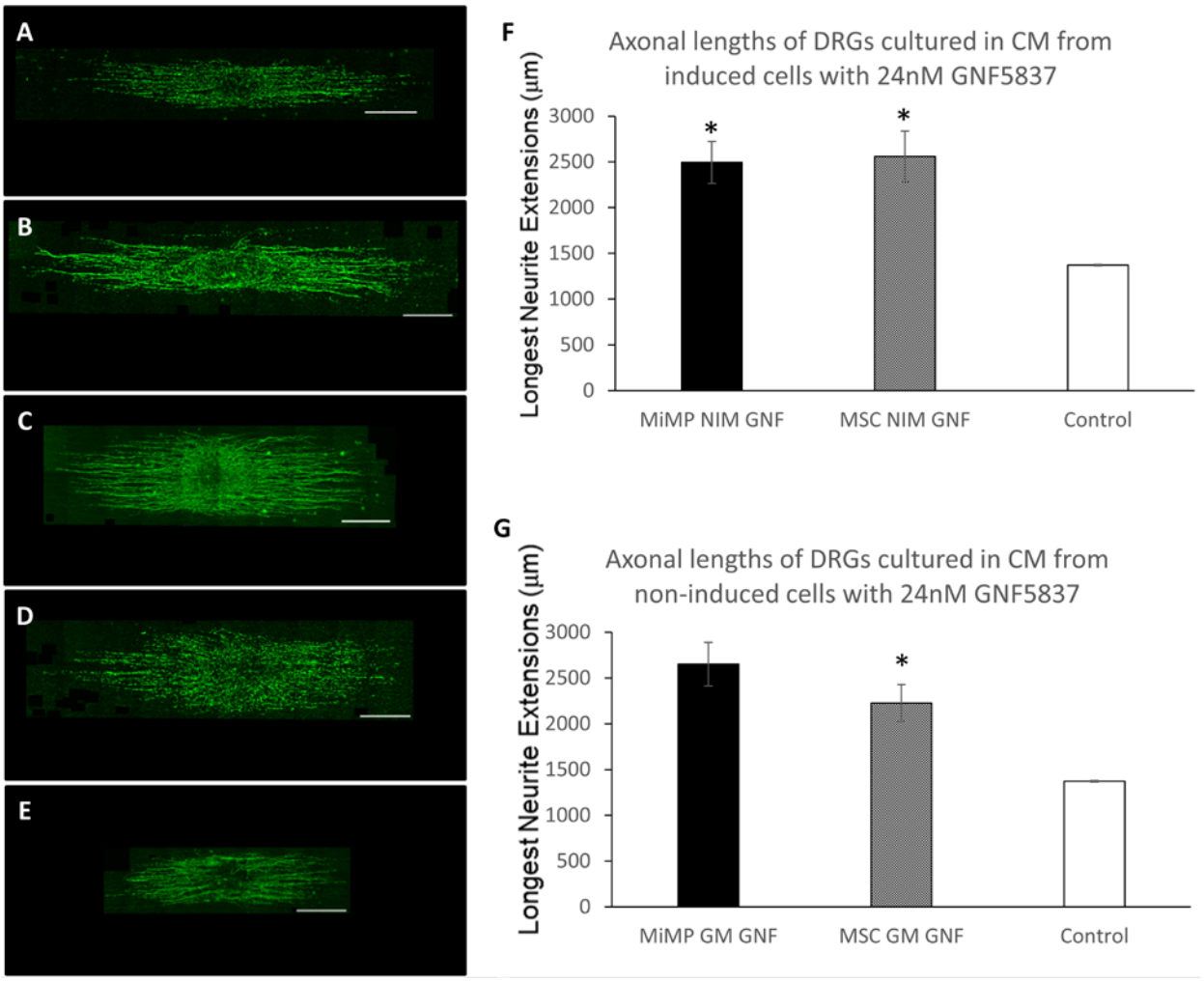

Figure 15: Morphologic and quantitative comparison of DRG axonal outgrowth supplemented with 24nM GNF5837

DRGs were cultured for 5 days on aligned electrospun scaffolds in medium conditioned for 48 hours by **(A)** NI-MiMPCs, **(B)** NI-MSC, **(C)** GM-MiMPCs, or **(D)** GM-MSCs. All cell conditioned medium was supplemented with 24 nM pan-Trk receptor inhibitor GNF5837. Controls in **(E)** show DRGs cultured for 5 days in unconditioned basal medium supplemented with 24 nM GNF5837. All DRGs presented in this figure are representative cultures, and were stained with anti-heavy neurofilament antibody and imaged via fluorescent microscopy. Morphological observation of DRGs in images **A-D** show an increase in axon extension lengths compared to controls. **(F)** Axonal extension tracings on DRGs show that conditioned medium (CM) collected from both NI- MiMPCs and MSCs significantly enhanced neurite extension lengths over controls. **(G)** The 10 longest axonal extensions were traced in ImageJ and averaged, and show that conditioned medium from GM- MiMPCs and MSCs significantly enhance neurite extension outgrowth ($p<0.05$) compared to controls. All images were taken at 10x, and scale bars represent 800 µm. * denotes a significant difference ($p<0.05$) as compared to controls, determined by Tukey's HSD test.

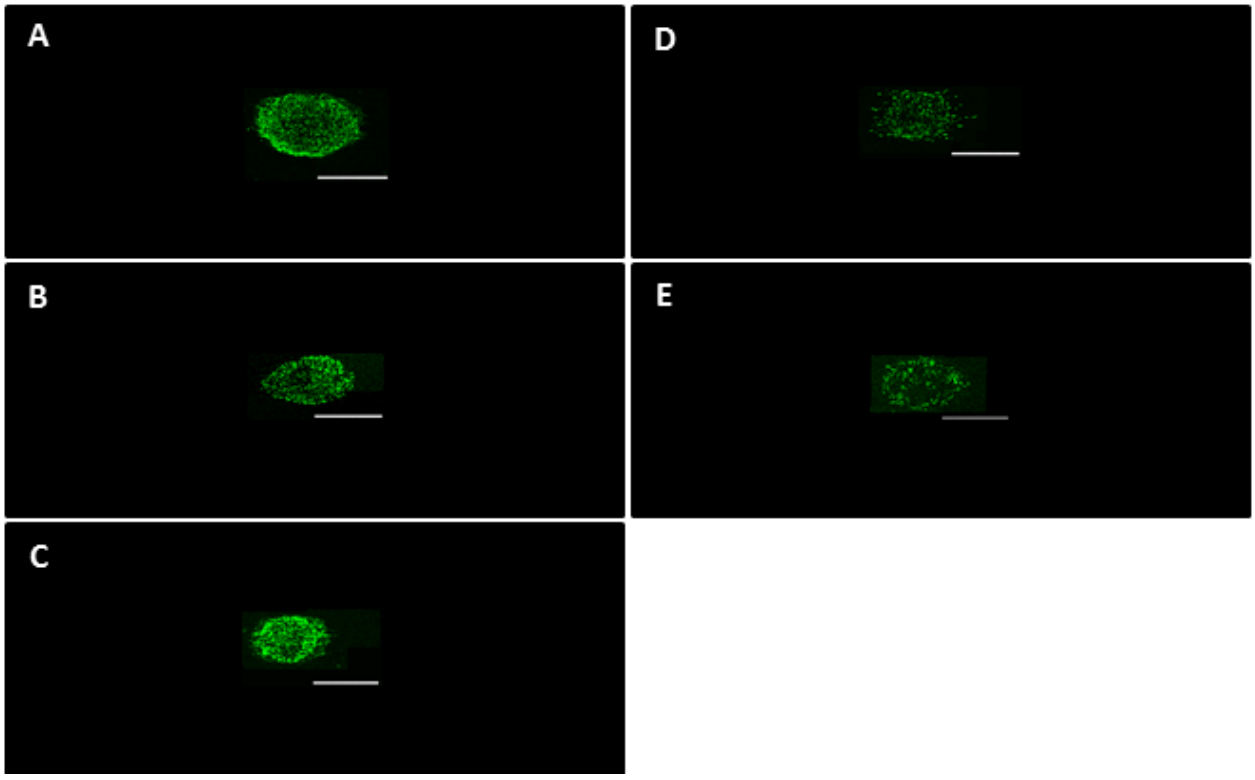

Figure 16: Morphologic and quantitative comparison of DRG axonal outgrowth supplemented with 60 nM cucurbitacin-I

DRGs were cultured for 5 days on aligned electrospun scaffolds in medium conditioned for 48 hours by **(A)** NI-MiMPCs, **(B)** NI-MSC, **(C)** GM-MiMPCs, or **(D)** GM-MSCs. All cell conditioned medium was supplemented with 60 nM Jak/STAT inhibitor cucurbitacin-I. Controls in **(E)** show DRGs cultured for 5 days in unconditioned basal medium supplemented with 60 nM cucurbitacin-I. All DRGs presented in this figure are representative cultures, and were stained with anti-heavy neurofilament antibody and imaged via fluorescent microscopy. Morphological observation of DRGs in images **A-E** show no visible axon extensions. All images were taken at 10x, and scale bars represent 800 µm.

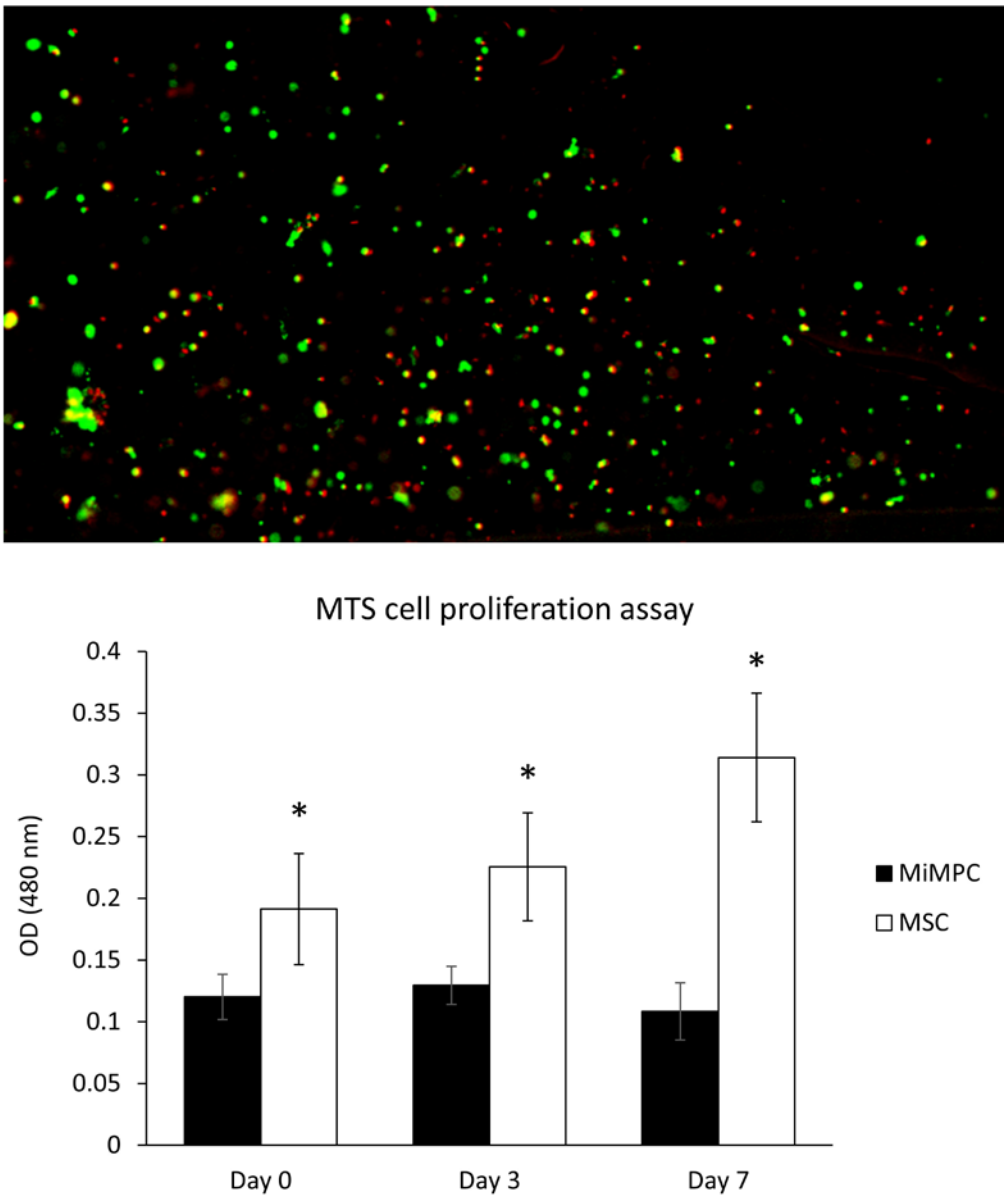

Figure 17: Viability of mGelatin encapsulated MiMPCs seeded onto composite scaffolds as determined by Live-Dead and MTS assays

MiMPCs encapsulated in mGelatin, seeded onto the random fibers side of crosslinked scaffold. Fluorescence microscopy image of live-dead assay shows over 50% of cells are viable after 24-hours in culture. MTS assays, where cells were incubated with MTS reagent for 1.5 hours on Days 0, 3 and 7 of culture shows that MSCs proliferate after encapsulation and seeding onto 2D scaffolds over the course of 7 days, while MiMPCs maintain steady cell numbers in scaffold cultures. * denotes a significant difference ($p<0.05$) as compared to MiMPCs, determined by Tukey's HSD test.

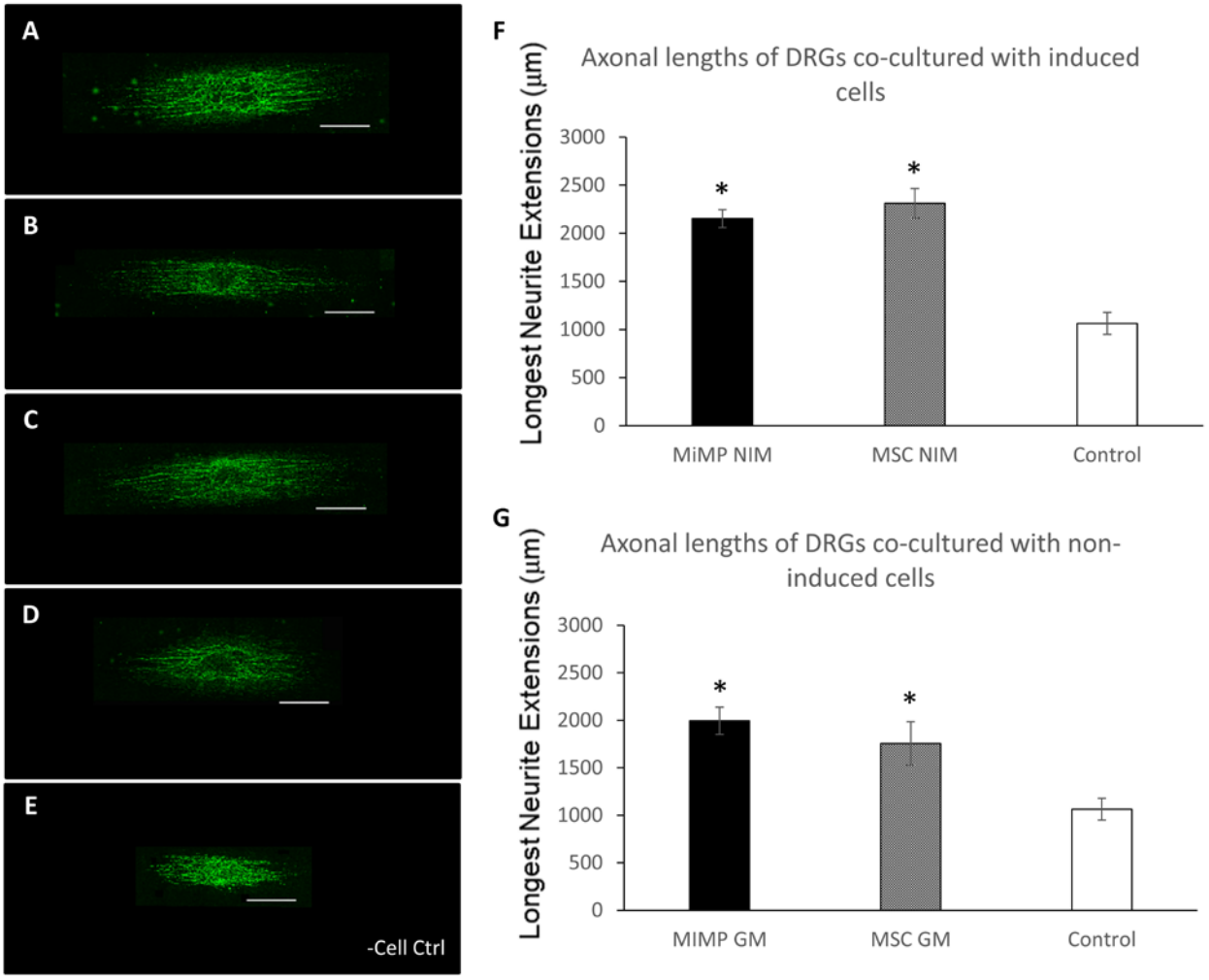

Figure 18: Morphologic and quantitative comparison of DRG axonal outgrowth when co-cultured with cells on 2D electrospun aligned scaffold

Dorsal root ganglia (DRGs) were co-cultured with **(A)** NI-MiMPCs, **(B)** NI-MSC, **(C)** GM-MiMPCs, or **(D)** GM-MSCs, for 5 days on aligned electrospun scaffolds in basal medium. Controls in **(E)** show DRGs cultured for 5 days in basal medium with no cells present. All DRGs presented in this figure are representative cultures, and were stained with anti-heavy neurofilament antibody and imaged via fluorescent microscopy. Morphological observation of DRGs in images **A-D** show an increase in axon extension lengths compared to controls. **(F)** Axonal extension tracings on DRGs show that co-culture with NI- MiMPCs and MSCs significantly enhanced neurite extension lengths over controls. **(G)** The 10 longest axonal extensions were traced in ImageJ and averaged, and show that co-culture with GM- MiMPCs and MSCs significantly enhance neurite extension outgrowth ($p<0.05$) compared to controls. All images were taken at 10x, and scale bars represent 800 µm. * denotes a significant difference ($p<0.05$) as compared to controls, determined by Tukey's HSD test.

4.4 DISCUSSION

Biomaterial scaffolds provide physical support and can mimic the microenvironmental textures and structures found in native tissue. Living cells can be interfaced with scaffolds to facilitate cell coverage and regeneration of the injured area. As living tissues are complex, heterogeneous systems comprised of multiple cell types and tissue layers that function in tandem, composite scaffolds have generally yielded better outcomes than homogenous scaffolds [197, 198]. The composite nature of our scaffolds allows for fabrication of a multilayered construct comprised of both aligned and random fibers. The methacrylated gelatin component of the scaffold allowed for crosslinking and forming a durable structure out of both types of fibers.

Topographical cues have long been found to affect cell adhesion, growth and differentiation [101, 102, 104]. Multiple studies have shown the advantages of culturing DRGs on aligned surfaces, with data showing improved adherence and axon elongation, as well as increased organization among regenerated axons [31, 103, 199]. Due to the favorable environment that an aligned nanotopographical surface might provide, we examined the potential advantage of combining our conditioned medium with scaffolds for DRG cultures. However, studies have shown that MSCs proliferate significantly more when cultured on randomly aligned nanofibers when compared to aligned fibers, as well as providing structural strength and suture retention for *in vivo* use later [200]. Due to the differences in topographical preferences of the cells, we felt it prudent to create a scaffold that could optimally house both nerves and their support cells.

Our results from the MTS assays of MSCs cultured on 2D randomly aligned nanofibers agree with those presented by Jahani, et al [197] as, over the course of 7 days, MSCs continued to proliferate in 2D scaffold cultures. However, while MiMPCs maintained a steady level of

metabolic activity, there was no indication of MiMPC proliferation comparable to that seen in MSCs (Figure 17). This suggests that encapsulation by gelatin doesn't necessarily impede cell proliferation, as MSCs are capable of growing, but rather that perhaps reduced proliferation is specific to the MiMPC. This may imply that MiMPCs are not as robust as MSCs in terms of hardiness and tolerance of growth environments. However, considering the growth enhancement results seen in DRG cultures, we do not feel that the discrepancy in proliferative prowess between MiMPCs and MSCs is a critical factor. The fact that fewer MiMPCs are needed to achieve the same results as MSCs may be an argument in favor of using MiMPCs over MSCs, as this property of the MiMPC may be more economical and time-saving in the end.

Length measurements showed enhanced DRG axon elongation from conditioned medium cultures compared to controls, though there were no significant differences between the various conditioned medium groups. When cells were seeded into the scaffold, DRGs also exhibited enhanced axon elongation, although again, there were no significant differences between the various cell types (i.e., between GM- or NI- cell groups). For practicality purposes, this finding may give us reason in future *in vivo* experiments to simply use GM- cells or conditioned medium taken from GM- cells. The reagents for NI- treatment can be costly, and as this parameter is seemingly unaffected by NI- treatment, it may be more economical to include only GM- cells in our studies.

BDNF has been extensively studied, and proven to play roles in peripheral nerves relating to survival, growth and repair. However, DRG axon elongation was seemingly unaffected with the supplementation of 24 nM of GNF5837, a potent pan Trk-receptor inhibitor. As MiMPCs do not produce CNTF or GDNF, and the actions of other Trk-receptor mediated neurotrophin signaling was blocked by GNF5837, it is again plausible that BDNF either does not play as large

a role in axon elongation as other factors (i.e. IL-6), or that there is a compensatory or crosstalk mechanism between signaling pathways that can promote axon elongation even in the absence of any Trk-receptor mediated signaling.

Cytokines in the IL-6 cytokine superfamily signal through the gp130 receptor to activate the Jak/STAT3 pathway, which has been shown to be important in the growth of neurite extensions and nerve regeneration [175, 201]. Our ELISA results (Figure 8) showed that NI-MiMPCs were able to maintain production of cytokines in this family, including IL-6 and LIF, but not others, such as oncostatin-M and ciliary neurotrophic factor (CNTF) (data not shown). We postulated that these pro-inflammatory cytokines secreted into the conditioned medium from NI-MiMPCs could act through the Jak/STAT3 pathway to maintain improved neurite outgrowth, even when Trk-receptors were blocked.

The addition of 60 nM of cucurbitacin-I inhibited axonal outgrowth from the DRG on the 2D scaffold, whereas on TCP, cucurbitacin-I truncated, but did not completely abolish, axonal outgrowth. This observation suggested that the effects of cucurbitacin-I on outgrowing neurites could be influenced by different substrate surfaces, i.e., tissue culture plastic *versus* nanofibers. All experiments were performed with MiMPCs differentiated from human MSC-derived iPSCs, and the results were compared to those achieved by human MSCs. For these reasons, scaffolds have become an important tissue engineering tool.

By blocking the activation of the Jak/STAT3 pathway with the pharmacological blocker, cucurbitacin-I, we observed that our conditioned medium could not rescue the length of neurite extension, regardless of whether the conditioned medium was taken from induced cells or not. From this, it is likely that the superior lengths of neurite extensions found in conditioned medium cultures are a result of these cytokines, particularly IL-6, produced by the cells, activating

STAT3. We cannot rule out that LIF may play a role as LIF is a more potent cytokine than IL-6, and may be able to exert the same effects at a lower concentration [177]. However, the potency of LIF versus IL-6 was assessed on microvascular and endothelial cells, so it may still be premature to assume that LIF is having the same effect in nerve regeneration.

Overall, our findings show that MiMPCs can provide similar advantages as MSCs, which makes MiMPCs clinically applicable, and can serve as a less invasive and, more importantly, sustainable therapeutic method. The growth advantages associated with MiMPC cells or conditioned medium can be coupled with the benefits yielded by aligned scaffolds. Together, the two components make a renewable, biodegradable, clinically relevant system that can improve nerve regeneration after traumatic injury.

5.0 SUMMARY AND FUTURE DIRECTIONS

Traumatic peripheral nerve injury remains a challenging field in regenerative medicine. The current gold standard of treatment is the nerve autograft, even though only 40-50% of patients exhibit functional recovery after the procedure [202]. Timely treatment is of utmost importance in nerve injuries, and though advances in microsurgical techniques and biomaterials have improved the outcome of surgical treatment, a purely surgical approach has seemingly reached its limit in effectiveness. Promising further advancement in peripheral nerve treatment may lie in delivery of supplementation of factors that can lend biochemical support. Current regenerative medicine research has shown significant interest in the use of stem cells, particularly induced pluripotent stem cells (iPSCs), in various applications, including peripheral nerve regeneration.

It is well established in the literature that mesenchymal stem cells (MSCs) can have neurotrophic effects given modulation of their chemical environment. As iPSCs are capable of differentiating into MSC-like cells (termed mesenchymally-induced mesenchymal progenitor cells [MiMPCs]), it was hypothesized that the same environmental modulation would yield clinically relevant neurotrophic MiMPCs. The preceding chapters attempted to optimize the use of MiMPCs in a neuro-regenerative capacity, and provided information on the molecular mechanism by which the MiMPC secretome was able to enhance axonal elongation from dorsal root ganglion (DRG) cultures. The most obvious and significant advantage of using MiMPCs as a replacement for MSCs is the fact that they are a virtually limitless source that does not require

invasive procedures to harvest. As MiMPCs are derived from iPSCs, rather than human embryonic stem cells (hESCs), their use also avoids the various ethical quandaries associated with the use of hESCs in research and the clinic. This, however, is counterbalanced by the fact that the MiMPCs are not as robust as the MSCs, and although they are capable of producing high levels of pertinent growth factors, they fail to thrive in neurotrophic induction medium.

In the second chapter, which dealt with optimization and choosing an appropriate line of iPSCs, it was found that iPSCs derived from mesenchymal parentage cells (MiMPCs), as opposed to amniotic epithelial parentage cells (AEiMPCs), yielded the more neurotrophic cell population after neuroinductive (NI) treatment. MiMPCs were able to produce comparatively higher levels of BDNF, and expressed the same mesenchymal and neuronal cell surface markers as MSCs and Schwann cells. As the neurogenic potential of MSCs have been repeatedly demonstrated, and as iPSCs retain epigenetic memory of their parental cell type, it stood to reason that MiMPCs, rather than AEiMPCs, may be more suited to use in nerve related studies, perhaps due to differences in the epigenetic nature of the original cell sources.

Further characterization of MiMPC in terms of their likeness to neurotrophic MSCs and their status as a cell therapy candidate may include studying the immunogenic effects of the MiMPC. This may be especially important as allogenic Schwann cells have been shown to be immunogenic and are rejected by the host *in vivo* [3], as stated previously, and even though this work has shown that MiMPCs share many characteristics with MSCs, it cannot be denied that MiMPCs also exhibit some Schwann-like properties. Of course, autologous Schwann cells do not provoke an immune response, however the drawback lies in the fact that few cells can be isolated, requiring extensive *ex vivo* expansion, and again, requires a secondary nerve injury to the patient that risks scarring, neuroma formation, and functional loss. The immunomodulatory

properties of MSCs are well documented [203]; however, such properties of the MiMPC have not yet been extensively studied. Preliminary *in vitro* studies from our laboratory indicated that, similar to the MSC, MiMPCs were unable to achieve T-cell activation (data not included). Further work into this subject has not been done and was not included in this body of work. However, future studies may require a focus on immunomodulatory characteristics of the MiMPC as neurotrophic work continues *in vivo*.

The third chapter described culturing embryonic chicken dorsal root ganglion (DRGs) with conditioned medium collected from NI-MiMPCs and NI-MSCs. Conditioned medium from all cells, both induced and uninduced, promoted neuritogenesis from the DRG. However, when a pan-Trk receptor inhibitor drug, GNF5837, was supplemented to block the action of BDNF, only conditioned medium from NI-MiMPCs still promoted increased neurite branching density. One possible explanation for this observation is that the NI-MiMPC is producing one or more non-neurotrophin molecules in its secretome that can enhance nerve regeneration independently of the Trk-receptors.

It should be reiterated that there were no significant differences in either neurite complexity or axon elongation lengths in DRG cultures between either co-culture with cells or cultures in conditioned medium from GM- and NI- MiMPC groups. It is noteworthy that while GM-MiMPCs are perfectly capable of enhancing neuritogenesis and axon elongation in traumatic injury, and should certainly be employed as treatments for these injuries to remain cost effective, the benefits NI-MiMPCs appear to convey to DRGs in the presence of Trk-receptor inhibitors may indicate an alternative treatment method in cases such as diabetic neuropathy, where injury is induced by a disease state other than exposure to traumatic injury. Growth factor related-tyrosine kinsases (GFR-TKs), a family of transmembrane proteins in which Trk receptors

are included, have been implicated as part of the disease process in diabetes [204, 205]. It may not be unreasonable to assume that if conditioned medium from NI-MiMPCs is robust enough to enhance DRG growth in the presence of a potent pan-Trk receptor inhibitor, that perhaps the same benefits may be conveyed in the presence of other drugs that can modulate GFR-TK behavior. If this is indeed the case, then it may be possible to treat both diabetic neuropathies in parallel with the underlying causes of the neuropathy itself. There are diabetic mouse models that may be of use in setting up *in vivo* studies for diabetic neuropathies, such as streptozotocin-induced (STZ) diabtetes, high fat diet model, or genetic models [223], and it is also especially promising as a possible future direction for the clinical application of MiMPCs, as MSCs have seen success in alleviating diabetic neuropathies [203, 206, 207].

As stated in the previous chapters, Taylor's group [32, 33, 58], along with others [208, 209], have previously reported that osteonectin is associated with axon regeneration. In order to determine if the MiMPC secreted osteonectin was playing a similar role, we knocked down osteonectin expression with siRNA to generate osteonectin-reduced conditioned medium. Our preliminary data from DRGs cultured with osteonectin-reduced CM suggested that while the presence of osteonectin may be beneficial in conditioned medium from GM- cells, it may play less of a role in conditioned medium from NI- cells (data not shown). Furthermore, when GNF5837 was supplemented to osteonectin-reduced medium, we did not observe the same marked reduction in neurite branching as the results of a similar experiment with Schwann cells that was reported by Taylor's group. This might indicate that NI-MiMPC secretions are distinct enough from those of Schwann cells, and compensatory enough that they are able to encourage neuritogenesis even in the presence of inhibitors or absence of beneficial factors, whereas

Schwann cells are unable. Further study and repetition will be required to determine the effect of osteonectin on DRG neuritogenesis in NI- cell conditioned medium.

It was established in chapter two that MiMPCs are capable of producing IL-6. In addition, there is a wealth of literature proclaiming beneficial effects of IL-6 signaling through the Jak/Stat pathway on nerves. From this, our prevailing hypothesis going forward was that the IL-6 produced by MiMPCs were exhibiting a neurotrophic effect on the DRGs, enhancing neuritogenesis despite the presence of pan-Trk receptor inhibitor. We tested this hypothesis in chapter three by supplementing conditioned medium with cucurbitacin-I, a Jak/Stat inhibitor. When applied to DRG cultures, we indeed observed decreased neurite outgrowth, particularly in length, though this parameter could not be accurately measured on tissue culture plastic. However, Sholl analysis showed a slight decrease in extension complexity. The fact that conditioned medium could not rescue neurite outgrowth in the presence of a Jak/Stat inhibitor indicated that molecules in the MiMPC secretome, presumably IL-6, were essential in axon formation and extension.

As stated in chapter 2, multiple studies have already shown the benefits of angiogenic factors during nerve regeneration [69, 71, 210], and that angiogenesis and restoration of blood supply improves functional recovery. However, VEGF is unlikely to be affecting DRG outgrowth in our studies, as, unlike MSCs, MiMPCs do not produce VEGF when cultured outside the NI treatment medium, and DRGs were cultured only in basal conditioned medium collected from cells, not NI conditioned medium. As MiMPCs will remain in NI medium when transplanted *in vivo,* it is likely that MiMPCs may not be able to support angiogenesis. Therefore, *in vivo* sciatic nerve crush models may require a supply of exogenous VEGF or the MiMPCs may need to be transfected with VEGF-expressing plasmids in order to promote full functional

recovery. As tissue culture plastic was suboptimal for determining parameters other than complexity, aligned scaffolds were employed in DRG cultures to organize neurite outgrowth, and thereby provided a more accurate means of neurite length measurement. In chapter four, conditioned medium from all cell types and induction states enhanced neurite length over controls. When cells were incorporated into scaffolds, similar results were observed—both NI- and GM- MiMPCs and MSCs were capable of enhancing neurite extension lengths.

Scaffold DRG cultures are inherently more clinically relevant than those on tissue culture plastic as surgical treatment of nerve injuries may involve the use of a scaffold as physical support for the native nerve. For this reason, in future *in vivo* studies, it may be more economical and efficient to incorporate conditioned medium only from GM-MiMPCs as the benefits are comparable between GM- and NI- cell groups.

Fibrotic infiltrates impede axon regrowth, and can ultimately cause neuroma formation. While the MiMPC itself may not be capable through cytokine secretions to turn cells away, it is possible to prevent cellular infiltration by physical barriers (i.e. a nanofibrous scaffold into which cells cannot infiltrate) [212]. It remains to be seen whether our layered, PCL/gelatin composite scaffolds can simultaneously encapsulate MiMPCs while keeping all other cells outside of the lumen. We believe it is possible that immune and fibroblastic infiltrates can be kept to a minimum while the scaffold is intact, but once the scaffold begins to degrade, there is an increased chance for cells to infiltrate through cracks in the scaffold [113]. Therefore, we believe that the scaffold must be tailored to accommodate the length of time required for complete nerve regeneration. PCL degrades slowly, and may be a suitable material for this purpose, but it may be beneficial for future studies to further examine and optimize the materials and design of the scaffold to act as a semi-permeable barrier between surrounding tissues and the healing nerve.

The investigations presented here demonstrate the neurotrophic potential of a virtually limitless cell source, the MiMPC. While previous data show that MiMPCs are a more heterogeneous population of cells than MSCs, they are comparably neurotrophic and capable of supporting neurite outgrowth. Insights gained from this work indicate that further studies may include elucidating the neurotrophic differences in secretome between the MiMPC and MSC; their immunogenicity when encapsulated in scaffolds and implanted *in vivo*; and possible immunomodulatory effects of the MiMPC in comparison to MSCs. Full comprehension of the MiMPC secretome in terms of neurotrophism along with immunogenic or immunomodulatory activity may be indispensable for the development of MiMPC-based cell therapies for peripheral nerve injuries.

APPENDIX A

VEGF PRODUCTION IN MEDIUM CONDITIONED BY MIMPCS AND MSCS

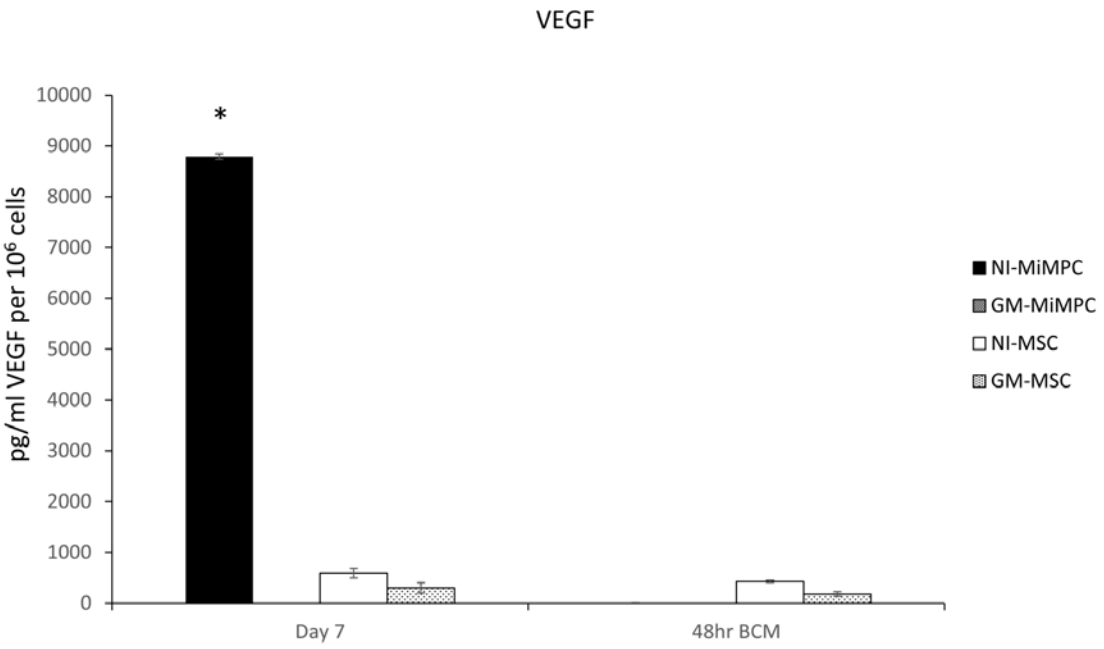

Figure 19: Production of vascular endothelial growth factor (VEGF) by NI-MiMPCs and MSCs, quantified via ELISA

MiMPCs and MSCs were cultured in neurotrophic induction medium or growth medium. Conditioned media taken from days 7 of induction culture, and basal conditioned medium taken from cultures 48 hours post-induction (48hr BCM). The conditioned media assayed include those from MiMPCs (induced, NI-MiMPCs; un-induced, GM-MiMPCs), and from MSCs (induced, MI-MSCs; un-induced, GM-MSCs), as well as basal medium (controls). Medium was assayed for levels of VEGF via ELISA, and measured in pg/ml of VEGF produced per million cells. Both NI- and GM- MSCs produced VEGF. However, MiMPCs were only able to produce VEGF while in neurotrophic induction medium, and could not maintain VEGF secretions when cells were moved to basal medium.

REPRESENTATIVE SHOLL CURVE MEASURING DRG NEURITE COMPLEXITY

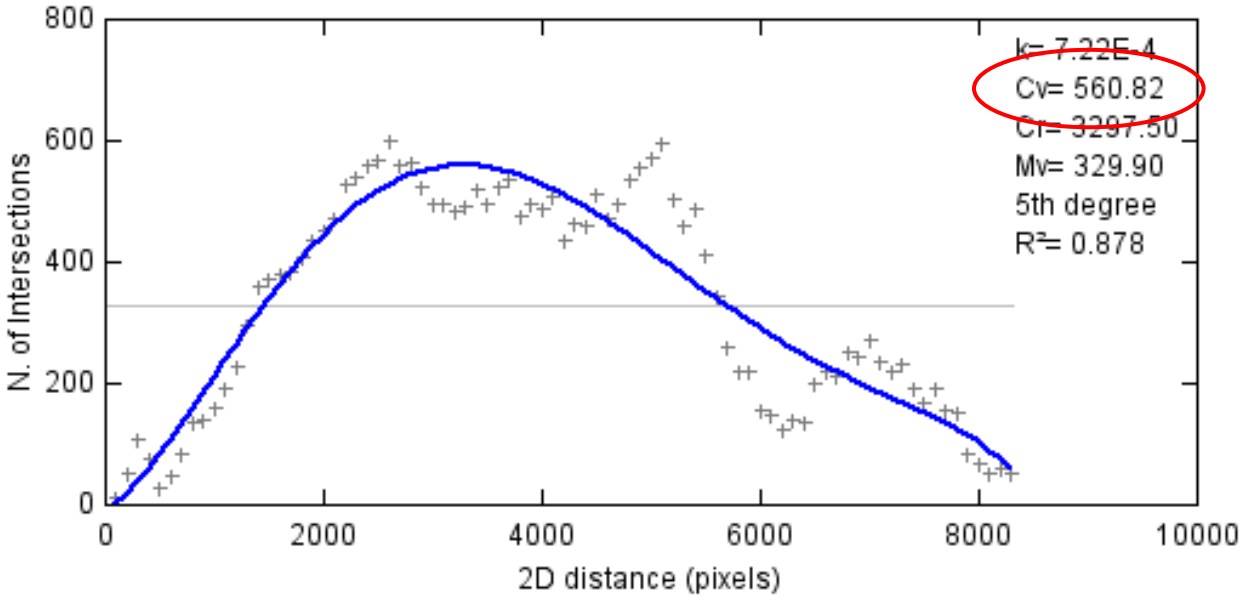

Figure 20: Representative Sholl analysis graph generated by Fiji/ImageJ measuring the branching complexity of neurite extensions from a DRG culture

All DRG cultures on tissue culture plastic were imaged via fluorescent microscopy and all images were analyzed via the Sholl analysis plugin included in Fiji/ImageJ. The figure represents a typical graph generated by the Sholl analysis. The critical value (Cv), highlighted by a red circle, represents the peak of the graph, corresponding to the maximum number of neurite extensions.

BIBLIOGRAPHY

1. Menorca, R. M. G., Fussell T. S., and Elfar J. C. Peripheral Nerve Trauma: Mechanisms of Injury and Recovery. *Hand clinics*. **29**(3):317-330. (2013).

2. Lee, S. K. and Wolfe S. W. Peripheral Nerve Injury and Repair. *Journal of the American Academy of Orthopaedic Surgeons*. **8**(4):243-252. (2000).

3. Mosahebi, A., et al. Effect of Allogeneic Schwann Cell Transplantation on Peripheral Nerve Regeneration. *Experimental Neurology*. **173**(2):213-223. (2002).

4. Keilhoff, G., et al. Transdifferentiated Mesenchymal Stem Cells as Alternative Therapy in Supporting Nerve Regeneration and Myelination. *Cellular and Molecular Neurobiology*. **26**(7):1233-1250. (2006).

5. Jackson, W. M., et al. Mesenchymal progenitor cells derived from traumatized muscle enhance neurite growth. *Journal of Tissue Engineering and Regenerative Medicine*. **7**(6):443-451. (2013).

6. Stadtfeld, M. and Hochedlinger, K. Induced pluripotency: history, mechanisms, and applications. *Genes & Development*. **24**(20):2239-2263. (2010).

7. Colohan, A. R., Pitts, L. H., Rosegay, H. Injury to the peripheral nerves. In: Feliciano DV, Moore EE, Mattox KL, editors. *Trauma*. 3rd ed. Stamford, Conn: Appleton and Lange; 1996. pp. 853–62.

8. Portland, G. H., et al. Injury to the infrapatellar branch of the saphenous nerve in anterior cruciate ligament reconstruction: Comparison of horizontal versus vertical harvest site incisions. *Arthroscopy: The Journal of Arthroscopic & Related Surgery*. **21**(3):281-285. (2005).

9. Sanders, B., et al. Prevalence of Saphenous Nerve Injury After Autogenous Hamstring Harvest: An Anatomic and Clinical Study of Sartorial Branch Injury. *Arthroscopy: The Journal of Arthroscopic & Related Surgery*. **23**(9):956-963. (2007)

10. Carofino, B. C., et al. Iatrogenic Nerve Injuries During Shoulder Surgery. *The Journal of Bone & Joint Surgery*. **95**(18): p. 1667-1674. (2013).

11. Rosberg, H. E., et al. Costs and outcome for serious hand and arm injuries during the first year after trauma – a prospective study. *BMC Public Health*. **13**:501-501. (2013).

12. Thorsén, F., et al. Digital nerve injuries: Epidemiology, results, costs, and impact on daily life. *Journal of Plastic Surgery and Hand Surgery*. **46**(3-4):184-190. (2012).

13. Grinsell, D. and Keating, C. P. Peripheral Nerve Reconstruction after Injury: A Review of Clinical and Experimental Therapies. *BioMed Research International*. **2014**:13. (2014).

14. Seddon, H. J. A Classification of Nerve Injuries. *British Medical Journal*. **2**(4260):237-239. (1942).

15. Tubbs, R. S., et al. Nerves and Nerve Injuries: Vol 2: Pain, Treatment, Injury, Disease and Future Directions. Elsevier Science. 2015. pp. 604-605.

16. Sunderland, S. A Classification of Peripheral Nerve Injuries Producing Loss of Function. *Brain*. **74**(4):491-516. (1951).

17. DeLisa, J. A., Gans B. M., and Walsh, N. E. Physical Medicine and Rehabilitation: Principles and Practice. Lippincott Williams & Wilkins. 2005. pp. 897.

18. Gaudet, A., Popovich P., and Ramer, M. Wallerian degeneration: gaining perspective on inflammatory events after peripheral nerve injury. *Journal of Neuroinflammation*. **8**(1): 110. (2011).

19. Svenningsen, Å. F. and Kanje, M. Regulation of Schwann cell proliferation in cultured segments of the adult rat sciatic nerve. *Journal of Neuroscience Research*. **52**(5):530-537. (1998).

20. Fex Svennigsen, Å. and Dahlin, L.B. Repair of the Peripheral Nerve—Remyelination that Works. *Brain Sciences*. **3**(3):1182-1197. (2013).

21. Murinson, B. B. and Griffin, J. W. C-Fiber Structure Varies with Location in Peripheral Nerve. *Journal of Neuropathology & Experimental Neurology*. **63**(3):246-254. (2004).

22. Orita, S., et al. Schwann cell LRP1 regulates Remak bundle ultrastructure and axonal interactions to prevent neuropathic pain. *The Journal of neuroscience : the official journal of the Society for Neuroscience.* **33**(13):5590-5602. (2013).

23. Saito, H. and Dahlin, L.B. Expression of ATF3 and axonal outgrowth are impaired after delayed nerve repair. *BMC Neuroscience*. **9**:88-88. (2008).

24. Levi-Montalcini, R. and Angeletti, P. U. Nerve growth factor. *Physiological Reviews*. **48**(3): p. 534. (1968).

25. Kalil, K. and Dent, E.W. Branch management: mechanisms of axon branching in the developing vertebrate CNS. *Nature reviews Neuroscience*. **15**(1):7-18. (2014).

26. Sun, W., et al. Improvement of Sciatic Nerve Regeneration Using Laminin-Binding Human NGF-β. *PLoS ONE*. **4**(7):e6180. (2009).

27. Kimpinski, K., Campenot, R. B. and Mearow, K. Effects of the neurotrophins nerve growth factor, neurotrophin-3, and brain-derived neurotrophic factor (BDNF) on neurite growth from adult sensory neurons in compartmented cultures. *Journal of neurobiology*. **33**(4):395-410. (1997).

28. Ma, S., et al. Sciatic nerve regeneration using a nerve growth factor-containing fibrin glue membrane. *Neural Regeneration Research.* **8**(36):3416-3422. (2013).

29. Wood, M. D. and Sakiyama-Elbert, S.E. Release rate controls biological activity of nerve growth factor released from fibrin matrices containing affinity-based delivery systems. *Journal of Biomedical Materials Research Part A*. **84A**(2):300-312. (2008).

30. Wood, M. D., et al., Heparin-Binding-Affinity-Based Delivery Systems Releasing Nerve Growth Factor Enhance Sciatic Nerve Regeneration. *Journal of Biomaterials Science, Polymer Edition.* **21**(6-7):771-787. (2010).

31. Patel, S., et al. Bioactive Nanofibers: Synergistic Effects of Nanotopography and Chemical Signaling on Cell Guidance. *Nano Letters*. **7**(7):2122-2128. (2007).

32. Ma, C. H. E., et al. Synergistic effects of osteonectin and brain-derived neurotrophic factor on axotomized retinal ganglion cells neurite outgrowth via the mitogen-activated protein kinase-extracellular signal-regulated kinase1/2 pathways. *Neuroscience*. **165**(2):463-474. (2010).

33. Eddie Ma, C. H., Palmer, A. and Taylor, J. S. H. Synergistic effects of osteonectin and NGF in promoting survival and neurite outgrowth of superior cervical ganglion neurons. *Brain Research*. **1289**:1-13. (2009).

34. Wilhelm, J. C., et al. Cooperative roles of BDNF expression in neurons and Schwann cells are modulated by exercise to facilitate nerve regeneration. *The Journal of Neuroscience*. **32**(14):5002-5009. (2012).

35. Tolwani, R. J., et al. BDNF overexpression produces a long-term increase in myelin formation in the peripheral nervous system. *Journal of Neuroscience Research.* **77**(5):662-669. (2004).

36. Takemura, Y., et al. Brain-Derived Neurotrophic Factor from Bone Marrow-Derived Cells Promotes Post-Injury Repair of Peripheral Nerve. *PLoS ONE*. **7**(9):e44592. (2012).

37. Lin, G., et al. Brain-derived neurotrophic factor promotes nerve regeneration by activating the JAK/STAT pathway in Schwann cells. *Translational Andrology and Urology*. 2016. **5**(2):167-175. (2016).

38. Bella, A. J., et al., Brain-Derived Neurotrophic Factor (BDNF) Acts Primarily via the JAK/STAT Pathway to Promote Neurite Growth in the Major Pelvic Ganglion of the Rat: Part I. *The Journal of Sexual Medicine*. **3**(5):815-820. (2006).

39. Jones, J., et al. Mesenchymal stem cells improve motor functions and decrease neurodegeneration in ataxic mice. *Molecular Therapy*. **23**(1): 130-138. (2014).

40. Li, Q., et al. Nerve conduit filled with GDNF gene-modified schwann cells enhances regeneration of the peripheral nerve. *Microsurgery.* **26**(2):116-121. (2006).

41. Wood, M. D., et al. Affinity-based release of glial-derived neurotrophic factor from fibrin matrices enhances sciatic nerve regeneration. *Acta Biomaterialia*. **5**(4):959-968. (2009).

42. Wood, M. D., et al. GDNF released from microspheres enhances nerve regeneration after delayed repair. *Muscle & Nerve*. **46**(1):122-124. (2012).

43. Ramer, M. S., et al. Neurotrophin-3-Mediated Regeneration and Recovery of Proprioception Following Dorsal Rhizotomy. *Molecular and Cellular Neuroscience*. **19**(2):239-249. (2002).

44. Sterne, G. D., et al. Neurotrophin-3–enhanced Nerve Regeneration Selectively Improves Recovery of Muscle Fibers Expressing Myosin Heavy Chains 2b. *The Journal of Cell Biology*. **139**(3):709-715. (1997).

45. Newman, J. P., et al. Ciliary neurotrophic factor enhances peripheral nerve regeneration. *Archives of Otolaryngology–Head & Neck Surgery*. **122**(4):399-403. (1996).

46. Terenghi, G. Peripheral nerve regeneration and neurotrophic factors. *Journal of Anatomy*. **194**(Pt 1):1-14. (1999).

47. Yao, M., et al. Peripheral Nerve Regeneration in CNTF Knockout Mice. *The Laryngoscope*. **109**(8):1263-1268. (1999).

48. Sendtner, M., et al. Endogenous Ciliary Neurotrophic Factor Is a Lesion Factor for Axotomized Motoneurons in Adult Mice. *The Journal of Neuroscience.* **17**(18):6999-7006. (1997).

49. Yamamori, T., et al. The Cholinergic Neuronal Differentiation Factor from Heart Cells is Identical to Leukemia Inhibitory Factor. *Science*. **246**(4936):1412-1416. (1989).

50. Hilton, D. J. LIF: lots of interesting functions. *Trends in Biochemical Sciences*. **17**(2):72-76. (1992).

51. McKay Hart, A., Wiberg, M. and Terenghi, G. Exogenous leukaemia inhibitory factor enhances nerve regeneration after late secondary repair using a bioartificial nerve conduit. *British Journal of Plastic Surgery*. **56**(5):444-450. (2003).

52. Ogai, K., et al. Upregulation of Leukemia Inhibitory Factor (LIF) during the Early Stage of Optic Nerve Regeneration in Zebrafish. *PLoS ONE*. **9**(8):e106010. (2014).

53. Pricola, K. L., et al. Interleukin-6 Maintains Bone Marrow-Derived Mesenchymal Stem Cell Stemness by an ERK1/2-Dependent Mechanism. *Journal of cellular biochemistry*. **108**(3):577-588. (2009).

54. Hirota, H., Hiroshi, K., Kishimoto, T., Taga, T. Accelerated Nerve Regeneration in Mice by upregulated expression of interleukin (IL) 6 and IL-6 receptor after trauma. *The Journal of Experimental Medicine.* **183**(6):2627-2634. (1996).

55. Leibinger, M., et al. Interleukin-6 contributes to CNS axon regeneration upon inflammatory stimulation. *Cell Death and Disease*. **4**:e609. (2013).

56. Yang, P., et al. IL-6 promotes regeneration and functional recovery after cortical spinal tract injury by reactivating intrinsic growth program of neurons and enhancing synapse formation. *Experimental Neurology*. **236**(1):19-27. (2012).

57. Lee, H. S., et al. Meteorin promotes the formation of GFAP-positive glia via activation of the Jak-STAT3 pathway. *Journal of Cell Science.* **123**(11):1959-1968. (2010).

58. Bampton, E. T. W., et al. Osteonectin is a Schwann cell-secreted factor that promotes retinal ganglion cell survival and process outgrowth. *European Journal of Neuroscience*. **21**(10):2611-2623. (2005).

59. Termine, J. D., et al. Osteonectin, a bone-specific protein linking mineral to collagen. *Cell*. **26**(1):99-105. (1981).

60. Wolford, L. M. and Stevao, E. L. L. Considerations in nerve repair. *Proceedings (Baylor University. Medical Center).* **16**(2):152-156. (2003).

61. Ray, W. Z. and Mackinnon, S. E. Management of nerve gaps: Autografts, allografts, nerve transfers, and end-to-side neurorrhaphy. *Experimental Neurology*. **223**(1):77-85. (2010).

62. Tuttle, H. K. Exposure of the brachial plexus with nerve-transplantation. *Journal of the American Medical Association.* **61**(1):15-17. (1913).

63. Moore, A. M. Nerve Transfers to Restore upper Extremity Function: A Paradigm Shift. *Frontiers in Neurology.* **5**:40. (2014).

64. Waikakul, S., Wongtragul, S., and Vanadurongwan, V. Restoration of elbow flexion in branchial plexus avulsion injury: Comparing spinal accessory nerve transfer with intercostal nerve transfer. *The Journal of Hand Surgery*. **24**(3):571-577. (1999).

65. Lee, S. K. M. W., Scott W. MD, Nerve Transfers for the Upper Extremity: New Horizons in Nerve Reconstruction. *Journal of the American Academy of Orthopaedic Surgeons*. **20**(8):506-517. (2012).

66. Lavasani, M., et al. Human muscle–derived stem/progenitor cells promote functional murine peripheral nerve regeneration. *The Journal of Clinical Investigation*. **124**(4):1745-1756. (2014).

67. Brohlin, M., et al. Characterisation of human mesenchymal stem cells following differentiation into Schwann cell-like cells. *Neuroscience Research*. **64**(1):41-49. (2009).

68. Sadan, O., et al. Mesenchymal stem cells induced to secrete neurotrophic factors attenuate quinolinic acid toxicity: A potential therapy for Huntington's disease. *Experimental Neurology*. **234**(2):417-427. (2012).

69. Man, A. J., et al. Neurogenic Potential of Engineered Mesenchymal Stem Cells Overexpressing VEGF. *Cellular and Molecular Bioengineering*. **9**(1):96-106. (2016).

70. Caddick, J., et al. Phenotypic and functional characteristics of mesenchymal stem cells differentiated along a Schwann cell lineage. *Glia*. **54**(8):840-849. (2006).

71. Hofer, H. R. and Tuan, R. S. Secreted trophic factors of mesenchymal stem cells support neurovascular and musculoskeletal therapies. *Stem Cell Research & Therapy*. **7**(1):131. (2016).

72. Tomita, K., et al. Glial differentiation of human adipose-derived stem cells: Implications for cell-based transplantation therapy. *Neuroscience*. **236**:55-65. (2013).

73. Tomita, K., et al. Differentiated adipose-derived stem cells promote myelination and enhance functional recovery in a rat model of chronic denervation. *Journal of Neuroscience Research*. **90**(7):1392-1402. (2012).

74. Dadon-Nachum, M., et al. Differentiated Mesenchymal Stem Cells for Sciatic Nerve Injury. *Stem Cell Reviews and Reports*. **7**(3):664-671. (2011).

75. Marconi, S., et al. Human Adipose-Derived Mesenchymal Stem Cells Systemically Injected Promote Peripheral Nerve Regeneration in the Mouse Model of Sciatic Crush. *Tissue Engineering Part A*. **18**(11-12):1264-1272. (2012).

76. Fairbairn, N. G., et al. Augmenting peripheral nerve regeneration using stem cells: A review of current opinion. *World Journal of Stem Cells*. **7**(1):11-26. (2015).

77. Bulken-Hoover, J. D., et al. Inducible Expression of Neurotrophic Factors by Mesenchymal Progenitor Cells Derived from Traumatically Injured Human Muscle. *Molecular Biotechnology*. **51**(2):128-136. (2012).

78. Friedenstein, A. J., Piatetzky-Shapiro, I. I., and Petrakova, K. V. Osteogenesis in transplants of bone marrow cells. *Journal of Embryology and Experimental Morphology*. **16**(3):381-390. (1966).

79. Dominici, M., et al. Minimal criteria for defining multipotent mesenchymal stromal cells The International Society for Cellular Therapy position statement. *Cytotherapy*. **8**(4):315-317. (2006).

80. Ankrum, J. A., Ong, J. F., and Karp, J. M. Mesenchymal stem cells: immune evasive, not immune privileged. *Nature Biotechnology*. **32**(3):252-260. (2014).

81. Thomson, J. A., et al. Embryonic Stem Cell Lines Derived from Human Blastocysts. *Science*. **282**(5391):1145-1147. (1998).

82. Kingham, E., et al. Nanotopographical Cues Augment Mesenchymal Differentiation of Human Embryonic Stem Cells. *Small*. **9**(12):2140-2151. (2013).

83. Kimbrel, E.A., et al. Mesenchymal Stem Cell Population Derived from Human Pluripotent Stem Cells Displays Potent Immunomodulatory and Therapeutic Properties. *Stem Cells and Development*. **23**(14):1611-1624. (2014).

84. Ziegler, L., et al. Efficient Generation of Schwann Cells from Human Embryonic Stem Cell-Derived Neurospheres. *Stem Cell Reviews and Reports*. **7**(2):394-403. (2011).

85. Xia, X. and Zhang, S. C. Differentiation of Neuroepithelia from Human Embryonic Stem Cells, in Neural Cell Transplantation. D. Gordon and N.J. Scolding, Editors. 2009, Humana Press. p. 51-58.

86. Rong, Z., et al. An Effective Approach to Prevent Immune Rejection of Human ESC-Derived Allografts. *Cell Stem Cell*. **14**(1):121-130. (2014).

87. Takahashi, K. and Yamanaka, S. Induction of Pluripotent Stem Cells from Mouse Embryonic and Adult Fibroblast Cultures by Defined Factors. *Cell*. **126**(4):663-676. (2006).

88. Hochedlinger, K., et al. Ectopic Expression of Oct-4 Blocks Progenitor-Cell Differentiation and Causes Dysplasia in Epithelial Tissues. *Cell*. **121**(3):465-477. (2005).

89. Maherali, N. and Hochedlinger, K. Guidelines and Techniques for the Generation of Induced Pluripotent Stem Cells. *Cell Stem Cell*. **3**(6):595-605. (2008).

90. Okita, K., Ichisaka, T. and Yamanaka, S. Generation of germline-competent induced pluripotent stem cells. *Nature*. **448**(7151):313-317. (2007).

91. Patel, M. and Yang, S. Advances in Reprogramming Somatic Cells to Induced Pluripotent Stem Cells. *Stem cell reviews*. **6**(3):367-380. (2010).

92. Agarwal, S. Cellular Reprogramming. *Methods in Enzymology*. **420:**265-283. (2006).

93. Kaji, K., et al. Virus free induction of pluripotency and subsequent excision of reprogramming factors. *Nature*. **458**(7239):771-775. (2009).

94. Bar-Nur, O., et al. Small molecules facilitate rapid and synchronous iPSC generation. *Nature Methods*. **11**(11):1170-1176. (2014).

95. Lyssiotis, C. A., et al. Reprogramming of murine fibroblasts to induced pluripotent stem cells with chemical complementation of Klf4. *Proceedings of the National Academy of Sciences*. **106**(22):8912-8917. (2009).

96. Lin, T. and Wu, S. Reprogramming with Small Molecules instead of Exogenous Transcription Factors. *Stem Cells International*. **2015**:11. (2015).

97. Gropp, M., et al. Standardization of the Teratoma Assay for Analysis of Pluripotency of Human ES Cells and Biosafety of Their Differentiated Progeny. *PLoS ONE*. **7**(9):e45532. (2012).

98. Diederichs, S. and Tuan, R. S. Functional Comparison of Human-Induced Pluripotent Stem Cell-Derived Mesenchymal Cells and Bone Marrow-Derived Mesenchymal Stromal Cells from the Same Donor. *Stem Cells and Development*. **23**(14):1594-1610. (2014).

99. Liu, Q., Swistowski, A. and Zeng, X. Human Neural Crest Stem Cells Derived from Human Pluripotent Stem Cells, in Stem Cells and Tissue Repair: Methods and Protocols, C. Kioussi, Editor. 2014, Springer New York: New York, NY. p. 79-90.

100. Chambers, S. M., et al. Combined small molecule inhibition accelerates developmental timing and converts human pluripotent stem cells into nociceptors. *Nature biotechnology*. **30**(7):715-720. (2012).

101. Moghadasi Boroujeni, S., et al. The synergistic effect of surface topography and sustained release of TGF-β1 on myogenic differentiation of human mesenchymal stem cells. *Journal of Biomedical Materials Research Part A*. **104**(7):1610-1621. (2016).

102. Yim, E. K. F., Pang, S.W. and Leong, K. W. Synthetic nanostructures inducing differentiation of human mesenchymal stem cells into neuronal lineage. *Experimental Cell Research*. **313**(9):1820-1829. (2007).

103. Brunetti, V., et al. Neurons sense nanoscale roughness with nanometer sensitivity. *Proceedings of the National Academy of Sciences.* **107**(14):6264-6269. (2010).

104. Hoffman-Kim, D., Mitchel, J. A., and Bellamkonda, R. V. Topography, Cell Response, and Nerve Regeneration. *Annual review of biomedical engineering*. **12**:203-231. (2010).

105. Mahoney, M. J., et al. The influence of microchannels on neurite growth and architecture. *Biomaterials*. **26**(7):71-778. (2005).

106. Yao, L., et al. Effect of functionalized micropatterned PLGA on guided neurite growth. *Acta Biomaterialia.* **5**(2):580-588. (2009).

107. Lietz, M., et al. Neuro tissue engineering of glial nerve guides and the impact of different cell types. *Biomaterials*. **27**(8):1425-1436. (2006).

108. Li, J., McNally, H. and Shi, R. Enhanced neurite alignment on micro-patterned poly-L-lactic acid films. *Journal of Biomedical Materials Research Part A.* **87A**(2):392-404. (2008).

109. de Luca, A. C., et al. Extracellular matrix components in peripheral nerve repair: how to affect neural cellular response and nerve regeneration? *Neural Regeneration Research*. **9**(22):1943-1948. (2014).

110. Ciardelli, G. and Chiono, V. Materials for Peripheral Nerve Regeneration. *Macromolecular Bioscience.* **6**(1):13-26. (2006).

111. Nectow, A. R., Marra, K.G. and Kaplan, D.L. Biomaterials for the Development of Peripheral Nerve Guidance Conduits. *Tissue Engineering. Part B, Reviews*. **18**(1):40-50. (2012).

112. Kokai, L. E., et al. Diffusion of soluble factors through degradable polymer nerve guides: Controlling manufacturing parameters. *Acta Biomaterialia*. **5**(7):2540-2550. (2009).

113. Jiang, X., et al. Current applications and future perspectives of artificial nerve conduits. *Experimental Neurology*. **223**(1):86-101. (2010).

114. Kehoe, S., Zhang, X. F., and Boyd, D. FDA approved guidance conduits and wraps for peripheral nerve injury: A review of materials and efficacy. *Injury.* **43**(5):553-572. (2012).

115. Arslantunali, D., et al. Peripheral nerve conduits: technology update. *Medical Devices (Auckland, N.Z.)*. **7**:405-424. (2014).

116. Weber, R. A., Breidenbach W. C., Brown, R. E., Jabaley, M. E., Mass, D. P. A Randomized Prospective Study of Polyglycolic Acid Conduits for Digital Nerve

Reconstruction in Humans. *Plastic and Reconstructive Surgery*. **106**(5):1036-1045. (2000).

117. Bertleff, M. J., Meek, M. F., and Nicolai, J. P. A. A Prospective Clinical Evaluation of Biodegradable Neurolac Nerve Guides for Sensory Nerve Repair in the Hand. *The Journal of Hand Surgery*. **30**(3):513-518. (2005).

118. Hudson, T. W., Zawko, S., Deister, C., Lundy, S., Hu, C. Y., Lee, K., and Schmidt, C. E. Optimized Acellular Nerve Graft Is Immunologically Tolerated and Supports Regeneration. *Tissue Engineering.* **10**(11-12):1641-1651. (2004).

119. Gilbert, T. W., Sellaro, T. L. and Badylak, S.F. Decellularization of tissues and organs. *Biomaterials*. **27**(19):3675-3683. (2006).

120. Whitlock, E. L., Tuffaha, S. H., Luciano, J. P., Yan, Y., Hunter, D. A., Magill, C. K., Moore, A. M., Tong, A. Y., Mackinnon, S. E., Borschel, G. H. Processed allografts and type I collagen conduits for repair of peripheral nerve gaps. *Muscle & Nerve*. **39**(6):787-99. (2009).

121. Sun, W., et al. The effect of collagen-binding NGF-β on the promotion of sciatic nerve regeneration in a rat sciatic nerve crush injury model. *Biomaterials*. **30**(27):4649-4656. (2009).

122. Diao, E., Andrews, A., and Diao, J. Animal models of peripheral nerve injury. *Operative Techniques in Orthopaedics*. **14**(3):153-162. (2004).

123. Greene, L. A. and Tischler, A. S. Establishment of a noradrenergic clonal line of rat adrenal pheochromocytoma cells which respond to nerve growth factor. *Proceedings of the National Academy of Sciences of the United States of America*. **73**(7):2424-2428. (1976).

124. Zerby, S. E. and Ewing, A. G. Electrochemical monitoring of individual exocytotic events from the varicosities of differentiated PC12 cells. *Brain Research*. **712**(1):1-10. (1996).

125. Stephens, R. M., et al. Trk receptors use redundant signal transduction pathways involving SHC and PLC-γ1 to mediate NGF responses. *Neuron*. **12**(3):691-705. (1994).

126. Das, K. P., Freudenrich, T. M. and Mundy, W. R. Assessment of PC12 cell differentiation and neurite growth: a comparison of morphological and neurochemical measures. *Neurotoxicology and Teratology*. **26**(3):397-406. (2004).

127. Westerink, R. H. S. and Ewing, A.G. The PC12 cell as model for neurosecretion. *Acta physiologica (Oxford, England)*. **192**(2):273-285. (2008).

128. Geuna, S., et al. In vitro models for peripheral nerve regeneration. *European Journal of Neuroscience.* **43**(3):287-296. (2016).

129. Chen, W., et al. Immortalization and characterization of a nociceptive dorsal root ganglion sensory neuronal line. *Journal of the peripheral nervous system.* **12**(2):121-130. (2007).

130. Melli, G. and Höke, A. Dorsal Root Ganglia Sensory Neuronal Cultures: a tool for drug discovery for peripheral neuropathies. *Expert opinion on drug discovery.* **4**(10):1035-1045. (2009).

131. Armstrong, S. J., et al. Laminin activates NF-κB in Schwann cells to enhance neurite outgrowth. *Neuroscience Letters*. **439**(1):42-46. (2008).

132. Magnaghi, V., et al. GABA synthesis in Schwann cells is induced by the neuroactive steroid allopregnanolone. *Journal of Neurochemistry*. **112**(4):980-990. (2010).

133. de Luca, A. C., Faroni, A. and Reid, A.J. Dorsal Root Ganglia Neurons and Differentiated Adipose-derived Stem Cells: An In Vitro Co-culture Model to Study Peripheral Nerve Regeneration. *Journal of Visualized Experiments:JoVE*. **2015**(96): p. 52543. (2015).

134. Webber, C. and Zochodne, D. The nerve regenerative microenvironment: Early behavior and partnership of axons and Schwann cells. *Experimental Neurology*. **223**(1):51-59. (2010).

135. Mackinnon, S. E., et al. Chronic Nerve Compression-an Experimental Model in the Rat. *Annals of Plastic Surgery*. **13**(2):112-120. (1984).

136. Mackinnon, S. E. and Dellon, A. L. Experimental study of chronic nerve compression. Clinical implications. *Hand Clinics*. **2**(4):639-650. (1986).

137. Dellon, A. L., Mackinnon, S. E,, Seiler, W. A. 4th. Susceptibility of the diabetic nerve to chronic compression. *Annals of Plastic Surgery*. **20**(2):117-9. (1988).

138. Gupta, R. and Steward O. Chronic nerve compression induces concurrent apoptosis and proliferation of Schwann cells. *Journal of Comparative Neurology*. **461**(2):174-186. (2003).

139. Rydevik, B., Lundborg, G., Bagge, U. Effects of graded compression on intraneural blood flow: An in vivo study on rabbit tibial nerve. *The Journal of Hand Surgery*. **6**(1):3-12. (1981).

140. Bauder, A. R. and Ferguson, T. A. Reproducible Mouse Sciatic Nerve Crush and Subsequent Assessment of Regeneration by Whole Mount Muscle Analysis. *Journal of Visualized Experiments:JoVE*. **2012**(60): p. 3606. (2012).

141. Burgette, R. C., et al. A Rat Model for Intracranial Facial Nerve Crush Injuries. *Otolaryngology-Head and Neck Surgery*. **146**(2):326-330. (2011).

142. Brushart, T. M. Preferential motor reinnervation: a sequential double-labeling study. *Resorative neurology and neuroscience*. **1**(3):281-7. (1990).

143. Al-Majed, A. A., et al. Brief Electrical Stimulation Promotes the Speed and Accuracy of Motor Axonal Regeneration. *The Journal of Neuroscience*. **20**(7):2602-2608. (2000).

144. Clark, B. D., et al. Performance of a High-Repetition, High-Force Task Induces Carpal Tunnel Syndrome in Rats. *Journal of Orthopaedic & Sports Physical Therapy*. **34**(5):244-253. (2004).

145. Abreu, R.d.S., et al. Global signatures of protein and mRNA expression levels. *Molecular bioSystems*. **5**(12):1512-1526. (2009).

146. Koussounadis, A., et al. Relationship between differentially expressed mRNA and mRNA-protein correlations in a xenograft model system. *Scientific Reports*. **5**:10775. (2015).

147. Vogel, C. and Marcotte, E. M. Insights into the regulation of protein abundance from proteomic and transcriptomic analyses. *Nature Reviews Genetics*. **13**(4):227-232. (2012).

148. Frostick, S. P., Yin, Q., Kemp, G. J. Schwann cells, neurotrophic factors, and peripheral nerve regeneration. *Microsurgery*. **18**(7):397-405. (1998).

149. Wright, M. C., et al. Novel Roles for Osteopontin and Clusterin in Peripheral Motor and Sensory Axon Regeneration. *The Journal of Neuroscience*. **34**(5):1689-1700. (2014).

150. Marolt, D., et al. Engineering bone tissue from human embryonic stem cells. *Proceedings of the National Academy of Sciences*. **109**(22):8705-8709. (2012).

151. Teramura, T., et al. Induction of Mesenchymal Progenitor Cells with Chondrogenic Property from Mouse-Induced Pluripotent Stem Cells. *Cellular Reprogramming.* **12**(3):249-261. (2010).

152. Zhang, R.-R., et al. Efficient Hepatic Differentiation of Human Induced Pluripotent Stem Cells in a Three-Dimensional Microscale Culture, in Stem Cells and Tissue Repair: Methods and Protocols. C. Kioussi, Editor. 2014, Springer New York: New York, NY. p. 131-141.

153. Batalov, I. and Feinberg, A.W. Differentiation of Cardiomyocytes from Human Pluripotent Stem Cells Using Monolayer Culture. *Biomarker Insights.* **10**(Suppl 1):71-76. (2015).

154. Nagai, A., et al. Multilineage Potential of Stable Human Mesenchymal Stem Cell Line Derived from Fetal Marrow. *PLoS ONE*. **2**(12):e1272. (2007).

155. Meyer, M., Matsuoka, I., Wetmore, C., Olson, L., Thoenen, H. Enhanced synthesis of brain-derived neurotrophic factor in the lesioned peripheral nerve: different mechanisms are responsible for the regulation of BDNF and NGF mRNA. *The Journal of Cell Biology*. **119**(1):45-54. (1992).

156. Ghosh-Roy, A., et al. Calcium and Cyclic AMP Promote Axonal Regeneration in Caenorhabditis elegans and Require DLK-1 Kinase. *The Journal of Neuroscience*. **30**(9): p. 3175-3183. (2010).

157. Borin, A., et al. Influence of cyclic AMP on facial nerve regeneration in rats. *Brazilian Journal of Otorhinolaryngology*. **74**(5):675-683. (2008).

158. Gao, Y., et al. Neurotrophins Elevate cAMP to Reach a Threshold Required to Overcome Inhibition by MAG through Extracellular Signal-Regulated Kinase-Dependent Inhibition of Phosphodiesterase. *The Journal of Neuroscience*. **23**(37):11770-11777. (2003).

159. Jackson, E. K. and Raghvendra, D. K. The Extracellular Cyclic AMP-Adenosine Pathway in Renal Physiology. *Annual Review of Physiology*. **66**(1):571-599. (2004).

160. Godinho, R. O. and Costa-Jr, V. L. Regulation of intracellular cyclic AMP in skeletal muscle cells involves the efflux of cyclic nucleotide to the extracellular compartment. *British Journal of Pharmacology*. **138**(5):995-1003. (2003).

161. Haase, G., et al. Signalling by death receptors in the nervous system. *Current opinion in neurobiology*. **18**(3):284-291. (2008).

162. Bamji, S.X., et al. The p75 Neurotrophin Receptor Mediates Neuronal Apoptosis and Is Essential for Naturally Occurring Sympathetic Neuron Death. *The Journal of Cell Biology*. **140**(4):911-923. (1998).

163. Bai, Y., et al. Chronic and Acute Models of Retinal Neurodegeneration TrkA Activity Are Neuroprotective whereas p75(NTR) Activity Is Neurotoxic through a Paracrine Mechanism. *The Journal of Biological Chemistry*. **285**(50):39392-39400. (2010).

164. Rosset, E. M. and Bradshaw, A. D. SPARC/osteonectin in mineralized tissue. *Matrix Biology*. **52–54**:78-87. (2016).

165. Kupprion, C., Motamed, K., Sage, E. H. SPARC (BM-40, Osteonectin) Inhibits the Mitogenic Effect of Vascular Endothelial Growth Factor on Microvascular Endothelial Cells. *Journal of Biological Chemistry*. **273**(45):29635-29640. (1998).

166. Denhardt, D. T., et al. Osteopontin as a means to cope with environmental insults: regulation of inflammation, tissue remodeling, and cell survival. *Journal of Clinical Investigation*. **107**(9):1055-1061. (2001).

167. Hashimoto, M., et al. Osteopontin-Deficient Mice Exhibit Less Inflammation, Greater Tissue Damage, and Impaired Locomotor Recovery from Spinal Cord Injury Compared with Wild-Type Controls. *The Journal of Neuroscience*. **27**(13):3603-3611. (2007).

168. May, P. C. and Finch, C. E. Sulfated glycoprotein 2: new relationships of this multifunctional protein to neurodegeneration. *Trends in Neurosciences.* **15**(10):391-396. (1992).

169. Yu, J.-T. and Tan, L. The Role of Clusterin in Alzheimer's Disease: Pathways, Pathogenesis, and Therapy. *Molecular Neurobiology.* **45**(2):314-326. (2012).

170. Dati, G., et al. Beneficial effects of r-h-CLU on disease severity in different animal models of peripheral neuropathies. *Journal of Neuroimmunology*. **190**(1–2):8-17. (2007).

171. Bonnard, A.-S., Chan, P., Fontaine, M. Expression of clusterin and C4 mRNA during rat peripheral nerve regeneration. *Immunopharmacology*. **38**(1):81-86. (1997).

172. Liu, L., Svensson, M., Aldskogius, H. Clusterin Upregulation Following Rubrospinal Tract Lesion in the Adult Rat. *Experimental Neurology.* **157**(1):69-76. (1999).

173. Fitzgerald, M., et al. Metallothionein-IIA promotes neurite growth via the megalin receptor. *Experimental Brain Research.* **183**(2):171-180. (2007).

174. Fleming, C.E., et al. Transthyretin Internalization by Sensory Neurons Is Megalin Mediated and Necessary for Its Neuritogenic Activity. *The Journal of Neuroscience*. **29**(10):3220-3232. (2009).

175. Elsaeidi, F., et al. Jak/Stat Signaling Stimulates Zebrafish Optic Nerve Regeneration and Overcomes the Inhibitory Actions of Socs3 and Sfpq. *The Journal of Neuroscience*. **34**(7):2632-2644. (2014).

176. Heinrich, P. C., et al. Interleukin-6-type cytokine signalling through the gp130/Jak/STAT pathway. *Biochemical Journal.* **334**(Pt 2):297-314. (1998).

177. Günthert, U. and Birchmeier, W. Attempts to Understand Metastasis Formation II: Regulatory Factors. 2012: Springer Berlin Heidelberg. pp. 56.

178. Decurtis, I. Intracellular Mechanisms for Neuritogenesis. 2007: Springer US. pp. 31-33.

179. Huang, E. J. and Reichardt, L. F. Trk Receptors: Roles in Neuronal Signal Transduction. *Annual Review of Biochemistry.* **72**(1):609-642. (2003).

180. Albaugh, P., et al. Discovery of GNF-5837, a Selective TRK Inhibitor with Efficacy in Rodent Cancer Tumor Models. *ACS Medicinal Chemistry Letters*. **3**(2):140-145. (2012).

181. Cazorla, M., et al. Cyclotraxin-B, the First Highly Potent and Selective TrkB Inhibitor, Has Anxiolytic Properties in Mice. *PLoS ONE*. **5**(3):e9777. (2010).

182. Dziennis, S. and Alkayed, N. J. Role of Signal Transducer and Activator of Transcription 3 in Neuronal Survival and Regeneration. *Reviews in the neurosciences*. **19**(4-5):341-361. (2008).

183. Nishi, R. Chapter 13 Autonomic and Sensory Neuron Cultures, in Methods in Cell Biology. B.-F. Marianne, Editor. 1996, Academic Press. pp. 249-263.

184. Sholl, D. A. Dendritic organization in the neurons of the visual and motor cortices of the cat. *Journal of Anatomy*. **87**(Pt 4):387–406. (1953).

185. Blaskovich, M. A., et al. Discovery of JSI-124 (Cucurbitacin I), a Selective Janus Kinase/Signal Transducer and Activator of Transcription 3 Signaling Pathway Inhibitor with Potent Antitumor Activity against Human and Murine Cancer Cells in Mice. *Cancer Research*. **63**(6):1270-1279. (2003).

186. Schindelin, J., et al. Fiji - an Open Source platform for biological image analysis. *Nature methods*. **9**(7):676-682. (2012).

187. Ferreira, T.A., et al. Neuronal morphometry directly from bitmap images. Nature Methods. **11**(10):982-984. (2014).

188. Brenner, M. J., et al. Repair of Motor Nerve Gaps With Sensory Nerve Inhibits Regeneration in Rats. *The Laryngoscope*. **116**(9):1685-1692. (2006).

189. Nichols, C. M., et al. Effects of motor versus sensory nerve grafts on peripheral nerve regeneration. *Experimental Neurology*. **190**(2):347-355. (2004).

190. Griffin, J. W., Hogan, M. V., Chhabra, A. B., Deal, D. N. Peripheral Nerve Repair and Reconstruction. *Journal of Bone & Joint Surgery - American Volume*. **95**(23):2144-2151. (2013).

191. Lin, H., et al. Application of Visible Light-based Projection Stereolithography for Live Cell-Scaffold Fabrication with Designed Architecture. *Biomaterials*. **34**(2):331-339. (2013).

192. Barbarisi, M., et al. Use of polycaprolactone (PCL) as scaffolds for the regeneration of nerve tissue. *Journal of Biomedical Materials Research Part A*. **103**(5):1755-1760. (2015).

193. Daly, W., et al. A biomaterials approach to peripheral nerve regeneration: bridging the peripheral nerve gap and enhancing functional recovery. *Journal of the Royal Society Interface*. **9**(67):202-221. (2012).

194. Chang, C. J. Effects of nerve growth factor from genipin-crosslinked gelatin in polycaprolactone conduit on peripheral nerve regeneration—In vitro and in vivo. *Journal of Biomedical Materials Research Part A.* **91A**(2):586-596. (2009).

195. Leong, K. F., et al. Engineering functionally graded tissue engineering scaffolds. *Journal of the Mechanical Behavior of Biomedical Materials*. **1**(2):140-152. (2008).

196. Fairbanks, B. D., et al. Photoinitiated polymerization of PEG-diacrylate with lithium phenyl-2,4,6-trimethylbenzoylphosphinate: polymerization rate and cytocompatibility. *Biomaterials*. **30**(35):6702-6707. (2009).

197. Han, L.-H., et al. Fabrication of three-dimensional scaffolds for heterogeneous tissue engineering. *Biomedical Microdevices*. **12**(4):721-725. (2010).

198. Atesok, K., et al. Multilayer scaffolds in orthopaedic tissue engineering. *Knee Surgery, Sports Traumatology, Arthroscopy*. **24**(7):2365-2373. (2016).

199. Zamani, F., et al. The influence of surface nanoroughness of electrospun PLGA nanofibrous scaffold on nerve cell adhesion and proliferation. *Journal of Materials Science: Materials in Medicine.* **24**(6):1551-1560. (2013).

200. Jahani, H., et al. The effect of aligned and random electrospun fibrous scaffolds on rat mesenchymal stem cell proliferation. *Cell Journal (Yakhteh)*. **14**(1):31-38. (2012).

201. Yadav, A., et al. JAK/STAT3 Pathway Is Involved in Survival of Neurons in Response to Insulin-like Growth Factor and Negatively Regulated by Suppressor of Cytokine Signaling-3. *Journal of Biological Chemistry*. **280**(36):31830-31840. (2005).

202. Deumens, R., et al. Repairing injured peripheral nerves: Bridging the gap. *Progress in Neurobiology*. **92**(3):245-276. (2010).

203. Abdi, R., et al. Immunomodulation by Mesenchymal Stem Cells: A Potential Therapeutic Strategy for Type 1 Diabetes. *Diabetes*. **57**(7):1759-1767. (2008).

204. Fountas, A., Diamantopoulos, L.-N., Tsatsoulis, A. Tyrosine Kinase Inhibitors and Diabetes: A Novel Treatment Paradigm? *Trends in Endocrinology & Metabolism.* **26**(11):643-656. (2015).

205. Stoleru, B., et al. Tropomyosin-Receptor-Kinases Signaling in the Nervous System. *Mædica*. **8**(1):43-48. (2013).

206. Waterman, R.S., et al. Anti-Inflammatory Mesenchymal Stem Cells (MSC2) Attenuate Symptoms of Painful Diabetic Peripheral Neuropathy. *Stem Cells Translational Medicine*. **1**(7):557-565. (2012).

207. Xia, N., et al. Human mesenchymal stem cells improve the neurodegeneration of femoral nerve in a diabetic foot ulceration rats. *Neuroscience Letters*. **597**:84-89. (2015).

208. Au, E., et al. SPARC from Olfactory Ensheathing Cells Stimulates Schwann Cells to Promote Neurite Outgrowth and Enhances Spinal Cord Repair. *The Journal of Neuroscience*. **27**(27):7208-7221. (2007).

209. Gillen, C., et al. Differentially expressed genes after peripheral nerve injury. *Journal of Neuroscience Research*. **42**(2):159-171. (1995).

210. Kingham, P. J., et al. Stimulating the neurotrophic and angiogenic properties of human adipose-derived stem cells enhances nerve repair. *Stem Cells and Development*. **23**(7):741-754. (2014).

211. Mohammadi, R., et al. Vascular endothelial growth factor promotes peripheral nerve regeneration after sciatic nerve transection in rat. *Chinese Journal of Traumatology* **16**(6):323-329. (2013).

212. Taras, J. S. and Jacoby S. M. Repair of lacerated peripheral nerves with nerve conduits. *Techniques in Hand & Upper Extremity Surgery.* **12**(2):100-106. (2008).

213. Appasani, K. and Appasani, R. K. *Stem Cells & Regenerative Medicine: From Molecular Embryology to Tissue Engineering*, Humana Press. 2010. pp. 206.

214. Kim, J.-H., et al. Suppression of in vitro murine T cell proliferation by human adipose tissue-derived mesenchymal stem cells is dependent mainly on cyclooxygenase-2 expression. *Anatomy & Cell Biology.* **46**(4):262-271. (2013).

215. Chen, M. B., et al. Luminal Fillers in Nerve Conduits for Peripheral Nerve Repair. *Annals of Plastic Surgery*. **57**(4):462-471. (2006).

216. Madison R. D., da Silva C. F., Dikkes P., et al. Peripheral nerve regeneration with entubulation repair: comparison of biodegradable nerve guides versus polyethylene tubes and the effects of a laminin-containing gel. *Experimental Neurology*. **95**(2):378 –390. (1987).

217. Williams, L. R. Exogenous fibrin matrix precursors stimulate the temporal progress of nerve regeneration within a silicone chamber. *Neurochemical Research.* **12**(10):851-860. (1987).

218. Rosen, J. M., et al. Artificial Nerve Graft Using Collagen as an Extracellular Matrix for Nerve Repair Compared with Sutured Autograft in a Rat Model. *Annals of Plastic Surgery*. **25**(5):375-387. (1990).

219. Rich, K. M., et al. Nerve growth factor enhances regeneration through silicone chambers. *Experimental Neurology.* **105**(2):162-170. (1989).

220. Hadlock, T., et al. A Novel, Biodegradable Polymer Conduit Delivers Neurotrophins and Promotes Nerve Regeneration. *The Laryngoscope.* **109**(9):1412-1416. (1999).

221. Hobson, M. I., et al. VEGF enhances intraneural angiogenesis and improves nerve regeneration after axotomy. *Journal of Anatomy.* **197**(Pt 4):591-605. (2000).

222. Subramanian, A., et al. Development of biomaterial scaffold for nerve tissue engineering: Biomaterial mediated neural regeneration. *Journal of Biomedical Science.* **16**(1):108-108. (2009).

223. O'Brien, P. D., et al. Mouse Models of Diabetic Neuropathy. *ILAR Journal*. **54**(3): 259-272. (2014).